UNIVERSIDAD DE MURCIA

ESCUELA INTERNACIONAL DE DOCTORADO

Benthic Diatoms from the Hypersaline Mar Menor Coastal Lagoon: Taxonomy, Phylogeny and Responses to Environmental Changes

Diatomeas Bentónicas de la Laguna Costera Hipersalina del Mar Menor: Taxonomía, Filogenia y Respuestas a Cambios Ambientales

Dª María Dolores Belando Torrentes

2017

UNIVERSIDAD DE
MURCIA

D. Arnaldo Marín Atucha, Profesor Titular de Universidad del Área de Ecología en el Departamento de Ecología y Hidrología, AUTORIZA:

La presentación de la Tesis Doctoral titulada "Diatomeas bentónicas de la laguna costera hipersalina del Mar Menor: taxonomía, filogenia y respuestas a cambios ambientales", realizada por D. Maria Dolores Belando Torrentes, bajo mi inmediata dirección y supervisión, y que presenta para la obtención del grado de Doctor por la Universidad de Murcia.

En Murcia, a 19 de septiembre de 2017

Fdo. Arnaldo Marín

UNIVERSIDAD DE
MURCIA

Dª. Marina Aboal Sanjurjo, Catedrática de Universidad del Área de Botánica en el Departamento de Biología Vegetal, AUTORIZA:

La presentación de la Tesis Doctoral titulada "Diatomeas bentónicas de la laguna costera hipersalina del Mar Menor: taxonomía, filogenia y respuestas a cambios ambientales", realizada por D. Maria Dolores Belando Torrentes, bajo mi inmediata dirección y supervisión, y que presenta para la obtención del grado de Doctor por la Universidad de Murcia.

En Murcia, a 19 de septiembre de 2017

MARINA ABOAL SANJURJO

Diatomeas bentónicas de la laguna costera hipersalina del Mar Menor: taxonomía, filogenia y respuestas a cambios ambientales.

Benthic diatoms from the hypersaline Mar Menor coastal lagoon: taxonomy, phylogeny and responses to environmental changes.

Maria Dolores Belando Torrentes

Facultad de Biología

Universidad de Murcia

2017

Contenido

Resumen

Las diatomeas son el grupo más diverso y abundante de las microalgas bentónicas que forman tapetes microbianos en los sistemas acuáticos. Estas comunidades tienen un papel ecológico fundamental en sistemas costeros poco profundos, como lagunas costeras y estuarios. También son responsables de una proporción significativa de la producción primaria total, intervienen en los ciclos biogeoquímicos y se consideran la base de la cadena trófica. Además, estas comunidades reaccionan de forma rápida ante cualquier variación ambiental o tipo de impacto. El conocimiento sobre la distribución, ecología y taxonomía de las diatomeas bentónicas en medio marino es muy escaso. Por otro lado, aunque la utilidad de estas microalgas como indicadores de estrés ambiental ha sido ampliamente probada en ríos, en medio marino hay escasa información que relacione los cambios en estas comunidades con variaciones ambientales. Este es el escenario en el que se engloba la presente tesis, ya que previamente no se tenía información sobre la composición de las comunidades de diatomeas bentónicas en la laguna del Mar Menor (SE España). Por la poca profundidad de la laguna y alto grado de confinamiento, que a su vez le aporta el carácter de hipersalinidad, se puede considerar un sistema estresando de forma natural. Además la laguna está sujeta a la presión ambiental de múltiples impactos antropogénicos, entre ellos los aportes de metales y nutrientes que entran a través de las ramblas que discurren por terrenos mineros y agrícolas, y desembocan en ella. Además, sus poblaciones se pueden ver muy afectadas por el aumento de temperatura asociado al cambio climático global. Por ello es un área de estudio ideal para investigar las relaciones entre especies y comunidades con los gradientes ambientales, y puede ayudar a entender los factores bióticos y abióticos que estructuran las comunidades de diatomeas bentónicas.

El objetivo general de la tesis es mejorar el conocimiento de la ecología y taxonomía de las comunidades de diatomeas bentónicas de la laguna costera del Mar Menor, y evaluar su potencial como indicadores biológicos de los múltiples factores de estrés que afectan y amenazan la laguna. La realización de cualquier trabajo sobre indicadores biológicos se sustenta en un buen conocimiento florístico, sin embargo en el Mar Menor se carece de esta información. El único trabajo que se ha podido tomar como referencia para el estudio taxonómico, ha sido la tesis doctoral de Xavier Tomás (1988), en el que se aporta información de la flora de dos salinas situadas en las inmediaciones de la laguna, El Cotorillo y de Marchamalo. Por ello, en esta tesis, primero se pretenden clarificar algunos aspectos taxonómicos, que han resultado fundamentales para poder testar e interpretar la respuesta de las comunidades de diatomeas bentónicas lagunares a los factores de estrés que se han investigado.

En el **capítulo 1** se ha realizado una revisión morfológica del género *Hyalosynedra*, acompañada de análisis filogenéticos de las secuencias disponibles para el género. Es un género de diatomeas arrafidiadas ampliamente distribuidas por todo el mundo y commúnmente encontradas formando parte de las comunidades de diatomeas bentónicas, ya sea como epífitos o colonizando sustratos duros. La apariencia hialina de las valvas y la elevada densidad de las estrías, que son imperceptibles a microscopio óptico, dificultan la identificación de la mayoría de las especies. Muy pocos estudios se han centrado en el estudio de su morfología, ecología y relaciones filogenéticas en detalle. Este trabajo forma parte de un proyecto más general que pretende mejorar el conocimiento sobre las comunidades de las diatomeas bentónicas de la laguna costera del Mar Menor (SE España), habida cuenta la escasa información florística existente. Basándonos en observaciones morfológicas, mediante microscopía óptica y electrónica, y datos moleculares (análisis filogenéticos y divergencia entre secuencias), *Hyalosynedra lanceolata* se propone como una nueva especie para la ciencia. La descripción morfológica des esta especie aporta nuevos caracteres morfológicos que no habían sido tenidos en cuenta anteriormente para el género, como son la forma de la colonia en racimo, estriación biseriada, esternum lanceolado y cloroplastos laminares y lobulados. Para incluir todos estos caracteres taxonómicos, se propone una ampliación de la descripción del género *Hyalosynedra*. Los análisis moleculares también revelan que *Hyalosynedra toxoneides,* recientemente incluida en el género*,* está más estrechamente relacionada con *Thalassionema* que con las otras especies de *Hyalosynedra*. Además no muestra semejanzas morfológicas con la descripción del género. Por ello, se propone mantener el nombre de *Synedra toxoneides* para este taxón. Nuestras investigaciones apuntan a que *S. toxoneides* podría pertenecer a un género diferente, relacionado filogenéticamente con *Hyalosynedra* pero también con *Thalassionema*, sin

embargo los análisis no cuentan con el soporte necesario, en parte, por la escasez de secuencias disponibles hasta la fecha. Por ello, estudios con un mayor número de secuencias de taxones relacionados como especies de la familia *Thalassionematales* e *Hyalosynedra* podría aportar información muy útil para desentrañar las relaciones filogenéticas entre estos tres grupos taxonómicos.

En el **capítulo 2** se realiza una descripción morfológica detallada con ilustraciones de microscopio óptico y electrónico de cinco especies epifíticas del género *Licmophora*; *L. proboscidea*, *L. debilis*, *L. tenuis*, *L. flabellata* y un taxón identificado como *Licmophora* sp. del que se ha observado amplia variabilidad morfológica y no encaja en la descripción de ninguna especie descrita hasta el momento. Para su correcta identificación es necesario el uso de técnicas moleculares que desvelen con claridad su posición taxonómica respecto a otros taxones morfológicamente similares como *L. gigantea*. La presencia de estas especies en la laguna hipersalina aporta información sobre su ecología como especies epífitas sobre *Cymodocea nodosa* y se amplía el rango de tolerancia a la alta salinidad de algunas de ellas. Se ha constatado que el taxón identificado como *Licmophora* sp. muestra una mayor abundancia relativa en comparación con las otras especies durante los meses de junio y julio. Las cinco taxones son nuevas citas para el Mar Menor, ya que el único estudio previo de estas comunidades sólo cita *Licmophora* cf. *proboscidea* y *L. remulus* en las salinas del Cotorillo y Marchamelo localizadas en las inmediaciones de dicho sistema lagunar.

En el **capítulo 3** se pone en evidencia que, a pesar del gran tamaño del algunas especies del género *Licmophora* (hasta 800 µm), para la identificación de algunos taxones, como ocurre en el caso del taxón identificado como *Licmophora* sp. en el capítulo anterior, es necesario el empleo de análisis filogenéticos. Esto se debe principalmente, a que la diagnosis de muchas especies se basa sólo en observaciones de microscopio óptico, o el tipo de material no está disponible para realizar una comparación morfológica. En este trabajo se han obtenido cultivos monoclonales de *Licmophora* sp., utilizando material de campo recolectado en julio de 2012 y también de *Licmophora remulus*, más abundante en septiembre del mismo año, que ha permitido un análisis filogenético y morfológico exhaustivo de ambas especies así como su comparación con otras especies (*L. gigantea* y *L. grandis*) morfológicamente similares. Los análisis comparativos avalan la descripción de *Licmophora colosalis* como nueva especie para la ciencia. Ambas especies, *L. colosalis* y *L. remulus* son nuevas citas para la laguna hipersalina del Mar Menor, aunque *L. colosalis* ha sido recolectada en la Bahía de Florida y el Mar Rojo, sugiriendo la naturaleza cosmopolita y el carácter eurihalino de esta especie.

En el **capítulo 4** se ha evaluado el posible efecto conjunto de la variación en el rango estequiométrico de nitrógeno y fósforo (N:P) del agua con el aumento de temperatura asociado al calentamiento global. Para ello, se ha llevado a cabo un experimento de laboratorio basado en un diseño multifactorial y utilizando cultivos monoclonales de la diatomea marina pedúnculada *Licmophora colosalis*. Los diferentes tratamientos consisten en cultivos celulares que contienen diversos medios de cultivo F/2 con una variación gradual del rango estequiométrico N:P, con el fin de evaluar diferentes grados de deficiencia en N y en P (5, 10, 16, 21 42). Cada uno de los cultivos replicados (n=5) han sido tratados con diferentes grados de estrés térmico a 26, 31 y 36 °C. Las temperaturas se han elegido tomando en consideración las observaciones en campo, siendo 26 °C, la temperatura observada en junio, cuando *L. colosalis* comienza a ser abundante en la laguna del Mar Menor. 31 °C corresponde al máximo observado en agosto, y 36 °C es la temperatura que se podrá alcanzar según las predicciones del calentamiento global. Los resultados revelan que las condiciones óptimas para el crecimiento de *L. colosalis* se aproximan a 26 °C y aguas con un rango estequiométrico comprendido entre 16 y 21. Diferente rango estequiométrico, sin embargo provoca una reducción significativa de su crecimiento. También se observó que el aumento de 26 a 31 °C puede tener efectos adversos sobre la viabilidad poblacional de la especie, produciendo un aumento de la mortalidad, de hasta el 70% de la población, y de la producción de carbohidratos, cuando el crecimiento es limitado por la deficiencia de nitrógeno o fósforo. Sin embargo, ese estrés térmico puede ser mejor soportado si se mantiene el rango estequiométrico N:P de 16. Por otro lado, un aumento de temperatura de hasta 36 °C puede resultar letal para la especie. Mientras que el aumento en la acumulación de carbohidratos está ligado a la reducción del crecimiento por limitación de nitrógeno o fósforo,

la producción de pedúnculos ha sido específicamente relacionada con los tratamientos en los que el crecimiento está limitado por déficit de fósforo. Esta respuesta ha sido consistente en ambas temperaturas, 26 y 31 °C, sugiriendo alta proporción de pedúnculos respecto al total de células, lo que podría servir como indicador de aguas enriquecidas en nitrógeno, y por ello sería una métrica potencialmente útil para la detección de la contaminación por nitratos, como es el caso de la laguna costera del Mar Menor.

El efecto conjunto de múltiples factores de estrés ambiental en las comunidades de diatomeas bentónicas en medio marino ha sido escasamente investigado hasta la actualidad. En el **capítulo 5** se investiga el impacto de descargas esporádicas de metales y nutrientes, de forma individual y conjuntamente, sobre tapetes de algas desarrolladas en una zona históricamente contaminada y en una zona relativamente inalterada (zona de referencia). Con el objetivo de ver la posible respuesta diferencial de ambos, se ha realizado un experimento de mesocosmos en campo basado en un diseño experimental multifactorial, en el que se han realizado descargas de una hora durante cuatro días, para simular los patrones de descarga en el medio natural cuando llueve de forma torrencial. Se han aplicado tres tratamientos: descargas de metales (Zn y Pb), nutrientes (N y P) y combinación de ambos, y un tratamiento control que consiste en adición de agua de cada zona de estudio. Los cambios en los tapetes se han monitorizado a diferentes niveles; composición y estructura de la comunidad (índices biológicos y abundancia relativa), y la caracterización química del tapete se ha realizado mediante medidas de concentración de metales acumulados, contenido en clorofilas y carbohidratos. Los principales resultados han mostrado que las comunidades desarrolladas en la zona crónicamente contaminada están dominadas por especies tolerantes (e.g. *Berkeleya fennica* y *Neosynedra provincialis*), y sólo han respondido con un aumento de carbohidratos ante las descargas de metales o nutrientes, lo que podría sugerir cierto grado de estrés, pero en general resultaron ser más resistentes a las descargas esporádicas que las comunidades desarrolladas en la zona de referencia. Estas comunidades estaban dominadas por especies que se podrían considerar sensibles a la contaminación por nutrientes y metales como *Opephora krumbeinii*, que fue afectada negativamente por todos los tratamientos aplicados y estaba escasamente representada en la zona contaminada. Estas comunidades fueron alteradas por todos los tratamientos, y se ha observado que, los nutrientes amplifican el impacto de los metales cuando actúan individualmente. Cuando ambos factores actúan conjuntamente, los metales actúan seleccionando y favoreciendo la colonización de especies tolerantes y el enriquecimiento por nutrientes beneficia la proliferación de aquellas con formas específicas de crecimiento (especies que forman colonias en zig-zag y tubos mucilaginosos). Todo ello se refleja en una amplificación en la concentración de metales acumulados, una reestructuración de la comunidad que tiende a parecerse a las comunidades de zonas contaminadas, y una mayor concentración de clorofilas y carbohidratos. Los cambios estructurales se reflejaron también en una mayor complejidad tridimensional del tapete, lo que podría sugerir el interés de estudiar el uso de los rasgos biológicos de las especies (formas de crecimiento) para una mejor interpretación de la respuesta de la comunidad.

Todos los trabajos realizados permiten concluir que las comunidades de diatomeas bentónicas pueden servir como potenciales bioindicadoras de los impactos antropogénicos a los que está sometida la laguna del Mar Menor. También se pone de manifiesto la importancia y el interés de los trabajos florísticos y taxonómicos como base del conocimiento de las diatomeas que componen las comunidades bentónicas de la laguna, y como primer paso para facilitar y mejorar los métodos de control y gestión de la laguna.

General Introduction

Benthic diatom communities in coastal lagoons

The term microphytobenthos refers to microscopic algae, mainly diatoms, dinoflagellates, euglonoids, and cyanobacteria that cover great extension on photic, apparently unvegetated sediments and seagrass beds in habitats such as salt marshes, estuarine and coastal ecosystems (MacIntyre *et al*., 1996). The term biofilm, as defined by Decho (2000), refers to microbial cells, such as microalgae, bacteria and fungi, which are embedded in a matrix of mucilaginous extracellular polymer (EPS) secretions by which they are attached to submerged surfaces. Wetzel (2001) proposed that a biofilm can be synonymous of periphyton, that in turns, it is usually applied as a synonym of microphytobenthos, mainly in freshwater and estuarine systems (e.g., Trobajo *et al*., 2007)

On the basis of substrata typology, different groups can be distinguished between benthic microalgae: the epiphyton includes taxa that grow attached to plants, such as angiosperms and macroalgae, and the epilithon refers to the taxa that live on hard substrata like rocks or other non-living surfaces (sediment). The diatoms that are associated with sediments are subdivided into epipsammon (attached to sand grains) and epipelon (motile form and not firmly attached to mud particles) (McIntire & Moore 1977). In shallow water systems, microphytobenthic populations are often enriched by phytoplanktonic species, which can settle on sediments in the absence of turbulent movements, tidal currents or water column stratification. In the event of strong turbulence, microphytobenthic organisms can be resuspended in the water column by entering the phytoplankton community (Delgado *et al*., 1991; MacIntyre *et al*., 1996). Moreover, some taxa have life cycles, including planktic and benthic phases (Lee, 2008). From a taxonomic point of view, the same taxa can be common in the water column and on surface sediments, which hence complicates the ecological characterisation of typical species in each habitat.

In shallow coastal environments, diatoms are often the dominant component of benthic microalgae assemblages (McIntire & Moore 1977; Sullivan 1999; Brotas *et al*.,, 1998). These diatom-dominated biofilms play a key ecological role in this aquatic ecosystems by contributing significantly to primary production (e.g., MacIntyre *et al*., 1996; Cahoon 2006; Underwood & Kromkamp 1999). They are also important mediators in several biogeochemical processes (e.g., nitrogen, phosphorus and silicon cycles) (e.g. Blanchard *et al*., 2000, Magalhães & Wiebe 2003), since the production of oxygen by photosynthesis may affect the oxic-anoxic state of sediments, and nutrient transformation and exchange at the sediment-overlaying water interface. Therefore, they may also attenuate the high nutrient concentration in the water column of usually enriched shallow coastal ecosystems, lagoons and estuaries. Diatoms constitute the main food source for meiofauna, being also relevant in biomass and energy transfers throughout benthic food webs (Blanchard *et al*., 2000). They also synthesise a extracellular matrix composed of exopolymers, extracellular polymeric substances (EPS) that mainly consist in polysaccharides, but also proteins, nucleic acids and lipids (Burmølle *et al*., 2014). This EPS fulfils a wide range of ecological functions, e.g., adhesion to surfaces and motility in raphe-bearing diatoms (Lind *et al*., 1997), and is the primary constituent of diatom stalks (Daniel *et al*., 1987). It contributes to sediment stabilisation, and the binding sites of these exopolymers confer biofilms a high adsorption capacity for nutrients and metals (Quigley *et al*., 2002; Aldridge *et al*., 2010), which can be potentially transferred through food chains (Marín-Guirao *et al*., 2008) and, therefore, act as a trophic link between dissolved compounds and higher trophic levels (Hynes 1970). Generally, EPS production is interpreted as a response to environmental stress, such as nutrient-limited conditions. Under these nutrient-deplete conditions with good light availability, EPS overproduction is interpreted as a "photosynthetic overflow", a mechanism for releasing surplus photosynthetically fixed carbon that cannot be stored within the cell (Smith & Underwood 2000, Staats *et al*.,, 2000).

Despite the ecological importance of these diatom-dominated biofilms in shallow coastal systems, knowledge of benthic communities from coastal lagoons is scarce compared with freshwater, phytoplankton, and even with estuarine communities (e.g., Trobajo 2007; Rovira *et al*., 2009; Delgado *et al*., 2012). Coastal lagoons are highly complex ecosystems where system dynamics and functioning are defined by specific conditions of wind,

the interchange with the open sea and runoff influence. Hence depending on the coastal area, each lagoon may have particular characteristics. In the Mediterranean region, these systems are not commonly affected by significant tidal influences, and are driven mainly by freshwater influence and winds. Salinity may vary from freshwater systems, with a high rivers interface, to hypersaline, which are usually found in arid coastal regions where evaporation is greater than runoff (Kjerfve & Magil 1989). These hypersaline systems have communities that are characterised by a low diversity, but highly specialised organisms, and they may be considered natural stressed environments. Being close to land, their ecological equilibrium is frequently subjected to multiple anthropogenic pressures, including climate change, nutrient loading, toxicants and fishing (e.g., Cloern *et al*., 2016) or tourism. In this context, signals of human disturbance can be confounded by the variability of the climate system through its separate influences on watersheds and ocean basins (Feyrer *et al*., 2015). Despite the difficulty of studying these highly dynamic systems, they are the ideal place to investigate the relationship of species and communities with environmental gradients, which may help us to understand the biotic and abiotic factors that structure communities.

Biological indicators

The ecological and chemical monitoring of coastal environments is compulsory in many countries in an attempt to quantify the level and nature of the imposed stress. Numerous biological or chemical ecosystem parameters can be used to describe the ecological state and quality of sampling sites. To satisfy future management needs (Water Framework (WFD; 2000/60/EC) and the Marine Strategy Framework Directives (MSFD; 2008/56/EC)), several indices have been developed based on the biological and water chemistry parameters defined by legislation. Water chemistry measurements can identify the causative factors that can explain further ecosystem perturbation (Ferreira *et al*., 2011). However, chemical sampling does not help to evaluate biological threats of specific stress to ecosystem health; e.g., changes in the structure and functioning of community components. Moreover, obtaining representative values of chemical characteristics of a location is complicated by the variability in concentration with time. Moreover, the detection of elements in some oligotropic water is difficult if they are lower than the detection threshold of analytical methods. For all these reasons, the use of bio-indicators may be a more representative approach since organisms integrate spatial and temporal changes into water quality. Bio-indicators can provide an integrative tool to measure these changes as they “relay a complex message in a simplified and useful manner providing insights about a trend or event that cannot be directly observed” (Linton & Warner 2003). In this context, a good bio-indicator must have a short life span to integrate short-term environmental variability, must be abundant and easy to sample, and be sessile to reflect conditions at one site, and response-specific to identify a particular impact on the ecosystem.

The biological quality elements required by the WDF to describe the ecological quality of a coastal site are phytoplankton, aquatic flora (macroaglae and angiosperms), and benthic invertebrate fauna (CIS-WFD, 2003). Actually used elements require months, or even years, to detect some environmental changes, while benthic diatom and phytoplanktonic communities can respond to impacts in just a few days. Diatoms have short life span as unicellular microalgae, respond to short-term environmental fluctuations at sampling sites, and are sensitive to numerous environmental parameters (e.g., pH, salinity, toxicants, nutrients and organic enrichment) (e.g., Ivorra *et al*., 2002; Soldo & Behra 2000; Cunningham *et al*., 2003). The main advantage of using benthic communities against phytoplacktonic is the fact that phytoplankton involve many taxonomic classes of organisms, such as dinoflagellates, euglenoides, diatoms, etc., while only training in identifying diatoms is required to detect changes in the benthic communities. Phytoplanktonic communities are non-sessile, while benthic communities can integrate both short- and long-term environmental conditions at a specific location, and they are also easy to sample.

It is widely recongnised that benthic diatoms are good biological indicators for monitoring the quality of freshwater environments (e.g., Van Dam *et al*., 1994; Kelly*et al*., 1995; Potapova *et al*., 2004) and numerous

diatom indices have been developed to be used for routing monitoring (e.g., PDI, TDI, BDI), as in the WDF context. For biomonitoring, this compartment is evaluated in the species assemblages that constitute biofilms, and is based on the fact that each organism that inhabits each site is adapted to the specific environmental conditions. In rivers, it is clear that diatom indices are suitable for detecting organic and nutrient enrichment, but the monitoring of toxic pollution (e.g., metal loads) remains difficult because no clear correlations between indices and concentrations of toxicant have been found (e.g., Blanco *et al*., 2007).

In marine environments most studies focus on the functional and global response of biofilms (e.g., Kociolek & Stoermer 2001; Blanck *et al*., 2009; Sanz *et al*., 2015) to water quality changes. Very few studies have focused on the community composition and the response of benthic diatom species to specific environmental characteristics, or a few are available for specific areas. On the other hand, the floristic or structural studies usually have a very descriptive approach that rarely shows an environmental characterisation of locality type. This scenario results from the traditional separation made between the disciplines of Taxonomy and Ecology in diatom studies, where a limited number of formally trained diatom taxonomists works in collaboration with ecologists (Kociolek & Stoermer 2001, Kociolek 2005).

In this context, most information has to be drawn from global studies that generally focus on the natural gradients related with the dynamics of systems (nutrients, salinity, turbulence), while approaches orientated to toxicant impacts are still scarce. Most marine studies have been orientated to the species that inhabit on or within sediments (epiphelic or epissamic species). Benthic communities are only well known in specific areas, e.g., in the Baltic Sea various studies have been specially focused on the microalgal flora (e.g., Snoeijs 1993, Snoeijs & Vilbaste 1994; Snoeijs & Balashova 1998), and on changes in the composition in response to salinity and turbidity (e.g., Busse & Snoeijs 2002; Ulanova & Snoeijs 2006). Various studies have also improved knowledge on estuarine composition, distribution and responses to gradients of nutrients, salinity and confinement in the Delta del Ebro, Spain (e.g., Delgado *et al*., 2012; Trobajo 2007; Trobajo *et al*., 2004), hypersaline environments (Clavero 2005; Tomás 1988), and also in Iberian Atlantic coasts (e.g., Ribeiro *et al*., 2013; Cabrita *et al*., 2000). On the other hand, some authors have indicated a metal and petroleum hydrocarbon modified composition of epiphelic communities from the Antarctica, as well as changes in the abundance of some potential tolerant species (Cunningham *et al*.,, 2005, Cunningham *et al*., 2003). Toxicity assays, which are widely used to evaluate ecological preferences, have been carried out essentially using the benthic marine diatom *Cylindrotheca closterium,* which has proved to be a reliable biomonitor of marine sediment quality assessments (Araújo *et al*., 2010).

Despite most studies having dealt with epiphelic or epissamic species, these diatoms have been excluded as potential indicators of water quality as their development is strongly influenced by nutrients from sediment and are not, therefore, representative of water conditions. Diatom assemblages that grow on hard substrates, however, have a promising bio-indication potential, and even the use of artificial substrata has been recommended to sample diatoms for routine monitoring, e.g., WFD procedures (Kelly *et al*., 1998), especially when there are no hard substrata available. However, much less information on epilithic communities is available. Some studies have implemented artificial substrata to assess species succession in response to antifouling agents, and although most studies have investigated toxicity at the functional level (e.g., Blanck & Wangberg 1988; Blanck *et al*., 2009), and some have shown responses of specific species (Dahl & Blanck, 1996). Epiphytic species have been rarely dealt with, rather the influence of nutrient and salinity on diatom assemblages in Florida Bay has been mainly assessed (Armitage *et al*.,, 2006; Frankovich *et al*., 2006, 2009; Wachnicka *et al*., 2010), and recently the first illustrated guide to the benthic diatom flora in Florida Bay has been published (Frankovich & Wachnicka 2015).

Studies showing fundamental data on the composition of diatom assemblages, and physico-chemical characteristics, are the basis of knowledge on species' ecological profile. Therefore, this kind of approach and bioassays are essential to implement diatoms in monitoring. However, some marine environments, such as shallow coastal lagoons, remain poorly investigated, and the only available description of most species stems from the pre-electronic microscopy era, without almost no information on ornamentation from striae density to type of areolae, etc. Therefore, developing a marine diatom index requires intensive work to define the ecological ranges of species, and taxonomic studies to provide managers (or the people implicated in monitoring) with complete species descriptions for easy species identification.

Biological traits: life-form and cell size

Diatoms are basically unicellular algae, but exhibit a considerable diversity of life forms and many of them can form colonies.

The life forms of benthic diatoms can be classified as follows:

1. Solitary cells that may live**:**

a. Unattached: diatoms move freely. We can differentiate two classes: a) mobile, cells with a raphe structure that may slowly glide (e.g. *Amphora* spp), and b) motile, including members of *Navicula* and *Nitzschia* sensu *lato*, which are generally selected as fast-moving mobile diatoms (Passy, 2007).

b. Attached: diatoms can be attached to substrates in several different ways:

- Adnate/prostrate: cells are firmly attached by their valve face, hypovalve (e.g. *Cocconeis placentula* , Plate 1 Fig. 2), or by their girdle view.
- Mucilage pad: cells produce a small cushion of mucilage on one pole that sticks to substrata.
- Mucilage stalk: cells can produce stalks through apical pore fields and these stick to substrata. Stalks can be simple (one-cell, e.g. *Achnanthes longipes* in Wang *et al*., 1997), or may be branched to form complex colonies, see the fan and arbuscular colonies below).

2. Considerable diversity exists in types of colonies, but the predominant classes found in our samples and the literature for marine benthic diatoms are:

a. Chain colonies: they refer to central diatoms whose cells are juxtaposed by their valves. These cells can be linked by spines (*Aulacoseira*) or other siliceous structures. In other cases adhesion is mediated by polysaccharide material (e.g. *Cyclotella*).

b. Ribbon colonies: pennate diatoms are juxtaposed by their valves, and are linked by spines (*Fragilaria capucina*, in Rimet phD) or are adhered by the mucilage excretions from their whole valve face (*Fragilariopsis*), or over only a part of it (Round *et al*., 1990).

c. Zig-zag colonies: pennate cells connected by mucilage on their opposed poles (e.g. *Neosynedra provincialis* Plate 1 Fig. 3*, Grammatophora*).

d. Rosette/Radiatte/tufted colonies: pennate cells produce a small cushion of mucilage at one pole that sticks to a substrate. After several cell divisions, they produce colonies that resemble radiatte/rosettes (e.g., *Hyalosynedra lanceolata* Figure X, *Synedra* spp in Round 1990, Plate 1 Figs. 5-6.

e. Arbuscular colonies: stalks produced by one valve pole diverge from each cell and form branching colonies, e.g. *Licmophora colosalis*, Plate 1 Fig. 4.

f. Fan-shaped colonies: cells are bound together in groups at the end of a copious amount of mucilage and stalks to resemble fans (e.g. *Licmophora flabellata*).

g. Mucilage tube colonies (Plate 1, Fig 1): the growth of species of several genera is included within mucilage tubes, enveloped or sheaths, and cells move inside them in a row (e.g. *Parlibellus*, *Berkeleya*).

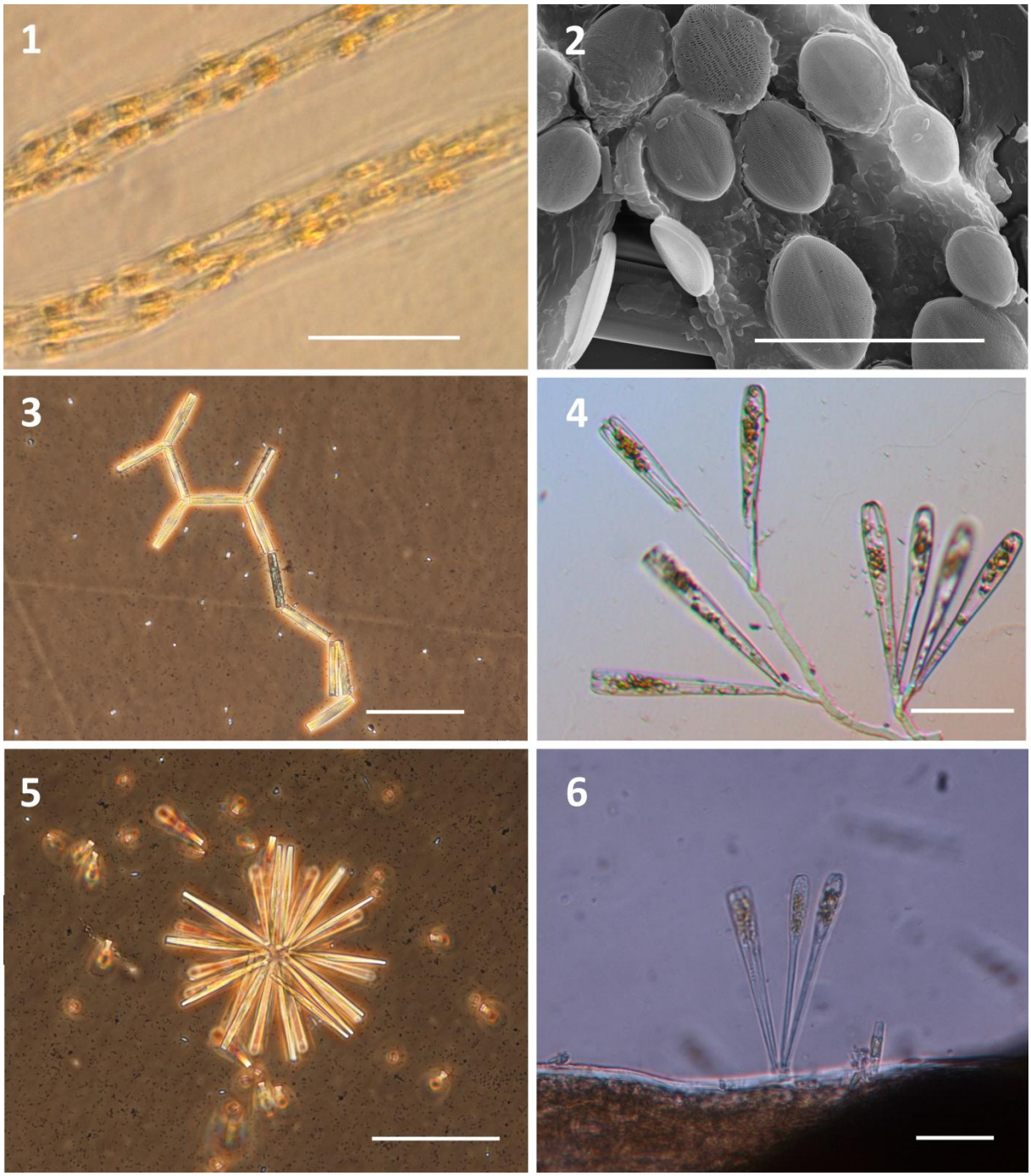

Plate 1. Examples of diatom life-form. **Fig. 1.** Mucous tubules. **Fig. 2.** Prostrated *Cocconeis* sp. **Fig. 3.** Zig-zag colony of *Neosynedra provincialis.* **Fig 4.** Long stalks of *Licmophora colosalis*. **Fig. 5** and **Fig 6.** Rosette-shaped colony of *Hyalosynedra lanceolata and Licmophora remulus* respectively. Scale bars: **Fig. 1** = 40 μm, **Fig. 2** = 30 μm, **Fig. 3** = 100 μm, **Fig. 4** = 75 μm, **Fig. 5** = 100 μm, **Fig. 6** = 50 μm

Life forms and cell size are responses to the evolutionary history of diatoms that have been subjected to strong selection in particular habitats, and in relation to attachment, light, nutrients capture (Round *et al*., 1990) and strong competition with other organisms. Investigation based on the relationship of life forms, cell size and environments may help to better understand ecological interactions (competition, predation) and provide a more realistic idea of the responses of a whole community to specific habitat characteristics. Studies based on this metrics can serve to obtain valuable information about the architecture and structure of biofilms and to reduce taxonomic resolution. Nowadays, the relationship between biological traits (life form and cell size) and environmental conditions has been investigated mainly in fluvial environments. The relationships between abundances of specific life forms and nutrients (Berthon *et al*., 2011) and pesticides (Rimet & Bouchez 2011) has been identified in rivers by experimental approaches. It is also generally indicated that benthic communities subjected to toxicant contamination tend to be dominated by small cell species (e.g., Tlili *et al*., 2011). In this context, it has been advocated by incorporating periphyton community responses to pollutants in terms of life history traits, ecological strategies, and morphological forms in ecotoxicology (Rimet and Bouchez, 2011; Elias *et al*., 2015), and as a water quality assessment tool (Medley & Clements (1998). However, it has also been highlighted that fine taxonomic determination is required for precise ecoregional bioassessments in fluvial ecosystems, e.g., to implement the Water Framework Directive, which requires the assessment of ecological quality to be organised on the ecoregions basis (Rimet & Bouchez 2012). Therefore, the use of these metrics for ecotoxicological and bioassessment testing needs to be further studied and demonstration to better determine concentration-dependent and/or time-dependent responses, and to gain wider acceptance (Renzi *et al*., 2014; Marcel *et al*., 2017).

In marine coastal waters, Majewska *et al*. (2013) highlighted that the bio-physicochemical characteristics of water affected the epiphytic diatom communities more than the substrate type (macroalgal host) for epiphytic communities in the Antarctica, but very little is known about the trait-based ecology of microphytobenthic communities. Most investigation on the life forms of benthic marine species are descriptive of the type and composition of stalks, and type of motility (Wang *et al*., 1997; Hundon & Legendre 1987). Only (Ravizza & Hallegraeff 2015) has stated that the stalks production of *Licmophora flabellate* is related more with light intensity than with temperature or nutrients. Other studies have also indicated that large or small benthic species can differentially respond to salinity and turbulence in the Baltic Sea (Busse & Snoeijs 2002; Ulanova & Snoeijs 2006), or have highlighted the potential suitability of size class or life form for detecting nutrient gradients (Ribeiro *et al*. (2010). However, these authors have also indicated that this requires further research, and that research at the species level is essential to provide a good understanding of the relationship between benthic communities and environmental variations.

This kind of approach remains difficult in marine environments because there is still very little knowledge on the type of colony that several marine species have. The observation of life form and other taxonomic aspects requires observing live cells or well-preserved material, while the morphological description is usually based on clean material, so a lot of relevant information is lost. An approach that involves changes at both the structural and biological traits level related with environmental contamination is still poorly investigated in marine benthic communities, but would very helpful for biomonitoring.

Study context: the Mar Menor lagoon

The present study was carried out at the coastal hypersaline Mar Menor lagoon located in a semi-arid region of southeast Spain (Figure 7.). It is one of the largest coastal lagoons on the Mediterranean coastline as it occupies an area of 132 km^2, has a mean depth of 3.7 m and a maximum one if 7 m. It is isolated from the Mediterranean Sea by a 22-kilometre long sandy bar (La Manga) located on the eastern side of the lagoon and crossed by five shallow channels (golas). Due to the restricted water communication with the adjacent Mediterranean Sea, scarce precipitation (<300 mm yr^{-1}) and high evaporation rates related with the high sea

temperatures in the area, the lagoon has high salinity values compared with the Mediterranean Sea. The lagoon is a macrophyte-dominate ecosystem, where sediments are characterised by the dominance of sand and mud. The most important benthic species are *Caulerpa prolifera* (Forsskål) J.V. Lamouroux and *Cymodocea nodosa* (Ucria). Traditionally, benthic primary production was more important than planktic production (Terrados & Ros, 1991), and microphytobenthic primary production was estimated to contribute to 11% of total primary production (Terrados & Ros 1991). After the eutrophication process that started in 2015, 85% of meadows disappeared (Belando *et al*., 2015) and the contribution to the primary production of all these compartments may have changed, but no information is yet available.

The importance of the lagoon and its salt marshes in biodiversity terms has been recognised in numerous international protection schemes: it has been a Ramsar International site since 1994; it is considered a Special Protected Area of Mediterranean Interest (SPAMI) established by the Barcelona Convention in 2001; and is a Site of Community Importance (SCI) to be integrated into the Nature 2000 Network (EU Habitats Directive). This zone is also a Specially Protected Area (SPA) for nest building, migration and hibernation of aquatic birds, and is protected by European legislation (Birds Directive 79/409/CEE; Seawages Directive 91/271/EEC, Nitrate Directive 91/676/EEC; Habitat Directive 92/43/EEC Water Framework Directive (2000/60/EC) and the Marine Strategy Framework Directive. Despite the numerous protection figures the lagoon has, the system's ecological equilibrium is threatened by waste from intensive agriculture, from former mining activities and from massive urban growth in surrounding areas, and it has undergone two eutrophication episodes since 2015. The contribution of continental water is made up mainly of six ephemeral watercourses, which are dry most of the year, but can carry vast quantities of water and sediment when the torrential rainfall events, which are characteristic of the area, occur mainly in autumn and winter.

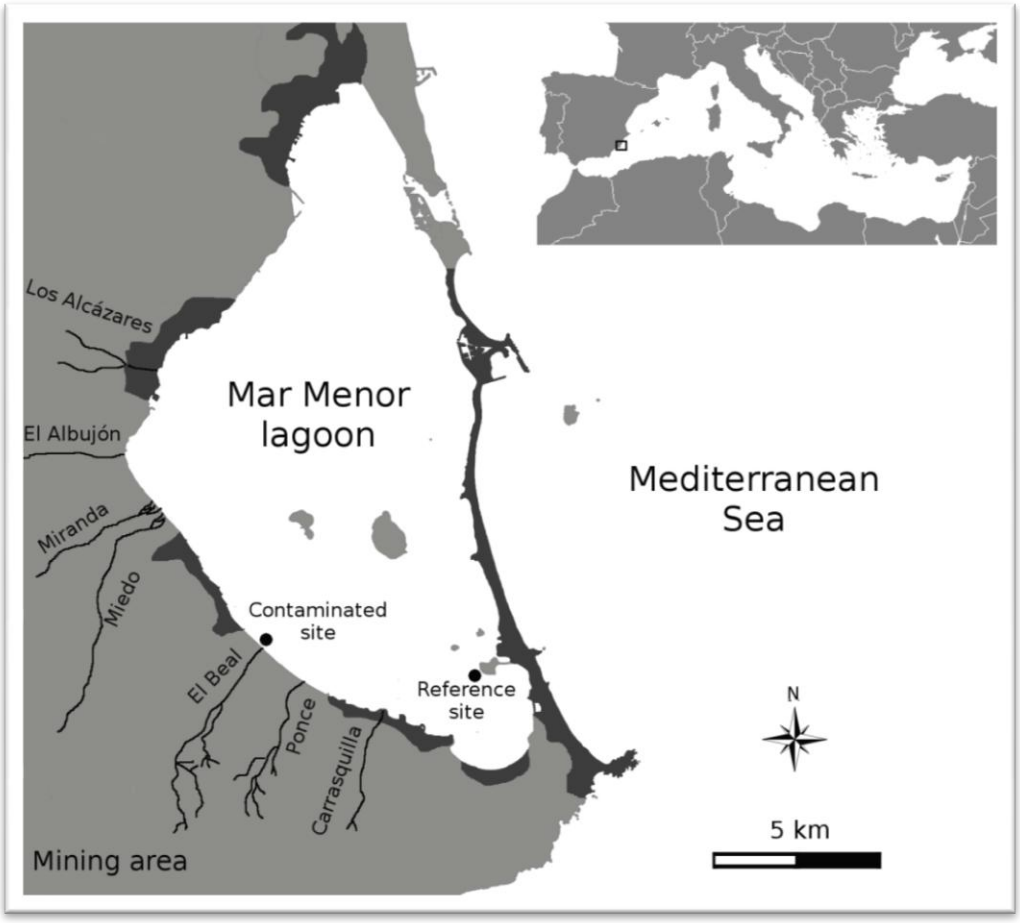

Figure 7. Map of the study area and location of the sampling sites.

The lagoon has been historically subjected to waste from the mining activity that has been undertaken in the Cartagena-La Unión mining area. This work took place south of the lagoon (Figure 7.), with intensive mining activity in the 19th and 20th centuries, which ceased in 1991. The sulphur mining activity in the area was based mainly on lead and zinc extractions, which came in high concentrations in the run-off water from the Sierra Minera (Robles-Arenas *et al*., 2006). Nowadays, the tailings that remain in mountains continue to erode and enter the lagoon (Marín-Guirao *et al*., 2005) through the draining wadis located in its south basis (The El Beal wadi, Carrasquilla, El Ponce and El Miedo wadis). On the other hand, over the last two decades, agriculture in the watershed has changed from extensive dry crop farming to intensively irrigated crops, and uses water from the Tajo-Segura river diversion. These changes have led to a rise in phreatic levels as the overexploited groundwater lessens. As a result, some watercourses, such as the Albujón wadi, now maintain a regular flux fed by ground water with high nitrate levels (Pérez-Ruzafa *et al*., 2002). Consequently, the run-off from agricultural lands and the exchange of water between lagoon and aquifers contaminated by nutrients mean nutrient enrichment of its water and the subsequently problem of microalgal blooms associated with the eutrophication process.

Contextualisation

Knowledge of the taxonomy and ecology of the microalgal communities at the Mar Menor lagoon is scarce. As far as we know, the few published studies are fairly old, and describe seasonal variability of phytoplankton (Ros & Miracle 1984), or its relationship with nutrient inputs (Ruzafa *et al*., 2002; Gilabert *et al*., 2001). Tomás (1988) has reported some benthic (epiphytic and epilithic) diatoms in two saltpan systems in the surrounding area of the lagoon, known as Marchamalo and Cotorillo, but he did not sample inside the lagoon. Marin-Guirao *et al*. (2005) has highlighted that the epiphytic compartment can be used as a sentinel of metal pollution in the lagoon. More recently, phytoplantic communities have been studied from the phylogenetic and metagenomic points of view (Ghai *et al*., 2012), but no studies prior to this thesis exist that have focused on composition or responses to the environmental changes of microphytobenthic communities.

According to the WFD, the Mar Menor is catalogued as natural coastal water (ES0701030005, Mar Menor,Type AC-T11). Benthic diatoms are not considered quality biomonitors for this type of ecosystem, so controls include studying the chlorophyll concentration of phytoplankton, macrophytes and macroinvertebrates. Diatoms have been used as a proxy of phytobenthos in the continental waters body, and as they react rapidly to environmental changes, their use in the lagoon could be very useful for the rapid detection of local and diffuse contamination, and to undertake and to easy implemen a monitoring routine.

Given the lagoon's singularity, it is an ideal place to detect biological indicators of metal and nutrient contamination, and to improve knowledge about the taxonomy of microphytobenthos from shallow coastal lagoons, specifically of hypersaline systems.

Objectives and thesis outline

The general aim of this thesis is to improve knowledge of the ecology and taxonomy of the benthic diatom communities from the Mediterranean coastal hypersaline Mar Menor lagoon, and to evaluate their potential use as biological indicators of the multiple environmental stressors that affect and threaten this ecosystem.

This thesis is structured in two main blocks: the first involves various morphologic and phylogenetic studies to clarify the taxonomic and phylogenetic position of the taxa that belong to the genera *Hyalosynedra* and *Licmophora* (**Chapters 1, 2 and 3**)**.** Once the taxonomic aspect of some dominant species is elucidated, the second block includes laboratory and field experiments, run to test the responses of benthic diatom

communities to multiple environmental stressors. We evaluated the combined effects of the stressors that derive from human activities (metal and nutrients), as well as the interactive effects of nutrients and rising temperature with climate change. We investigated the responses at different organisation, population and community levels, and structural changes were also combined with the changes in the biological traits of the biofilm components.

The more specific objectives addressed in each thesis chapter are:

- ✓ To describe and identify new species of *Hyalosynedra* and to investigate interspecific phylogenetic relationship within the genus and with closely related genera (**Chapter 1**).
- ✓ To study the composition and abundance of the *Licmophora* species in the Mar Menor lagoon, and to investigate the interspecific phylogenetic relationship in order to identify potential new species (**Chapter 2 and 3**).
- ✓ To assess the interactive effects of temperature and the N:P stoichiometry of water on the marine diatom stalked-forming *Licmophora colosalis* populations, and to evaluate if stalks overproduction may serve as an indicator of high N:P ratios in water (**Chapter 4**).
- ✓ To study the composition, structure and biological traits of the species of two benthic diatom communities from areas with different degrees of metal and nutrient contamination, and to evaluate their responses to sporadic discharges of metals and nutrients in order to evaluate the suitability of these communities as a tool for the environmental monitoring of the lagoon (**Chapter 5**).

References

Aldridge, K.T., Brookes, J.D., Ganf, G.G. 2010. Changes in abiotic and biotic phosphorus uptake across a gradient of stream condition. River research and applications,26: 636-649.

Araújo, C. V., Blasco, J., & Moreno-Garrido, I. 2010. Microphytobenthos in ecotoxicology: a review of the use of marine benthic diatoms in bioassays. Environment international, 36 (6), 637-646.

Armitage, A.R., T.A. Frankovich and J.W. Fourqurean. 2006. Variable responses within epiphytic and benthic microalgal communities to nutrient enrichment. Hydrobiologia 569: 423–35.

Belando, M.D., Bernardeau-Esteller, J., García-Muñoz, R., Ramos-Segura, A., Santos-Echeandía, J., García-Moreno, P. &Ruiz, J.M. 2017. Evaluación del estado de conservación de las praderas de Cymodocea nodosa en la laguna costera del Mar Menor. 2014-2016. Informe del Instituto Español de Oceanografía y la Asociación de Naturalistas del Sureste. Murcia. 157pp.

Berthon, V., Bouchez, A. and Rimet, F. 2011. Using diatom life-forms and ecological guilds to assess organic pollution and trophic level in rivers: a case study of rivers in south-eastern France. Hydrobiologia, 673(1), pp.259-271.

Blanchard, G. F., Paterson, D. M., Stal, L. J., Richard, P., Galois, R., Huet, V. & Christie, M. 2000. The effect of geomorphological structures on potential biostabilisation by microphytobenthos on intertidal mudflats. Continental Shelf Research, 20(10), 1243-1256.

Blanck, H., Eriksson, K.M., Grönvall, F., Dah,l B., Guijarro, K.M., Birgersson, G., Kylin, H. 2009. A retrospective analysis of contamination and periphyton PICT patterns for the antifoulant irgarol 1051, around a small marina on the Swedish west coast. Marine Pollution Bulletin. 58(2): 230-7.

Blanck, H., Wangberg, S.A. 1988. Validity of an ecotoxicological test system - short-term and long-term effects of arsenate on marine periphyton communities in laboratory systems Canadian Journal of Fisheries and Aquatic Sciences. 25: 1807-1815.

Blanco, S., Bécares, E., Cauchle, H.M., Hoffrnanrr, L. and Ecto, L. 2007. Comparison of biotic indices for water quality diagnosis in the Duero Basin (Spain). Arch. Hydrobiol. Suppl, 161, pp.3-4.

Breitburg, D.L, Sanders, J.G., Gilmour, C.C., Hatfield, C.A., Osman, R.W., Riedel, G.F., *et al*., 1999. Variability in responses to nutrients and trace elements, and transmission of stressor effects through an estuarine food web. Limnol. Oceanogr. 44: 837-863.

Brotas, V., Plante-Cuny, M.R. 1998. Spatial and temporal patterns of microphytobenthic taxa of estuarine tidal flats in the Tagus Estuary (Portugal) using pigment analysis by HPLC. Marine Ecology Progress Series. 171:43–57.

Burmølle, M., Ren, D., Bjarnsholt, T., Sorensen, S. J. 2014. Interactions in multispecies biofilms: do they actually matter?. Trends Microbiology 22, 84–91.

Busse, S., & Snoeijs, P. 2002. Gradient responses of diatom communities in the Bothnian Bay, northern Baltic Sea. Nova Hedwigia, 74(3-4), 501-525.

Cabrita, M.T. & Brotas, V. 2000. Seasonal variation in denitrification and dissolved nitrogen fluxes in intertidal sediments of the Tagus estuary, Portugal. Marine Ecology Progress Series, 202, pp.51-65.

Cahoon, L.B. 2006. Upscaling primary production estimates: Regional and global scale estimates of microphytobenthos production In: Kromkamp J, de Brouwer JFC, Blanchard GF, Forster RM, Créach V, editors. Functioning of microphytobenthos in estuaries. Royal Netherlands Academy of Arts and Sciences pp. 99-106.

CIS, W. 2003. Guidance Document No. 5–Transitional and Coastal Waters–Typology, Reference Conditions and Classification Systems. Produced by Working Group 2.4–COAST. Office for Official Publications of the European Communities, Luxembourg. ISBN 92-894-5125-4, ISSN 1725-1087.

Clavero, E. 2005. Diatomees d'ambients hipersalins costaners. Taxonomia, distribució y emprentes en el register sedimentary. Barcelona University, Spain.

Cloern, J.E., Abreu, P.C., Carstensen, J., Chauvaud, L., Elmgren, R., Grall, J., Greening, H., Johansson, J.O.R., Kahru, M., Sherwood, E.T. and Xu, J. 2016. Human activities and climate variability drive fast-paced change across the world's estuarine–coastal ecosystems. Global change biology, *22* (2), pp.513-529.

Cunningham, L., Raymond, B., Snape, I. and Riddle, M.J. 2005. Benthic diatom communities as indicators of anthropogenic metal contamination at Casey Station, Antarctica. Journal of Paleolimnology, *33*(4), pp.499-513.

Cunningham, L., Stark, J.S., Snape, I., McMinn, A. and Riddle, M.J. 2003. Effects of metal and petroleum hydrocarbon contamination on benthic diatom communities near Casey Station, Antarctica: an experimental approach. Journal of phycology, 39(3), pp.490-503.

Daniel, G. F., Chamberlain, A. H. L., & Jones, E. B. G. 1987. Cytochemical and electron microscopical observations on the adhesive materials of marine fouling diatoms. British phycological journal, 22(2), 101-118.

Decho, A.W. 2000. Microbial biofilms in intertidal systems: an overview. *Continental Shelf Research* 20: 1257-1273.

Delgado, M., De Jonge, V. N., & Peletier, H. 1991. Effect of sand movement on the growth of benthic diatoms. Journal of Experimental Marine Biology and Ecology, 145(2), 221-231.

Delgado, C., Pardo, I., & García, L. 2012. Diatom communities as indicators of ecological status in Mediterranean temporary streams (Balearic Islands, Spain). Ecological Indicators, 15(1), 131-139.

Dahl, B., Blanck, H. 1996. Toxic effects of the antifouling agent Irgarol 1051 on periphyton communities in coastal water microcosms. Marine Pollution Bulletin 32: 342-350.

Elias, C.L., Calapez, A.R., Almeida, S.F.P., Feio, M.J. 2015. From perennial to temporary streams: an extreme drought as a driving force of freshwater communities' traits. Marine and Freshwater Research 66: 469–480.

Ferreira, J.G., Andersen, J.H., Borja, A., Bricker, S.B., Camp, J., Da Silva, M.C., Garcés, E., Heiskanen, A.S., Humborg, C., Ignatiades, L. and Lancelot, C. 2011. Overview of eutrophication indicators to assess environmental status within the European Marine Strategy Framework Directive. Estuarine, Coastal and Shelf Science, 93(2), pp.117-131.

Feyrer, F., Cloern, J.E., Brown, L.R., Fish, M.A., Hieb, K.A., Baxter, R. 2015. Estuarine fish communities respond to climate variability over both river and ocean basins. Global Change Biology, 21, 3608–3619.

Frankovich, T.A., Gaiser, E.E., Zieman, J.C., & Wachnicka, A.H. 2006. Spatial and temporal distributions of epiphytic diatoms growing on Thalassia testudinum Banks ex König: relationships to water quality. Hydrobiologia 569: 259–71.

Frankovich, T.A., Armitage, A.R., Wachnicka, A.H., Gaiser, E.E. & Fourqurean, J.W. 2009. Nutrient effects on seagrass epiphyte community structure in Florida Bay. Journal of Phycology 45: 1010-1020.

Frankovich, T.A. & Wachnicka, A. 2015. Epiphytic Diatoms along Phosphorus and Salinity Gradients in Florida Bay (Florida, USA), an Illustrated Guide and Annotated Checklist. Microbiology of the Everglades Ecosystem, p.241.

Ghai, R., Hernandez, C.M., Picazo, A., Mizuno, C.M., Ininbergs, K., Díez, B., Valas, R., DuPont, C.L., McMahon, K.D., Camacho, A. and Rodriguez-Valera, F. 2012. Metagenomes of Mediterranean coastal lagoons. Scientific reports, 2.

Gilabert, J., 2001. Seasonal plankton dynamics in a Mediterranean hypersaline coastal lagoon: the Mar Menor. Journal of Plankton Research, 23(2), pp.207-218.

Hudon, C. & Legendre, P. 1987. The ecological implications of growth forms in epibenthic diatoms. Journal of Phycology, 23(3), pp.434-441.

Hynes, H.B.N, 1970. The Ecology of Running Waters. Liverpool University Press, Liverpool.

Ivorra, N., Hettelaar, J., Kraak, M.H.S., Sabater, S., Admiraal, W. 2002. Responses of biofilms to combined nutrient and metal exposure. Environ. Toxicology and Chemisty 21: 626-632.

Lee, R. E. 2008. Phycology. 4 th Edition. Cambridge University Press, Cambridge, UK.

Lind, J. L., K. Heimann, E. A. Miller, C. van Vliet, N. J. Hoogenraad, & Wetherbee, R. 1997. Substratum adhesion and gliding in a diatom are mediated by extracellular proteoglycans. Planta.203:213–221.

Linton, D.M. & Warner, G.F. 2003. Biological indicators in the Caribbean coastal zone and their role in integrated coastal management. Ocean & Coastal Management, 46(3), pp.261-276.

Kelly, M.G. & Whitton, B.A. 1995. The trophic diatom index: a new index for monitoring eutrophication in rivers. Journal of Applied Phycology, 7(4), pp.433-444.

Kjerfve, B. & Magill, K.E. 1989. Geographic and hydrodynamic characteristics of shallow coastal lagoons Marine Geology, 88 (3–4) (1989), pp. 187-199.

Kociolek, J.P. 2005. Taxonomy and ecology: Further considerations. Proceedings of the California Academy of Sciences 56:97-187.

Kociolek, J.P., Stoermer, E.F. 2001. Opinion: Taxonomy and Ecology: a marriage of necessity. Diatom Research 16:433-442

MacIntyre, H. L., Geider, R. J., & Miller, D. C. 1996. Microphytobenthos: the ecological role of the "secret garden" of unvegetated, shallow-water marine habitats. I. Distribution, abundance and primary production. *Estuaries*, *19*(2), 186-201.

Magalhães, C. M., Bordalo, A. A., & Wiebe, W. J. 2003. Intertidal biofilms on rocky substratum can play a major role in estuarine carbon and nutrient dynamics. Marine Ecology Progress Series, 258, 275-281.

Majewska, R., Gambi, M.C., Totti, C.M., Pennesi, C. and De Stefano, M. 2013. Growth form analysis of epiphytic diatom communities of Terra Nova Bay (Ross Sea, Antarctica). Polar Biology, 36(1), pp.73-86.

Marcel, R., Berthon, V., Castets, V., Rimet, F., Thiers, A., Labat, F. and Fontan, B. 2017. Modelling diatom life forms and ecological guilds for river biomonitoring. Knowledge & Management of Aquatic Ecosystems, (418), p.1.

Marín-Guirao, L., Atucha, A.M., Barba, J.L., López, E.M. and Fernández, A.J.G. 2005. Effects of mining wastes on a seagrass ecosystem: metal accumulation and bioavailability, seagrass dynamics and associated community structure. Marine Environmental Research, 60(3), pp.317-337.

Marín-Guirao, L., Lloret, J., Marín, A., Garcia, G., Garcia Fernández, A.J. 2007. Pulse-discharges of mining wastes into a coastal lagoon: Water chemistry and toxicity. Chemistry and Ecology. 23: 217-231.

Marín-Guirao, L., Lloret, J., Marín A. 2008. Carbon and nitrogen stable isotopes and metal concentration in food webs from a mining-impacted coastal lagoon. Science of the Total Environment. 393: 118-130.

McIntire, C.D., Moore, W.W. 1977. Marine litoral diatoms: ecological considerations. In: Werner D (ed) The Biology of Diatoms. Blackwell Scientific Publications, Oxford, p 333-371

Medley, C.L., Clements, W.H. 1998. Responses of diatom communities to heavy metals in streams: the influence of longitudinal variation. Ecolological Applications, 8, 631e644.

Passy, S.I. 2007. Diatom ecological guilds display distinct and predictable behavior along nutrient and disturbance gradients in running waters. Aquatic Botany. 86: 171-178.

Pérez-Ruzafa, A., Gilabert, J., Gutiérrez, J.M., Fernández, A.I., Marcos, C., Sabah, S. 2002. Evidence of a planktonic food web response to changes in nutrient input dynamics in the Mar Menor coastal lagoon, Spain. Hydrobiologia, 475/476, 359-369.

Potapova, M.G., Charles, D.F., Ponader, K.C. and Winter, D.M. 2004. Quantifying species indicator values for trophic diatom indices: a comparison of approaches. Hydrobiologia, 517(1), pp.25-41.

Quigley, M.S., Santschi, P.H., Hung, C.C., Guo, L.D., Honeyman, B.D. 2002. Importance of acid polysaccharides for Th-234 complexation to marine organic matter. Limnology and Oceanography. 47: 367-377

Ravizza, M. and Hallegraeff, G. 2015. Environmental conditions influencing growth rate and stalk formation in the estuarine diatom Licmophora flabellata (Carmichael ex Greville) C. Agardh. Diatom research, 30 (2), pp.197-208.

Renzi, M., Roselli, L., Giovani, A., Focardi, S.E., Basset, A. 2014. Early warning tools for ecotoxicity assessment based on Phaeodactylum tricornutum. Ecotoxicology 23, 1055-1072.

Ribeiro, L.L.C.S. 2010. Intertidal benthic diatoms of the Tagus estuary: taxonomic composition and spatial-temporal variation. phD Thesis.

Ribeiro, L., Brotas, V., Rincé, Y. and Jesus, B. 2013. Structure and diversity of intertidal benthic diatom assemblages in contrasting shores: a case study from the Tagus estuary1. Journal of phycology, 49(2), pp.258-270.

Rimet, F., Bouchez, A. 2011. Use of diatom life-forms and ecological guilds to assess pesticide contamination in rivers: Lotic mesocosm approaches. Ecological Indicators. 11: 489-499.

Robles-Arenas, V.M., Rodríguez, R., García, C., Manteca, J. I., Candela, L. 2006. Sulphide-mining impacts in the physical environment: Sierra de Cartagena–La Unión (SE Spain) case study. Environmental Geology 51, 47–64.

Ros, M. and Miracle, M. R. 1984ª. Distribución temporal de las dinoflageladas del Mar Menor. Analales de Biología. 2, 169–180.

Ros, M. and Miracle, M. R. 1984b. Variación estacional del fitoplancton del Mar Menor y sus relaciones con la de un punto próximo en el Mediterráneo. Limnetica, 1, 32–42.

Round, F.E., Crawford, R.M., Mann, D.G., 1990. The diatoms. Biology and morphology of the genera. Cambridge University Press, New York, Port Chester, Melbourne, Sydney, 747 pp.

Sanz-Lázaro, C., Fodelianakis, S., Guerrero-Meseguer, L., Marín, A. and Karakassis, I. 2015. Effects of organic pollution on biological communities of marine biofilm on hard substrata. Environmental Pollution, 201, pp.17-25.

Smith, D. J., & Underwood, G. J. C. 2000. The production of extracellular carbohydrates by estuarine benthic diatoms: the effects of growth phase and light and dark treatment. Journal of Phycology. 36:321-333

Snoeijs, P. 1993. Intercalibration and distribution of diatom species in the Baltic Sea, Vol 1. Opulus Press, Uppsala

Snoeijs, P., Balashova, J. 1998. Intercalibration and distribution of diatom species in the Baltic Sea, Vol 5. Opulus Press, Uppsala

Snoeijs, P., Vilbaste, S. 1994. Intercalibration and distribution of diatom species in the Baltic Sea, Vol 2. Opulus Press, Uppsala

Soldo, D., Behra, R. 2000. Long-term effects of copper on the structure of freshwater periphyton communities and their tolerance to copper, zinc, nickel and silver. Aquat. Toxicol. 47: 181-189.

Staats, N., Stal, L. J., de Winder, B., & Mur, L. R. 2000. Oxygenic photosynthesis as driving process in exopolysaccharide production of benthic diatoms. Marine Ecology Progress Series, 261-269.

Sullivan, M. J. 1979. Taxonomic Notes on Epiphytic Diatoms of Mississippi Sound, U.S.A. Nova Hed-wigia 64:237, 249.

Sullivan, M. J. 1999. Applied diatom studies in estuaries and shallow coastal environments. In: Sto-ermer, E. F. & Smol J. P. (eds), The Diatoms: Applications for the Environmental and Earth Sciences, pp. 334 -351, Cambridge Univ. Press.

Sullivan, M.J., Moncreiff, C.A. 1990. Edaphic algae are an important component of salt marsh food-webs: evidence from multiple stable isotope analyses. Marine Ecology Progress Series. 62:149–160.

Terrados, J. & Ros, J. 1991. Production dynamics in a macrophyte dominates ecosystem: the Mar Menor coastal lagoon (SE Spain). Oecologia aquatica 10: 255-270.

Tlili, A., Corcoll, N., Bonet, B., Morin, S., Montuelle, B., Bérard, A. and Guasch, H. 2011. In situ spatio-temporal changes in pollution-induced community tolerance to zinc in autotrophic and heterotrophic biofilm communities. Ecotoxicology, 20(8), p.1823.

Tomás, X. 1988. Diatomeas de las aguas epicontinentales saladas del litoral mediterráneo de la Penínnsula Ibérica. phD. Thesis. University of Barcelona, Spain.

Trobajo, R. 2007 Ecological analysis of periphytic diatoms in Mediterranean coastal wetlands (Empordá wetlands, NE Spain). Diatom Monographs. A.R.G.Gantner Verlag, Ruggell.

Trobajo, R., Quintana, X.D., Sabater, S. 2004. Factors affecting the periphytic diatom community in Mediterranean coastal wetlands (Emporda wetlands, NE Spain). Archiv Fur Hydrobiologie 160: 375-399.

Ulanova, A., & Snoeijs, P. 2006. Gradient responses of epilithic diatom communities in the Baltic Sea proper. Estuarine, Coastal and Shelf Science, 68(3), 661-674.

Underwood, G.J.C., Kromkamp, J. 1999. Primary production by phytoplankton and microphytobenthos in estuaries. Advances in Ecological Research 29:93-153

Van Dam, H., Mertens, A. and Sinkeldam, J. 1994. A coded checklist and ecological indicator values of freshwater diatoms from the Netherlands. Aquatic Ecology, 28(1), pp.117-133.

Wachnicka, A., Gaiser, E., Collins, L. & Boyer, J. 2010. Distribution of diatoms and development of diatom-based models for inferring salinity and nutrient concentrations in Florida Bay and adjacent coastal wetlands of south Florida (USA). Estuaries and Coasts 33: 1080-1098.

Wang, Y., Lu, J., Mollet, J.C., Gretz, M.R. and Hoagland, K.D. 1997. Extracellular matrix assembly in diatoms (Bacillariophyceae)(II. 2, 6-Dichlorobenzonitrile inhibition of motility and stalk production in the marine diatom Achnanthes longipes). Plant Physiology. 113(4), pp.1071-1080.

Wetzel, R. G. 2001.Limnology: lake and river ecosystems. Academic Press, San Diego

Chapter 1

Morphology and molecular phylogeny of *Hyalosynedra lanceolata* sp. nov. and extended description of *Hyalosynedra* (Bacillariophyta)

Introduction

Some studies on the phylogenetic relationship and diversity of marine diatoms have lately appeared (e.g. Li *et al*., 2015; Theriot *et al*., 2015; Li *et al*., 2016). Benthic marine species, however, are still poorly known everywhere, even in the Mediterranean Sea, where several new species have been described in recent years (Car *et al*., 2012; Álvarez-Blanco & Blanco 2014; Lobban *et al*., 2015; Belando *et al*., 2016; Carballeira *et al*., 2017). In particular, very little attention has been paid to the hypersaline coastal systems that lodge fairly diverse and relatively unknown communities (Tomás 1988; Clavero 2005; Belando *et al*., 2017). The araphid diatom genus *Hyalosynedra* is a worldwide distributed common component of marine benthic communities that grows as epiphytic and also colonises hard substratum like rocks (e.g. Round *et al*.*„* 1990; Álvarez-Blanco & Blanco 2014). It was one of the seven genera that derived from the division of *Synedra*: *Catacombas*, *Hyalosynedra*, *Tabularia*, *Ctenophora*, *Neosynedra, Synedropsis* and *Ulnaria*. These genera were clearly separated by their morphological grounds, and some authors have also indicated that several *Synedra* species with indiscernible ornamentation under a light microscope (LM) probably belong to the genus *Hyalosynedra* (Round *et al*.*„* 1990; Williams & Round 1986).

Until quite recently, *Hyalosynedra* was regarded as monospecific with *H. laevigata* (Grunow) Williams & Round as the only species. Currently, it comprises four species: three transferred from *Synedra, H. laevigata*, *H. hyalina* (Grunow) Álvarez-Blanco & Blanco, and *Hyalosynedra toxoneides* (Castracane) Perez Coca, Chang, Wang & Wang, plus the recently described *H. sublaevigata* Álvarez-Blanco & Blanco. Most of these nomenclatural changes are based mainly on morphological characters, and only Coca *et al*. (2016) have used molecular data to propose the transfer of *Synedra toxoneides* (Castracane) to *Hyalosynedra*.

Recent phylogenetic studies that have involved large numbers of the araphid pennate genus have shown how *Hyalosynedra* clusters in the same clade of species with rimoportulae that belong to the Fam. Flagilariaceae, including: *Tabularia*, *Catacombas*, *Ulnaria*, *Synedropsis*, *Grammonema*, *Ctenophora* and *Centronella* (Li *et al*., 2015; Li *et al*., 2016). However, these studies only include one *Hyalosynedra* strain, but not *Synedra toxoneides* and *Thalassionema* spp, which have been found to be closely related to *Hyalosynedra* in other previous works (Medlin *et al*., 2008; Kooistra *et al*., 2009; Lobban & Ashworth 2014). Coca *et al*. (2016) recently proposed transferring *Synedra toxoneides* to the genus *Hyalosynedra,* but it is clustered as a sister group with *Thalassionema* in other studies (Medlin *et al*., 2008; Kooistra *et al*., 2009). Since only one strain or two of *Hyalosynedra* have been included in these previous phylogenetic trees, and given the variability in the results reported in different studies, the relationship among these groups remains uncertain. Moreover, very few of these taxa have been morphologically studied in detail. Hence much remains to be investigated before we can unravel the relationship that connects these araphid genera.

While an extensive study was being done of epiphytic diatom communities from the hypersaline Mar Menor coastal lagoon (Belando *et al*., 2017), we found specimens of a strain that potentially belongs to the genus *Hyalosynedra*, but did not match any *Hyalosynedra* species description, and other taxa seem to be *H. toxoneides,* but did not match exactly the diagnosis of the genus. Based on morphologic and phylogenetic research, we aimed to assess whether the strain found in the Mar Menor corresponded to a new *Hyalosynedra* species*,* and the interspecific phylogenic relationship both within the genus and with closely related genera.

Materials and methods

Study area, sampling and sample processing

Samples were collected from two Mar Menor lagoon sites (Murcia Region, SE Spain), which is one of the largest hypersaline coastal lagoons in the Mediterranean Sea. In this shallow system (mean depth of 3.5 m, 7 m

maximum), temperature ranges from 10-31ºC, and salinity from 42-47. Despite its protection at regional, national and international levels, it is subjected to several pressures that derive from human activities: discharges of metals and pharmaceuticals through ephemeral streams, diffuse pollution from agriculture fields and tourism-related impacts (e.g. Marín-Guirao *et al*., 2007; Moreno-Gonzalez *et al*., 2014). The predominant macrophytes at the sampling sites were *Cymodocea nodosa,* which forms monospecific or mixed meadows with *Caulerpa prolifera*, and other macroalgae such as *Cladophora dalmatica*.

The samples used to conduct the morphological study of *H. lanceolata* and *H. toxoneides* were collected from *C. nodosa* leaves at a depth of 0.3-1 m in July 2008 and July 2012. Several extra samples were collected from the leaves of *C. nodosa* and *C. dalmatica* from January to September in different years (2009-2012). Biological samples were taken at a relatively unaltered site (El Ciervo Island, 37º39.595´ N, 00º44.435´ W) and a contaminated one (El Beal wadi, 37º39.975´ N, 00º48.750´ W). The physico-chemical background of the water at the sampling sites is summarised in a more general study (Belando *et al*., 2016). *Hyalosynedra lanceolata* was isolated in culture in July 2012. Cells were isolated with micropipettes under an inverted microscope in f/2 culture medium (SAG Culture Collection). Cultures were maintained at 20 °C in a photoperiod of 16:8 light-dark and 35 µmol photons m^{-2} s^{-1} (PAR).

Morphological observations

The morphological characterisation of both taxa was based on individuals of natural populations, and on H. lanceolata cultures. The colonies and chloroplasts of live cells of H. lanceolata, and also the cleaned material of both taxa, were examined by light microscopy (Leica DMRB, Wetzlar, Germany). The field and cultured material were cleaned with 33% H_2O_2 solution (70 ºC, 2 h), filtered (0.2 µm nylon membrane filter, MILLIPORE), washed with distilled water and resuspended in 96% ethanol solution. For the LM observations, the cleaned material was air-dried on glass cover slips, and permanent slides were mounted using Naphrax (refractive index 1.69, Brune Microscopes Ltd, UK). A Leica DC-500 camera was employed for the light micrographs. For scanning electron microscopy, the glass cover slips with the cleaned material of each taxon were mounted on stubs and were gold-/palladium-coated. Electron micrographs were taken with a JEOL-6100 scanning electron microscope (SEM).

Molecular methods

Hyalosynedra lanceolata DNA was extracted from the pelleted culture material by the CTAB extraction method described by Doyle & Doyle (1987), and was stored frozen at -20 ºC until the PCR reaction was carried out. For the phylogenetic analysis, the nuclear-encoded small subunit ribosomal DNA (SSU rDNA), and the large subunit of RUBISCO (*rbc*L) of the chloroplast, were amplified. The primers used for amplification and sequencing were selected from Alverson *et al*. (2007): SSU (primers SSU 1+ / 568-, 301+ / 1147-, 1004+ / ITS D-); *rbc*L (*rbc*L 66+ / *rbc*L 1255-). Amplification reactions were conducted in 50-µl volumes, which contained approximately 20 ng of genomic DNA, 0.2 mM of each dNTP, 2.5 mM of $MgCl_2$, 2 units of Taq polymerase (Biotools, Madrid, Spain), the buffer provided by the manufacturer, the combinations of primers at a final concentration of 0.4 mM, and ddH_2O to the final volume. Polymerase chain reactions (PCR) were performed in a thermocycler (Eppendorf mastercycler gradient, Hamburg, Germany) according to the following programme, as outlined in Alverson *et al*. (2007): 94 ºC for 3:30 min, 35 cycles of 94 ºC for 50 s, 53 ºC for 50 s, and 1 min at 72 ºC. A final 8-minute step at 72 ºC was included to terminate the amplification products. Finally, 2 ml of the amplification products were visualised on 1.5% agarose gel and successful amplifications were cleaned with the GenElute PCR clean-up kit (Sigma Aldrich). For sequencing, the purified PCR products were reacted with the BigDye terminator cycle sequencing ready reaction (Applied Biosystems, Foster City, California) using the amplification primers.

Phylogenetic analysis

Maximum likelihood (ML) and Bayesian inference (BI) analyses were performed with 56 SSU rDNA, and the 51 *rbc*L sequences, including the taxa related with *Hyalosynedra* in previous phylogenetic studies, and also selected by BLAST. Two *Bolidomonas pacifica* strains were used as the outgroup in accordance with previous araphid diatoms phylogenetic trees (e.g. Li *et al*., 2015). The Genbank accession numbers of all the taxa are listed in Table Ap1 1.

Sequences were checked for inaccurate base calling using Chromas Lite, v. 2.01 (Technelysium Pty. Ltd.). The consensus sequences of the *rbc*L gene fragments were aligned with CLUSTALX (Thompson *et al*., 1997), and the SSU rDNA sequence alignments were performed with the SSU-Align package (Nawrocki 2009; Nawrocki *et al*., 2009). SSU-Align performs secondary structure alignments based on the covariance model (CM) (Cannone *et al*., 2002; Alverson *et al*., 2007; Theriot *et al*., 2009). Sequences were aligned to the consensus CM of Eukarya, integrated into the SSU-Align package. The alignment columns with a low posterior probability (PP), which generally corresponded to large loops for which positional homology and covarying nucleotides were not easy to assign, were removed by the SSU-Mask routine from the SSU-Align package. Bioedit (Hall, 1999) was employed to make minor manual adjustments of alignments. Bayesian analyses were performed using MrBayes, v. 3.1 (Ronquist & Huelsenbeck, 2003). Two simultaneous runs were initiated by starting from random trees. To ensure that the two runs converged onto a stationary distribution, analyses were run until the average standard deviation of the split frequencies was 0.01. Convergence was evaluated using the potential scale reduction factor (PSRF), and 1,000,000 generations were run by sampling every 100^{th} generation with the following settings: Nst = 6, rates = gamma. Burnin (the number of starting generations discarded from further analyses) was set at 200,000 generations after visually inspecting the likelihood values in Excel. A 50% majority rule consensus tree was constructed using the "sumt" command of MrBayes.

ML phylogenetic trees were conducted with 1000 bootstrap replicates using the rapid Bootstrap analysis in RAxMLGUI v.1.5b1 (Silvestro & Michalak, 2012). The best-scoring ML trees were chosen as the final trees and bootstrap values were added to nodes. Both analyses were performed with GTR + G (general time reversible model of DNA substitution), because it was selected as the optimal evolution model for the two genes by JModeltest (Guindon & Gascuel, 2003; Darriba *et al*., 2012). Trees were edited with Figtree, v.1.3.

Given the uncertainty of the relationship of *Synedra toxoneides* (*=Hyalosynedra toxoneides)* with *Hyalosynedra* and *Thalassionema*, we investigated the hypothesis of monophyly of *S. toxoneides* with both these genera. RAxMLGUI was used to generate ML trees from the unconstrained data set and two constrained trees (*S. toxoneides + Hyalosynedra* or *S. toxoneides* + *Thalassionema*). The probability that the monophyly hypothesis was as likely as the unconstrained ML tree showed herein was tested by calculating per-site log likelihood values using RAxMLGUI, and by implementing the AU test in the Consel programme (Shimodaira & Hasegawa, 2001). In the AU test, the analysed tree topology was compared with a set of trees generated by a multiscale bootstrap technique of per site log likelihoods. If the tested tree topology falls outside the 95% confidence interval of the generated trees, the hypothesis can be rejected (if $p<0.05$).

The uncorrected p-distances of the SSU rDNA data set were also used to study genetic divergences among species, which were calculated with MEGA 7 (Kumar *et al*., 2016).

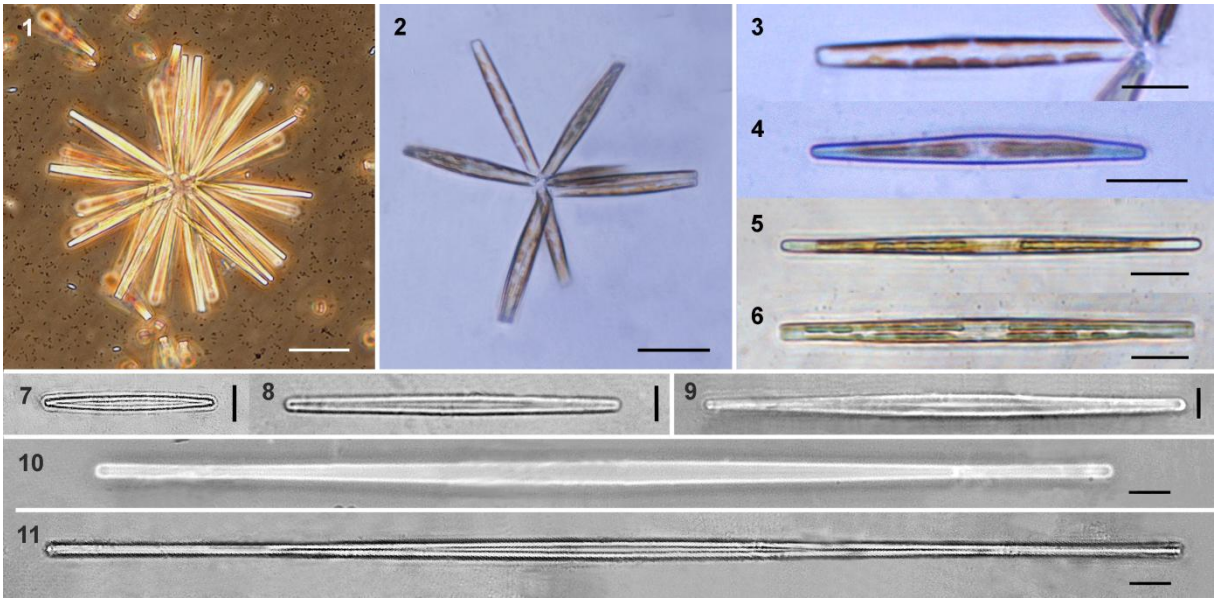

Plate 2. Figs. 1-11. Light microscopy micrographs of *Hyalosynedra lanceolata* sp. nov. **Figs. 1-6**. Colonies and chloroplasts in live cells**. Figs. 7-11**. Cleaned specimens showing the lanceolate sternum and the wide cell size range. Scale bars: **Figs. 1-2** = 40 µm, **Figs. 3-6** = 20 µm, **Figs. 7-11** = 5 µm.

Results

Species description

***Hyalosynedra lanceolata* Belando, Jiménez & Aboal sp. nov.**

DIAGNOSIS: Cells forming radiate colonies attached to substrata by a mucilage pad. Two long lobed laminar chloroplasts covering the whole length of the cell. Valves linear to linear-lanceolate with rounded poles and lanceolate sternum. Frustules 20.7-266 µm long, 1.3-3.7 (4.0-5.5) µm width at the centre, and 1.0-2.7 in the apices. 47-52 biseriate parallel striae in 10 µm. Striae uninterrupted at the junction of the valve face and mantle margin. Striae open externally by two rows of alternate pores, and internally by a rounded foramen. Valve ends with plain areas and lateral poroids where the striation ceases. One rimoportula at each pole of the valve, rounded externally and "parrot beak-like" internally. Apical pore field type ocellulimbus composed of three rows of poroids which are larger than pores of striate, and with a few small spines overhanging it. Internally smooth valves, with slightly depressed apices and pores at both sides of the rimoportula. Cingulum composed of two copula and a pleura with a single row of poroids.

GENBANK SEQUENCES: KY679465 (SSU rDNA), KY679464 (*rbc*L).

HOLOTYPE: permanent slide of natural material deposited at the Herbarium Universitatis Murcicae-Bacillariophyta, Spain, MUB-ALGAS (Diatomeas) 2785. Coll. Belando, M.D., in the Mar Menor lagoon (SE Spain), July 2012.

TYPE STRAIN: HyaLan-MMen. Cultures are available in the Department of Botany at the University of Murcia (Spain). Aboal, M.

TYPE LOCALITY: El Ciervo Island (37º39.595´N, 00º44.435´W) from the Mar Menor lagoon (SE Spain), at a depth of 0.4 m.

ECOLOGY: Epiphyte on *Cymodocea nodosa* and macroalgae as *Cladophora dalmatica* in hypersaline coastal waters. It is abundant in summer (25-28ºC) in locations far from the influence of metal and nutrient contamination. In a more general study, the seawater background of the type locality was characterised by: salinity 44.2, pH=8.1, dissolved O_2 = 8.22 mg · L^{-1}, NO_3^- and PO_4^{3-}= 2.9±0.39 and <1.05 µmol · L^{-1} respectively, and Zn and Pb = <0.45 and 3.01±2.80 µg · L^{-1} respectively. For further details, see Belando *et al*. (2017).

ETYMOLOGY: from Latin lanceolatus, refers to the lanceolate form of sternum.

DESCRIPTION: The two long lobed chloroplasts lie against the girdles along the whole length of the cell (Plate 2 Figs. 1-3), they may split up in unhealthy material, giving the impression of numerous discoid chromatophores (Plate 2 Figs. 4-6). Under LM the lanceolate sternum is a white line that becomes fainter in the apices (Plate 2 Figs. 7-11). Cells hyaline, and in the internal view the depressed zone of the apex appear obscure (Plate 2 Fig. 10). The wide range of cell sizes found in the field (20.7-266 µm) is persistent in cultures, but cultured cells are wider in the centre (4.0-5.5 µm). Large cells tend to be linear, while smaller ones are linear-lanceolate (Plate 3 Figs. 12-17). Cells tend to decrease to the minimum size when they are long time in cultures, according to the asexual reproduction process. Recovery of the largest size (Plate 3 Fig. 14) was observed as a fast and synchronized process in which most of cultured cells reached the largest size during one or two days, and small ones died. Auxospores have not been observed. The lanceolate sternum can reach up 1/3 of the valve width in the centre (Plate 4 Fig. 18). The areolae are usually broken appearing elongate and oblique to the transapical axis. The rounded external apertures of rimoportulae are located at the end of the striation (Plate 4 Figs. 19-20), and the internal opening is in a depressed area with a peak-like appearance in most cases (Plate 4 Fig. 21), but also by two almost parallel lips (Plate 4 Fig. 22). The ocelullimbus is formed by three rows of pores, larger than pores of areolae, and three or four small spines overhanging it at each apex (Plate 4 Fig. 20). Valves are structureless internally, except for the small pores connecting the valve chambers (Plate 4 Figs. 21-22). The cingulum consists in a serie of alternating, imcomplete and ligulate bands (Plate 4 Fig. 25). It is formed by a plain valvocopula, a copula (similar in structure but shorter), and by much narrower pleura with a single row of poroids (Plate 4 Figs. 23-25).

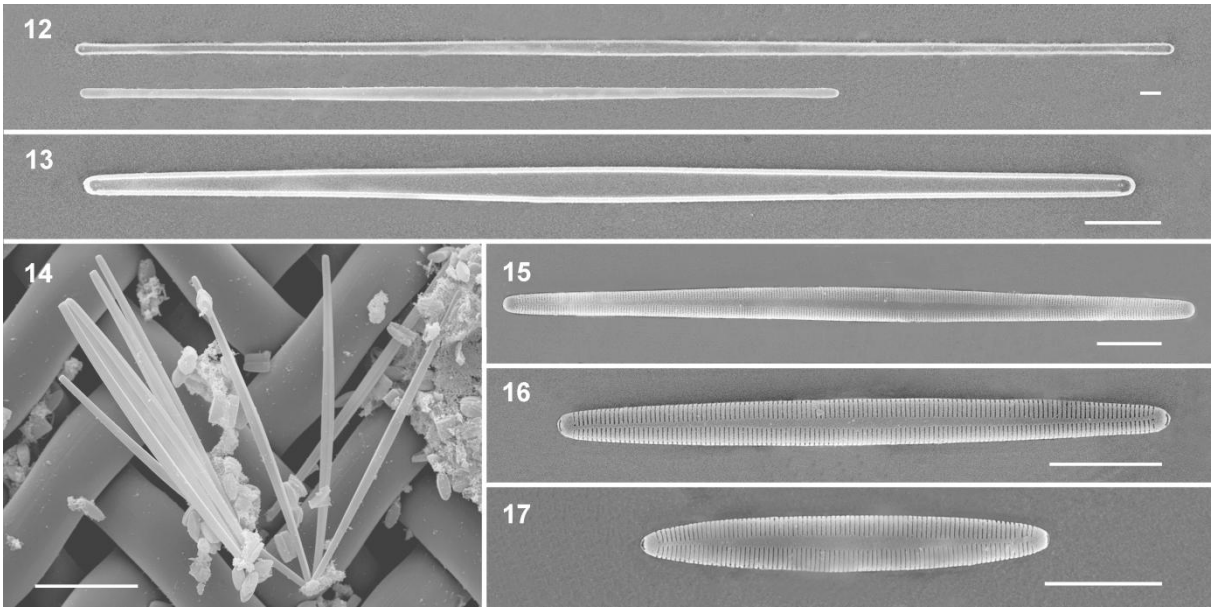

Plate 3. Figs. 12-17. Scanning electron micrographs of *Hyalosynedra lanceolata* sp. nov. **Fig. 12.** Giant cells (200-300 µm long) with almost linear valves. **Fig. 13.** Internal view of valves, less than 100 µm long and with a lineal-lanceolate shape. **Fig. 14.** Colony of large cells and very small others showing the wide cell size range in culture. **Figs. 15-17.** Cleaned specimens showing the lanceolate sternum. All scale bars = 5 µm, except **Fig. 14** = 50 µm.

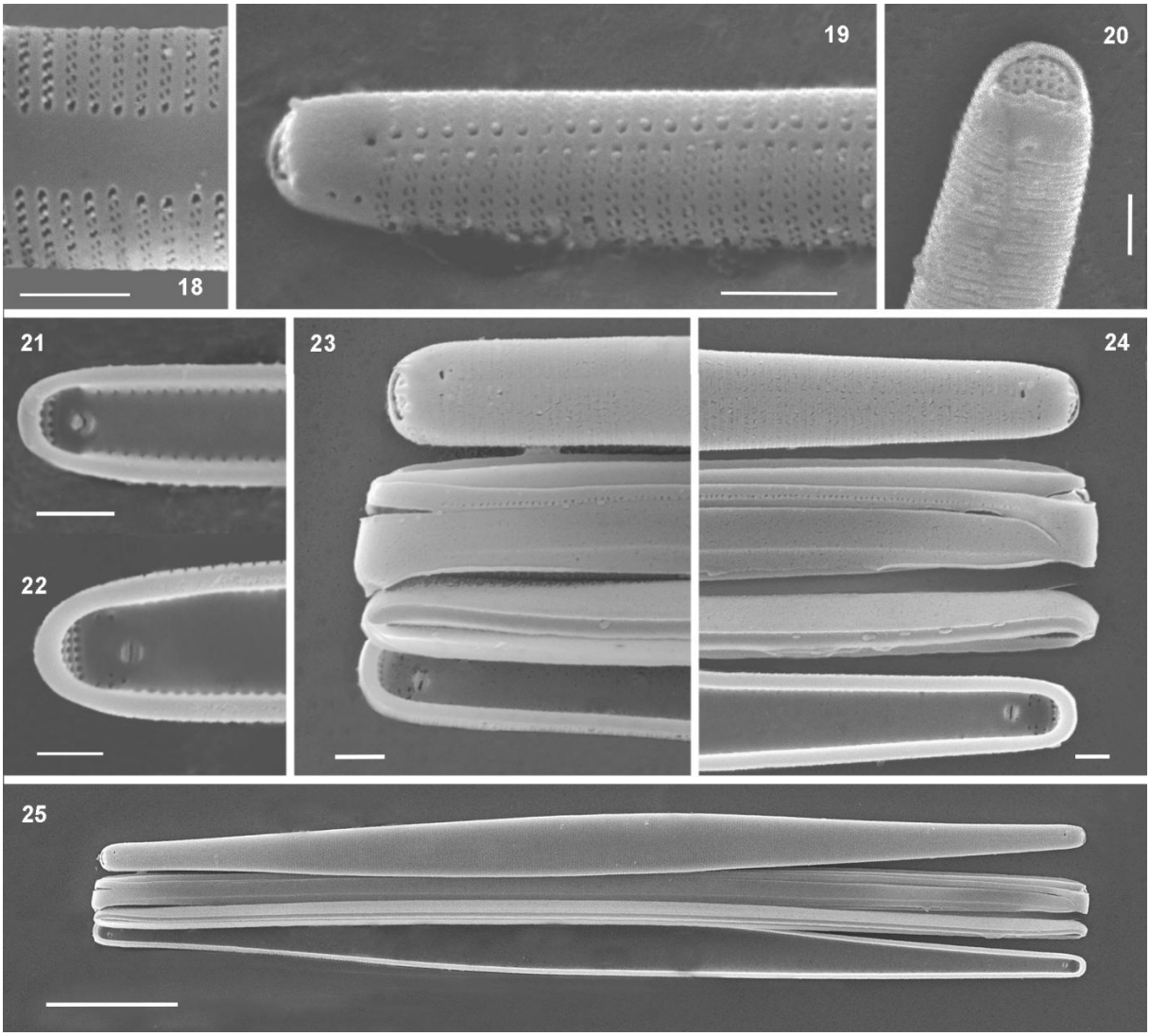

Plate 4. Figs. 18-25. Scanning electron micrographs of *Hyalosynedra lanceolata* sp. nov. **Fig. 18.** Detail of the biseriate striation with alternate areolae and the lanceolate sternum at the centre of valves (up to 1/3 total wide). **Fig. 19.** Apical part of cells showing areolae and thin sternum. **Fig. 20.** Detail of the external openings of rimoportula and the rows of pores in ocellolimbus. **Figs. 21-22.** Internal view of the smooth valves showing small rounded pores on both sides and the apperture of rimoportulae. **Figs. 23-24.** Detail of valvocopula, copula and pleura with a row of pores (one apex at each image). **Fig. 25.** Cingular view of cells with the three girdle bands. Scale bars: **Figs. 18-24**= 1 µm, **Fig. 25**= 10 µm.

COMPARISON WITH *HYALOSYNEDRA* SPECIES*:* The morphological and diagnostic characters of the studied material and *Hyalosynedra* species are summarised in Table 1. It morphologically matches the description of *Hyalosynedra,* except for the lanceolate sternum. The valve shape of the small specimens is similar to *H. laevigata*, but this is broader, has a less dense striation, and the striation has been described as uniseriate where each areola is occluded by a small closing plate with struts orientated on the transapical plane. Under LM, small specimens may also be confused with *H. sublaevigata* (26.5-34.1 length, 2.3-3.0 wide), but it does not fit the biseriate striation, the lanceolate sternum and non-occluded poroids on the valve apex. The valve of *H. hyalina* is strongly lanceolate, with capitately constricted ends.

Table 1. Diagnostic characters of *Hyalosynedra lanceolata* compared with other species of the genus.

Character	*H. lanceolata* sp. nov.	*H. sublaevigata* Álvarez-Blanco & S.Blanco	*H. laevigata* Grunow	*H. hyalina* (Grunow) Álvarez-Blanco & S.Blanco
Mucilage stalk	Mucilage pad	n.d.	n.d.	n.d.
Colony form	Radiate colony	n.d.	n.d.	n.d.
Valve shape	Linear to linear-lanceolate	Linear-lanceolate	Linear-lanceolate	Lanceolate
Poles	Rounded	Rounded	Rounded or tapered	Capitate
Apical spines	Yes	n.d.	Yes	n.d.
Valve length (µm)	20.7-266	26.5-34.1	80-400	40-70
Valve width (µm)	1.3-3.7(4.0-5.5)	2.3-3.0	5-7	4-4.8
Striae in 10 µm	47-53 (biseriate)	50-54	34-38 (uniseriate)	34-38
Sternum	Lanceolate	Narrow, straight	Narrow	Narrow
Rimoportulae per valve	2, one at each pole	2, one at each pole	2, one at each pole	n.d.
Apical pore field	3 rows of poroids	5-6 rows of poroids	3-9 rows of poroids	n.d.
Cingulum structure	Valvocopula, copula and pleura with a single row of poroids	n.d.	Valvocopula, copula and pleura with a single row of poroids	n.d.
Plastids	2 lobed laminar plate-like	n.d.	n.d.	n.d.
Ecology	Epiphyte	Epilithic	Epiphyte	n.d.
References	This study	Álvarez-Blanco & S. Blanco (2014)	Hustedt (1959) Williams & Round (1986)	Hustedt (1959) Álvarez-Blanco & S. Blanco (2014)

Synedra toxoneides Castracane

Synonym: Hyaloynedra toxoneides (Castracane) Perez Coca, Chang, Wang & Wang. Nova Hedwigia, 104.1-2: 1-2 (2017).

DESCRIPTION: Solitary cells or forming radiate colonies. Long cells, narrow, slightly curved towards the ends (Plate 5 Figs 26-27). Valves linear-lanceolate, slightly inflated at the centre and close to the slightly capitate poles (Plate 5 Figs. 26-28). Under LM sternum appeared wide, delimited by the visible striation (Plate 5 Fig. 29). Cells are 221-310 µm long, 2.3-4.0 (4.2) µm wide in the centre and 2.3-2.9 µm in the pole, with 23-25 transapical striae in 10 µm. Biseriate parallel striation with elongated and curved areolae, and one terminal areola, crescent-shaped (Plate 5 Figs. 30-31). Two rows of areolae not interrupted in the valve and mantle junction. Internally the valve is structureless, except for the small rounded openings between the valve face and mantle (Plate 5 Fig. 32). Sternum very wide (1/3 or more of valve width in the centre), slightly tapering towards apices (Plate 5 Fig. 30, Fig. 33). One rimoportula at each pole of valves, opening to the outside by a small pore located in a depressed area (Plate 5 Fig. 33), and internally by two parallel small lips (Plate 5 Fig. 34). 1-3 single pores located at both sides of the unornamented extreme of valves, opening also inside. Apical pore fields consisting in a rectangular grid of pores organized in rows and columns that occupy the whole margin of the ends valve (Plate 5 Fig. 33).

ECOLOGY: Epiphytes on *C. nodosa* and macroalgae, with low abundance in summer in the hypersaline Mar Menor lagoon, 0.4 m depth.

COMPARISON WITH OTHER TAXA AND REMARKS ON ITS INCLUSION IN THE GENUS: It morphologically resembles strain *S. toxoneides* WK57 included in the phylogenetic analysis (personal communication, Kooistra W.H.C.F.), but does not match the description of *Hyalosynedra.* It has no sunken apical pore plate (type ocellulimbus), nor are

spines in the apices as described for the genus. The valve shape of *Hyalosynedra* is linear-lanceolate, and striae are composed of small rows of pores. Areolae are similar to *Tabularia affinis* (Kützing) Snoeijs, but also have the apical pore plate, ocellulimbus-type, but no chambered valves. Because of the long thin shape of *S. toxoneides*, it could be confused with specimens of Fam. Thalassionemataceae (*Thalassionema* Grunow ex Mereschkowsky, *Thalassiothrix* (Grunow) Grunow and *Thrichotoxon* F.M.H.Reid & Round), but these genera have no or a small apical pore field in a single minute pore. *Thalassionema* has areolae with externally bar across them, and spines in the apices. *Thalassiothix* possesses heteropolar valves and spines along the entire valve. The curved shape of *S. toxoneides* coincides with *Trichotoxon,* but is longer (800-3,500 µm) and broader (5-8 µm, mid-section), only has a small pore in the apices (rimoportule aperture), with areolae occluded by cribra, and the striae are located on the valve face, only slightly extended towards the mantle. Internally the valve surface is slightly tabbed, especially in the centre.

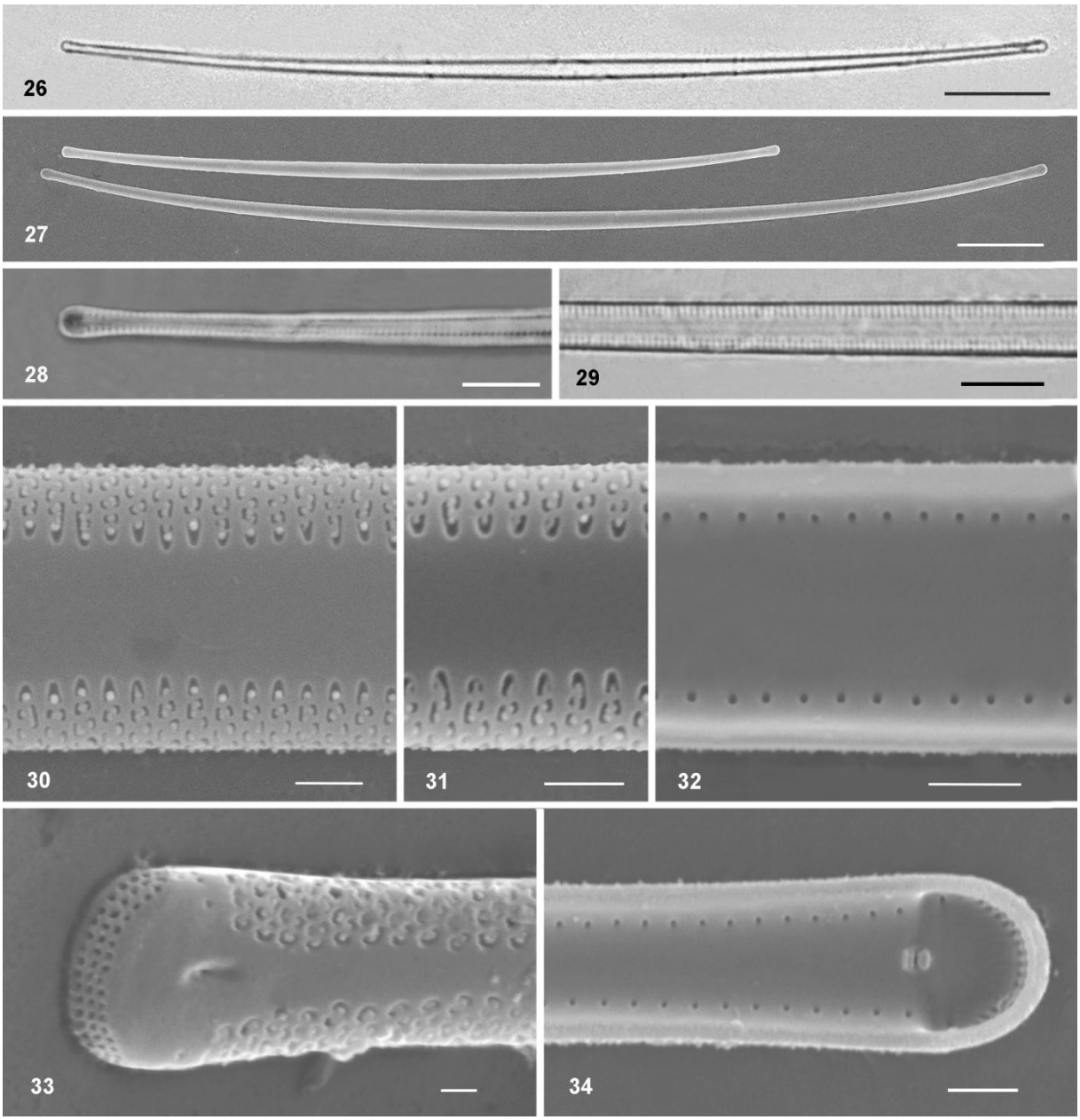

Plate 5. Figs 26-34. Light and scanning electron micrographs of *S. toxoneides* from the Mar Menor lagoon. **Fig. 26.** Hyaline thin and curved cells under LM. **Fig. 27.** SEM micrographs of large curved cell with capitate poles. **Figs. 28-29.** Detail of the visible striation under LM with inmersion oil. **Figs. 30-31.** External view of the wide sternum, striae and areolae. **Fig. 32.** Internal view of valves with rounded pores. **Fig. 33.** External view of rimoportula in a depressed area and a row of pores occupying the whole apex. **Fig. 34.** Internal opening of rimoportulae showing two parallel lips. Scale bars: **Figs. 26-27** =20 µm, **Figs. 28-29**= 5 µm, **Figs. 30-34** =1 µm.

Extended description of the genus *Hyalosynedra* D. M. Williams & F. E. Round (1986)

Some new distinctive morphological characters based on *H. lanceolata* sp. nov are described below to extend the description of *Hyalosynedra* Williams & Round (1986). Radiate colonies, two long chloroplasts lying against the girdles to the valve. Valves linear or linear-lanceolate, with rounded or capitate poles. Sternum narrow connecting both poles or wider lanceolate tapering gradually to the apices. Striae parallel uniseriate or biseriate externally open by one row or two rows of small pores, and internally by small rounded pores.

Type species: *Synedra laevigata* Grunow (1877) p.166, pl. 193, Fig. 3.

Phylogeny results

A concatenated alignment of both the nuclear and plastid regions from 56 taxa yielded 3,035 nucleotide sites (1598 SSU rDNA after masking with SSUalign, 1437 *rbc*L), of which 2,188 were constant, 176 variable, but parsimony-uninformative, and 671 were parsimony-informative. Aligned sequences have been deposited in TreeBase (study accession number XXXX, http://www.treebase.org/treebase/). Both the ML and Bayesian inference searches resulted in trees with a similar topology on each branch. Therefore, the Bayesian posterior probability/ ML bootstrap values (Bpp/MLb) are provided in the same tree for all the analyses. The outgroup taxa have been pruned away from the unconstrained tree, and they have been shown in the supplementary material (Figure Ap1 1, Figure Ap1 2).

The phylogenetic tree (Figure 35.) indicated that all *Hyalosynedra* strains were clustered in a clade that was split into two different branches: the upper branch grouped the strains of *Hyalosynedra* and *Thalassionema, which* were separated by a high support (1.00/95) from a clade that was dichotomically branched several times to cluster the seven sister genera *Tabularia*, *Ctenophora*, *Catacombas*, *Centronella*, *Ulnaria*, *Grammonema* and *Synedropsis.* The new species *Hyalosynedra lanceolata* HyaLan-MMen was separated by a high support (1.00/93) from the two strains of *Hyalosynedra laevigata* (15VI11-2A and GU44AI), and they all constituted a monophyletic clade. This clade was separated by a high support (1.00/84) from the three strains of *Hyalosynedra toxoneides,* which clustered in an unresolved dichotomically branched clade with *Thalassionema* spp (0.82/57).

The most likely tree topologies, inferred from the two gene data sets by RAxML and used in the AU test, had similar log likelihood values for the unconstrained and constrained trees (Table 2). The AU test results returned a $P > 0.05$ for the three tested topologies which, with the current data, does not allow the rejection of the hypothesis that *S. toxoneides* is a monophyletic group with *Thalassionema* or the other *Hyalosynedra* species.

The results for the divergence analysis (Table Ap1 1) showed that the p-distance ranged 1.26-1.79% when compare the three strains of *Hyalosynedra* (*H. lanceolata* and two strains of *H. laevigata*) with *Thalassionema* and *S. toxoneides* stains. The values of divergence among *S. toxoneides* and *Thalassionema* strains were lower and ranged from 0.63-0.94% (0.42 for one species). The interspecific distance ranged 0.63-0.74% if compared *H. lanceolata* and the two strains of *H. laevigata* (0.1% between these two). The p-distance between *S. toxoneides* WK57 and AQ9 or AQ10 was 0.1% or 0.0% respectively. Values of divergence among strains of *Thalassionema* ranged 0.31-0.52%, except for strain 5 and CCMP1100 that had p-distance=0.0%.

Table 2. AU test for the topologically unconstrained (Fig. 35) and constrained trees in the analysis of the monophyly of *S. toxoneides* with *Thalassionema* (Figure Ap1 1) or *Hyalosynedra* (Figure Ap1 2).

Best trees	-lnL	AU (p)	Confidence tree
Unconstrained tree	−20494.76	0.388	yes
Constrained *S. toxoneides+Hyalosynedra* tree	−20493.32	0.467	yes
Constrained *S. toxoneides+Thalassionema* tree	−20493.21	0.607	yes

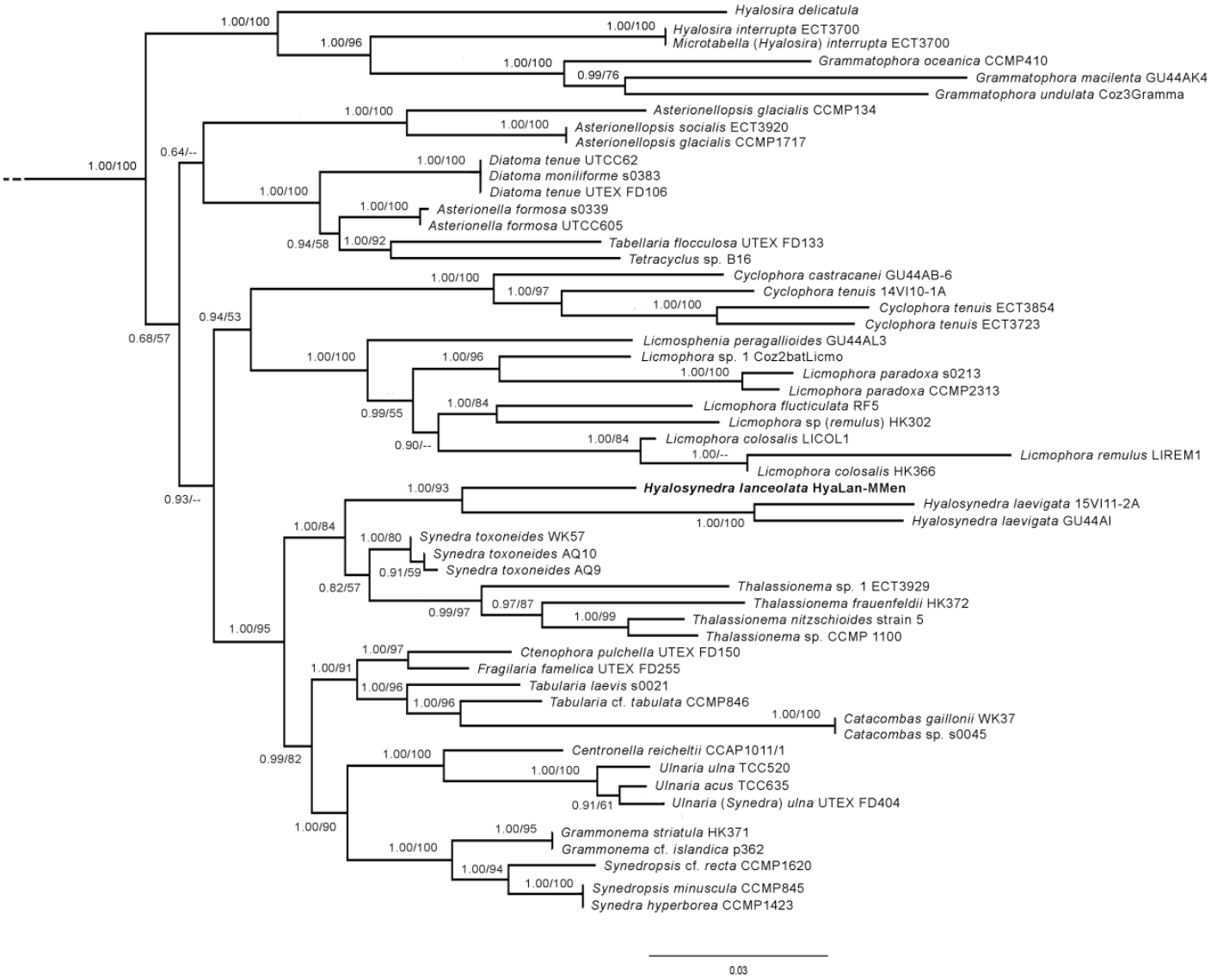

Figure 35. Maximum likelihood tree inferred from a concatenated alignment of SSU rRNA and *rbc*L markers of 56 araphid diatoms. The numbers on the nodes are Bayesian posterior probability/maximum likelihood bootstraps (Bpp/MLb). The newly described species is shown in bold. Any support values lower than 50% were omitted.

Discussion

In this study, we describe the new species *Hyalosynedra lanceolata* Belando, Jiménez & Aboal, based on the general morphological features shared by *Hyalosynedra*, e.g., valve shape, apical field of pores ocellulimbus-type and striae composed of rows of small pores, and molecular data that clearly separated it from the two *Hyalosynedra* strains with which it formed a monophyletic clade. This is the first study that contributes new distinctive characters of live cells of the genus, and the description of *Hyalosynedra* has been extended to include the radiate shaped colonies, the biseriate striation, lanceolate sternum and the two long laminar lobed plastids. The diagnosis of the genus was based on the uniseriate striation of the typus species *H. laevigata*, but in agreement with our proposal, Round *et al*., (1990) have already mentioned that areolae could become smaller and form biseriate rows in the mantle in some (undescribed) *Hyalosynedra* species. Clavero (2005) has also reported a *Hyalosynedra* sp. with a biseriate striation, and has suggested the need to modify the diagnosis of the genus.

Based on the morphological revision of both the described taxa and some strains included in the phylogenetic tree, we highlight that further molecular and SEM studies could provide wider interspecific variability of the genus. We observed that *H. lanceolata* sp. nov. coincides in various morphological features with *Hyalosynedra* sp. described by Clavero (2005) from hypersaline waters in Baja California South. It has a wide-ranging length (22.2-116.1 µm) and width (1.9-4.0 µm), and 45-(48)-53 striae in 10 µm, but is not indicated in any lanceolate sternum. So we cannot ensure that these specimens correspond to *H. lanceolata*. Clavero (2005) has also mentioned the possible confusion of this *Hyalosynedra* sp. with *H. laevigata* var. *angustata* Grunow because, according to Hustedt (1959), the differential character of the variety was a smaller valve (3 µm wide). The structureless and hyaline characters of the *H. lanceolata* valves seen under LM can easily lead to confusion with the aforementioned variety, but no detailed study of its morphology has been published to date as far as we know. Tomás (1988) identified this var. *angustata* in a salt marsh from the Mar Menor lagoon, close to our study site. The cell size range of Tomás' specimens (Lam. 18, Fig. 7) was similar to our material (10.2-204.5 long, 2.0-3.1 wide), with an indiscernible striation under LM (more than 40 striae in 10 µm, according to that author). It is not easy to differentiate the sternum shape (lanceolate or not) in the LM images shown due to the narrowness of cells, but these individuals probably belong to *H. lanceolata*. Overall our findings also indicated that *Hyalosynedra* sp. GU44AI should be named *H. laevigata*. The phylogenetic trees grouped it with *H. laevigata* (strain 15VI11-2A, Bpp/MLb: 1.00/100, 0.11% divergence), and it morphologically matched the description of this species (e.g., 37 striae/10µm), see http://www.protistcentral.org/Taxa/get/taxa_id/586040 (Jordan *et al*., 2009-2017). *Hyalosynedra* cf. *laevigata* (WK52), which was one of the few strains used in previous phylogenetic studies, was grouped with the monophyletic clade of *H. lanceolata* and *H. laevigata* in our preliminary trees. Finally it has not been considered, as it only has SSU rDNA marker available, and its inclusion diminished the resolving power of the analysis. Further research into this strain is recommended.

The morphological and molecular data indicated that *S. toxoneides* does not belong to *Hyalosynedra*, so we propose retaining the name *S. toxoneides* for the time being. The ultrastructure of this taxon has only been studied in detail for two deformed strains (AQ9, AQ10), from which the new combination has been proposed (Coca *et al*., 2016). As far as we know, the present study provides the first detailed description of this taxon, supported by LM and SEM micrographs, and using material found in the Mar Menor lagoon. It morphologically resembles the description of *S. toxoneides* in Hustedt (1959), and also *S. toxoneides* strain WK57 included in phylogenetic trees (material provided by Kooistra, W. H.C.F.). The large, thin and curved valve shape, the rectangular grid of pores (does not sunken in the end of valves) and the coarse striation (visible under LM) do not match the general features of *Hyalosynedra*. With the current data, the phylogenetic trees also support the notion that *S. toxoneides* does not belong *Hyalosynedra*, as the monophyletic clade consisting in *H. lanceolata* and *H. laevigata* was separated by a high support of the three *S. toxoneides* strains.

The phylogeny results also revealed that *S. toxoneides* was more closely related to *Thalassionema* spp, just as some studies have already mentioned (Kooistra *et al*., 2009; Medlin *et al*., 2008). The *S. toxoneides* strains (AQ9, AQ10, WK57) clustered in a different clade to *Thalassionema* spp, but the unconstrained trees showed each one not as a monophyletic group because of the unresolved dichotomy (Bpp/MLb: 84/57). The AU test demonstrated that unconstrained tree (Figure 35) did not significantly differ from the constrained trees (Figure Ap1 1, Figure Ap1 2) in that *S. toxoneides* was monophylectic with *Hyalosynedra* or *Thalassionema*. Therefore, we cannot confidently reject the monophyly of *S. toxoneides* with each one of this genus, our taxon sampling and our molecular data.

Based on the observed morphology, the epiphytic *S. toxoneides* did not match the general characteristics of the planktonic and needle-shaped diatoms that constitute *Thalassionema* and the other genera that belong to the Fam. Thalassionemataceae (*Thalassiothrix* and *Trichotoxon*). The most notable difference was that these genera have no apical pore field or a small one in a single minute pore. *Thalassionema* has areolae with an externally bar across them, and spines in apices, and *Thalassiothix* possesses heteropolar valves and spines along the entire valve, but these characters are not present in *S. toxoneides*. It shares some features of the genus *Thrichotoxon;* e.g. long and thin valves, curved and inflated at the centre and apices, but the valves of *S.*

toxoneides are much smaller, 221-310 µm long *vs.* 800 to 3,500 µm long (Reid & Round 1987; Round *et al*., 1990). The *Trichotoxon* striae present a valve and are constituted by elliptical to quadrate areolae with external criba (Figures 6-8 in Reid & Round, 1987, Figure d in Round *et al*., 1990), but the biseriate rows of areolae in *S. toxoneides* extend to the mantle. The valves of *Trichotoxon* may externally have a few areolae scattered on the valve face and, internally, are slightly ribbed, especially in the central region, while they are not in *S. toxoneides*. The numerous small chromatophores do not coincide with the large plate of *S. toxoneides* (Coca *et al*., 2016).

Overall our morphological findings seem to indicate that *S. toxoneides* could belong to a new different genus as its general features do not match any genera described to date. However, as suggested by Williams & Kociolek (2011), the natural diatom classification should be based on the monophyly concept. As it is not possible to reject the monophyly with *Thalassionema,* we decided to maintain the name of *S. toxoneides* for the time being. Lack of a high support in phylogenetic trees among the dichotomically clades separating both *S. toxoneides* and *Thalassoinema* could be related to the fact that the strains of *S. toxoneides* only had one available sequence (SSUrDNA), that could reduce the resolution power of the analysis. Hence further sequences of these strains and related genera such as *Trichotoxon* could help to elucidate the taxonomic identity of *S. toxoneides* and its relationship with species that belong to the Fam. Thalassionematacea. Therefore, further work is required.

Over the several years that the study lasted, *H. lanceolata* was observed as being epiphytic of *C. nodosa,* at least from January to September. In summer, *H. lanceolata* is one of the dominant species in benthic diatom communities from relatively unaltered sites in the Mar Menor lagoon, while *H. laevigata* exclusively occurred at the historically contaminated site (Belando *et al*., 2017). *S. toxoneides* was not abundant in any sample. The present record is the first of this species in the hypersaline Mar Menor lagoon (Murcia). Tomás (1988) also cited it as *S. toxoneides* in another Spanish hypersaline lagoon (Almería, SE Spain), and it appears to be widely distributed in the Mediterranean Sea (Hustedt 1959; Kooistra *et al*., 2009).

REFERENCES

Álvarez-Blanco, I. and Blanco, S. 2014. Benthic diatoms from Mediterranean coasts. *Acta Botanica Hungarica*, *56*, pp.3-4.ALVERSON, A.J., JANSEN, R.K., & THERIOT, E.C. 2007. Bridging the Rubicon: Phylogenetic analysis reveals repeated colonizations of marine and fresh waters by thalassiosiroid diatoms. Molecular Phylogenetics and Evolution 45: 193-210.

Belando, M.D., Aboal, M., Jiménez, J.F. and Marín, A. 2016. Licmophora colosalis sp. nov.(Licmophoraceae, Bacillariophyta), a large epiphytic diatom from coastal waters. *Phycologia*, *55*(4), pp.393-402.

Belando, M.D., Marín, A., Aboal, M., García-Fernández, A.J., & MARIN-GUIRAO, L. 2017. Combined in situ effects of metals and nutrients on marine biofilms: Shifts in the diatom assemblage structure and biological traits. Science of the Total Environment 574: 381-389.

Cannone, J.J., Subramanian, S., Schnare, M.N., Collet, J.R., D'Souza, L.M., Du, Y.S., Feng, B., Lin, N., Madabusi, L.V., Muller, K.M., Pande, N., Shang,Z.D., Yu,N., & Gutell, R.R. 2002. The Comparative RNA Web (CRW) Site: an online database of comparative sequence and structure information for ribosomal, intron, and other RNAs. Bmc Bioinformatics 3.

Car, A., Witkowski, A., Dobosz, S., Burfeind, D.D., Meinesz, A., Jasprica, N., Ruppel, M., Kurzydłowski, K.J. and Płociński, T. 2012. Description of a new marine diatom, *Cocconeis caulerpacola* sp. nov.(Bacillariophyceae), epiphytic on invasive *Caulerpa* species. European journal of phycology, *47*(4), pp.433-448.

Carballeira, R., Trobajo, R., Leira, M., Benito, X., Sato, S. and Mann, D.G. 2017. A combined morphological and molecular approach to *Nitzschia varelae* sp. nov., with discussion of symmetry in Bacillariaceae. European Journal of Phycology, pp.1-18.

Clavero, E. 2005. Diatomees d'ambients hipersalins costaners. Taxonomia, distribució y emprentes en el register sedimentary. University of Barcelona, Spain.

Perez Coca, J.J., Chang, Y.T., Lai, S.Y., Wang, W.L. and Wang, M.Y. 2017. Artificial culture conditions induce irreversible deformations in *Hyalosynedra toxoneides*. Nova Hedwigia, 104(4), pp.499-519.DARRIBA D, TABOADA, GL., DOALLO, R., POSADA, D. 2012. jModelTest 2: more models, new heuristics and parallel computing. Nature Methods 9: 772.

Doyle, J.J. & Doy, J.L. 1987. A rapid DNA isolation procedure for small quantities of fresh leaf tissue. Phytochemical Bulletin 19: 11-15.

Grunow, A. 1877. New diatoms from Honduras. The Montly Microscopical Journal 18: 165-186.

Guindon, S. & Gascuel, O. 2003. A simple, fast and accurate method to estimate large phylogenies by maximum-likelihood. Systematic Biology 52: 696-704.

Hall, T.A. 1999. BioEdit: a user-friendly biological sequence alignment editor and analysis program for Windows 95/98/NT. Nucleic Acids Symposium Series 41: 95-98.

Hustedt, F. 1959. Bemerkungen über die Diatomeen flora des Neusiedler Sees und des Salzlackengebietes. In *Landschaft Neusiedler See* (23) (Burgenland., W.A., editor), 180-240.

Jordan, R.W., Lobban, C.S. & Theriot, E.C. 2009-2017. Western Pacific Diatoms Project.ProtistCentral. http://www.protistcentral.org. Revised in 2017.

Kooistra, W.H., Forlani, G. and De Stefano, M. 2009. Adaptations of araphid pennate diatoms to a planktonic existence. Marine Ecology, 30(1), pp.1-15.

Kumar, S., Stecher, G. and Tamura, K. 2016. MEGA7: Molecular Evolutionary Genetics Analysis version 7.0 for bigger datasets. Molecular biology and evolution, 33(7), pp.1870-1874.

Li, C. L., Ashworth, M. P., Witkowski, A., Dąbek, P., Medlin, L. K., Kooistra, W. H., ... & Sabir, J. S. 2015. New insights into Plagiogrammaceae (Bacillariophyta) based on multigene phylogenies and morphological characteristics with the description of a new genus and three new species. PloS one, 10(10), e0139300.

Li, C.L., Ashworth, M.P., Witkowski, A., Lobban, C.S., Zgłobicka, I., Kurzydłowski, K.J. and Qin, S. 2016. Ultrastructural and molecular characterization of diversity among small araphid diatoms all lacking rimoportulae. I. Five new genera, eight new species. Journal of phycology, 52(6), pp.1018-1036.

Lobban, C.S., Ashworth, M.P. 2014. *Hanicella moenia*, gen. et sp. nov., a ribbon forming diatom (Bacillariophyta) with complex girdle bands, compared to *Microtabella interrupta* and *Rhabdonema* cf. adriaticum: implications for Striatellales, Rhabdonematales, and Grammatophoraceae, fam. nov. Journal of Phycology 50: 860-884.

Lobban, C.S., Ashworth, M.P., Car, A., Herwig, W. and Ulanova, A. 2015. *Licmosphenia* revisited: transfer to *Licmophora*, redescription of *L. clevei* Mereschkowsky and descriptions of three new species. Diatom research, 30(3), pp.227-236.MARIN-GUIRAO, L., LLORET, J., MARIN, A., GARCIA, G., & GARCIA FERNANDEZ, A.J. (2007). Pulse-discharges of mining wastes into a coastal lagoon: Water chemistry and toxicity. Chemistry and Ecology 23: 217-231.

Medlin, L., Jung, I., Bahulikar, R., Mendgen, K., Kroth, P. and Kooistra, W.H.C.F. 2008. Evolution of the diatoms. VI. Assessment of the new genera in the araphids using molecular data. Nova Hedwigia, 133, pp.81-100.

Moreno-González, R., Rodríguez-Mozaz, S., Gros, M., Pérez-Cánovas, E., Barceló, D. and León, V.M. 2014. Input of pharmaceuticals through coastal surface watercourses into a Mediterranean lagoon (Mar Menor, SE Spain): sources and seasonal variations. Science of the Total Environment, 490, pp.59-72.

Nawrocki, E.P. 2009. Structural RNA homology search and alignment using covariance models, Washington University, St. Louis, Missouri, USA.

Nawrocki, E.P., Kolbe, D.L. and Eddy, S.R. 2009. Infernal 1.0: inference of RNA alignments. Bioinformatics, 25(10), pp.1335-1337.

Reid, F.M. and Round, F.E. 1987. The Antarctic diatom *Synedra reinboldii*: taxonomy, ecology and transference to a new genus, Trichotoxon. Diatom Research, 2(2), pp.219-227.

Ronquist, F. & Huelsenbeck, J.P. 2003. MrBayes 3: Bayesian phylogenetic inference under mixed models. Bioinformatics, 19(12), pp.1572-1574.

Round, F.E., Crawford, R.M., & Mann, D.G. 1990. The Diatoms - Biology & Morphology of the genera. Cambridge University Press.

Shimodaira, H. and Hasegawa, M. 2001. CONSEL: for assessing the confidence of phylogenetic tree selection. Bioinformatics, 17(12), pp.1246-1247.

Silvestro, D. & Michalack, I. (2012). raxmlGUI: a graphical front-end for RAxML. Organisms Diversity & Evolution 12: 335-337.

Theriot, E.C., Cannone, J.J., Gutell, R.R. and Alverson, A.J. 2009. The limits of nuclear-encoded SSU rDNA for resolving the diatom phylogeny. European Journal of Phycology, 44(3), pp.277-290.

Theriot, E. C., Ashworth, M. P., Nakov, T., Ruck, E., & Jansen, R. K. 2015. Dissecting signal and noise in diatom chloroplast protein encoding genes with phylogenetic information profiling. Molecular phylogenetics and evolution 89: 28-36.

Thompson, J.D., Gibson, T.J., Plewniak, F., Jeanmougin, F. and Higgins, D.G. 1997. The CLUSTAL_X windows interface: flexible strategies for multiple sequence alignment aided by quality analysis tools. Nucleic acids research, 25(24), pp.4876-4882..

Tomás, X. (1988). Diatomeas de las aguas epicontinentales saladas del litoral mediterráneo de la Penínnsula Ibérica. University of Barcelona, Spain.

Williams, D.M., & Kociolek, J.P. (2011). An overview of diatom classification with some prospects for the future, in The Diatom World (Seckbach, J. & Kociolek, J.P., editors), 47–91, Springer, The Netherlands.

Williams, D.M. & Round, F.E. (1986). Revision of the genus Synedra Ehrenb. Diatom Research 1: 313-339.

Chapter 2

Licmophora species from a mediterranean hypersaline coastal lagoon (Mar Menor, SE Spain)

Introduction

In coastal lagoons and estuaries, microphytobenthos plays an important role in the total primary production (Barnes & Mann 1982). Although diatoms are an important and frequently dominant component of benthic microalgal assemblages (Sullivan 1999), studies on epiphytic diatom communities are very scarce in such habitats.

The Mar Menor, a hypersaline ecosystem, is one of the largest coastal lagoons on the Medi-terranean Sea. The environment of the lagoon has historically been affected by mining wastes and, more recently, by developments in agriculture and tourism. Several ephemeral wadis flow into the lagoon when torrential rains occur. In the Mar Menor lagoon the main macrophytes are the vascular plant Cymodocea nodosa (Ucria) Ascherson and the macroalga Caulerpa prolifera (Forsskal) Lamouroux. The latter has expanded its distribution and now occupies most of the bottom of the lagoon, while C. nodosa is restricted to small patches in shallow areas (Calvín-Calvo 1999, Lloret *et al*., 2005). Epiphytic biofilm growing on macrophytes can play an important role in dynamic and trophic relationships in this lagoon (Marin-Guirao *et al*., 2005, Lloret *et al*., 2008). Benthic primary production is greater than planktonic (Terrados & Ros 1992) and the microphytobenthos contributes to 11% of total primary production (Terrados & Ros 1991) in the Mar Menor. However, while several previous studies have examined seasonal phytoplankton dy-namics in this shallow system (Ros & Miracle 1984, Gilabert 2001) as well as biomass changes related to agricultural activities (Pérez Ruzafa *et al*., 2002, Lloret *et al*., 2005). The community dynamics, taxonomy and autoecology of microalgal epiphyte species in the lagoon are unknown.

Honeywill (1998) made an extensive study of several species of Licmophora (habitat, hosts, seasonability, colony formation, cell morphology and structure) in the British Isles and more recently Lobban *et al*. (2011) described a new species from the Pacific Ocean. The first documen-tation of epiphytic diatoms in the Mar Menor was provided by Tomás (1988), who reported three different species of Licmophora: *L. gigantea, L. remulus and L.* cf. *proboscidea.* In a preliminary survey Licmophora species were observed to be remarkable in abundance and morphologically variable close to Beal wadi (Mar Menor) suggesting that they are a common inhabitant of the lagoon. The main goal of the present study was to investigate the variability of *Licmophora* species in the hypersaline Mar Menor coastal lagoon.

Material and methods

The sampling was carried out between 13th June to 20th July 2008 in the Mar Menor lagoon (135 km2, mean depth 4 m, maximum depth 6.5 m), located in a semi-arid region of southeast Spain. It is isolated from the Mediterranean Sea by a 22 km long sand bar (La Manga) located on the eastern side of the lagoon and crossed by five very shallow channels. Wadis in the area are mainly located in the southwest side, although they remain dry during most of the year, watercourses flow into the lagoon after episodic rainfall events. The study sites were located in the southern part of the Mar Menor. The first sampling station, in the south-west of the lagoon, faces the Beal wadi outlet and is influenced by the wastes washed down from mining areas. The second corresponds to El Ciervo Island which is located in the east of the lagoon far from influ-ence of the mining area. The bottoms of both sampling stations are dominated by C. nodosa meadow which is included in Annex I of the Bern Convention (strictly protected flora species). The salinity of the lagoon ranges between 42 and 47, due to low precipitation (< 300 mm yr–1) and high evaporation rates. Water temperature ranges from 10 °C in winter to 31 °C in summer. During the sampling period water column was characterized by 7.6 – 9.8 mg O2 · l–1, 7.6–8.2 pH, 0.001–

0.002 mg Chl a · l^{-1}, PO_4^{3-} levels undetected and high salinity (43 – 44.8); the temperature ranged between 24.5 and 29.8 °C. The values corresponding to Ciervo Island were: 1.15 µmol NO_3^- · l^{-1}, 10.65 mg D. W. · l^{-1} (suspended solids), 3 µg Zn · l^{-1} and 2 µg Pb · l^{-1} (reaching 5 µg Zn · l^{-1} and 20 µg Pb · l^{-1} when torrential rains occur (Marin-Guirao *et al*., 2007). In Beal wadi: 1.98 µmol NO_3^- · l^{-1} and 12.35 mg D. W. · l^{-1} (suspended solids), 4.2 µg Zn · l^{-1} and 11.7 µg Pb · l^{-1} reaching 170 µg Zn · l^{-1} and 2000 µg Pb · l^{-1} when the wadi flows into the lagoon (Marín-Guirao *et al*., 2007). No stratification exists in the water column.

The epiphytic diatoms were collected monthly during the summer sampling period. The pres-ence of the species was checked in *C. nodosa* leaves at both sampling points. Alternatively artifi-cial substrata were used for 19 days each month (13th June-1st July, 2nd July-20th July 2008). These consisted of glass slides (76 × 26 mm) placed parallel to the current by means of polyethylene racks that held 25-30 slides. Diatoms were fixed in formaldehyde (3.5%) and analyzed in the laboratory.

Four replicates were used to study the relative abundance of the Licmophora species. Organic matter was removed by digestion in a 33% H_2O_2 solution for 2 hours. Cleaned diatom frustules were filtered (0.2 µm GNWP nylon membrane filter, MILLIPORE) and washed out with distilled water. The material was resuspended in ethanol (70%) using sonication. This solution was pipet-ted onto coverslips, air-dried and then mounted onto slides using Naphrax (R. I.1.69). Diatoms were examined using light microscopy (LM) (Leica DMRB). A minimum of 400 valves of dia-tom species with a maximum of 428 was counted for each sample. Later, the relative abundance of species (in percentage) and species richness were estimated. Taxa were identified according to Peragallo & Peragallo (1897–1908), Hustedt (1959), Tomás (1988), Honeywill (1998), Wit-kowski *et al*. (2000) and Clavero (2004).

Fresh material was studied using light microscopy to observe and record colony forms and chloroplasts. Colonies were also observed on calcined material. Cell dimensions and striae were estimated from light micrographs. With finely striated species, striae, areolae, rimoportulae and slits were read on a scanning electron microscope (SEM). Cleaned diatom frustules were de-hydrated in graded acetone, dried by the critical-point method using CO_2 as transition fluid, mounted, coated with gold, and viewed with a JEOL-6100 SEM microscope operating at 20 kV.

Results and discussion

The araphid genus *Licmophora* C. Agardh, a common component of epiphytic communities (Woods & Fletcher 1991), has a cosmopolitan distribution in coastal waters (Round *et al*., 1990). Valves are spathulate and clavate in valve view and cuneate in girdle view. Frustules usually form colonies attached to branching stalks or mucilage pads. They have uniseriate striation, radiate near apical pole with elliptic or elongate areolae (in some cases separated by means of vimines). The basal pole has a variable number of slits in multiscissura. Each cell has two or three rimopor-tula per cell with an orientation that differs between species (Honeywill 1998). Five species of *Licmophora* were identified in the samples studied from the Mar Menor and two different groups can be separated: small species with a low density of slits in multiscissura (*L. proboscidea, L. debilis* and *L. tenuis*) and large species with a high number of slits in multiscissura (*L. flabellata* and *Licmophora* sp.). The morphological characteristics for all species are summarized in Table 3.

Together, these species represented 2% in June and 5% in July of the total diatom community of Ciervo sland. In Beal wadi this genus contributed 1% in June and 11% in July to the total diatom population. *Licmophora* sp. was the most abundant species, contributing 92% of the cells in the samples, while the other species together (*L. proboscidea, L. debilis, L. tenuis* and *L. flabellata*) only provided 8% of the total abundance.

Table 3. Taxonomic characters of the *Licmophora* species from the Mar Menor coastal lagoon.

Licmophora species	Valve length µm	Valve width µm	Striae in 10 µm at the head pole	Striae in 10 µm at the basal pole	Areolae apical pole 10 µm	Areolae basal pole 10 µm	Number of rimoportulae per cell	Head rimoportulae	Basal rimoportulae	Number of slits (multicissura)	Mucilage stalk
L. proboscidea n=12	25-36-(43)	2.5-3.6	(25)-29-30	36	35-36	40	2	1	1 (Towards head pole)	5	Branched stalks
L. debilis n=11	16-34.5	2.4-5.7	(26)-30-34	(26)-30-34	(34)-40-50	40-50	2	1	1 (Towards head pole)	5	Short stalks
L. tenuis n=5	39-42.4	7-7.5	16-18	16	57 vimines	57 vimines	-	-	1 rounded	7	Mucilage pads
L. flabellata n= 33	104-174	5.8-7.4	30-32	30-32	40	40	14-18	1+	1 elongate	30	Long and branched stalks
Licmophora sp. morpho 1 n= 64	322 - 335	20 - 23.5	23 - 24	23 - 24	24 - 25 E	40	2	1	1 elongate	32 - 38	Long branched stalk
Licmophora sp. morpho 2 n= 48	220 - 255	14.5 - 18.8	25 - 27	25 - 27	40 (doble within criba)	28	2	1	1 rounded	28 - 30	
Licmophora sp. morpho 3 n= 53	177 - 281	13 - 15	25 - 26	25 - 26	21 - 23	56	2	1	1 elongate	24 - 28	

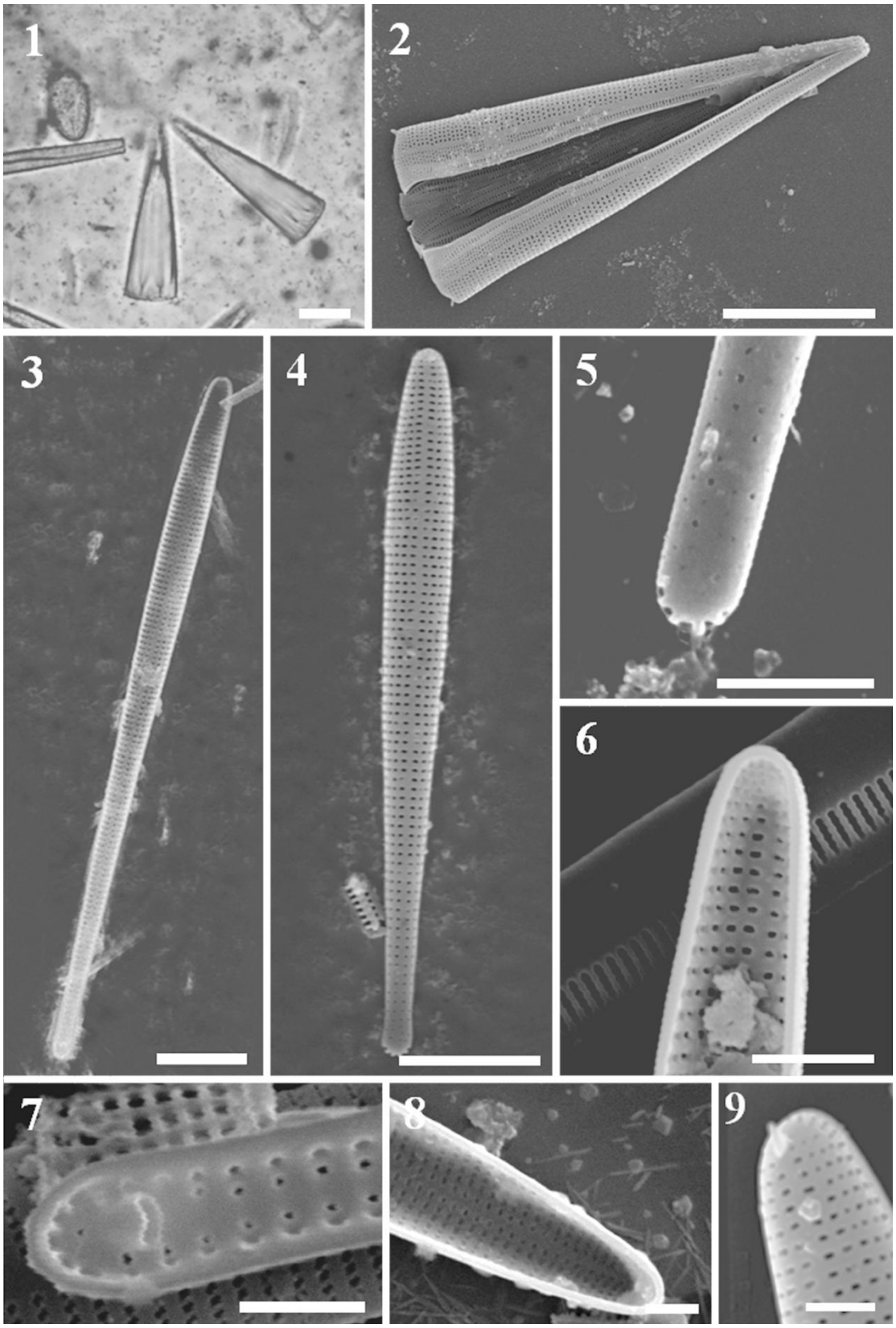

Plate 6. Fig. 1–9. *L. proboscidea.* **Fig. 1.** LM. Pairs of cells attached to long stalk, **Fig. 2.** SEM. Girdle view of valve showing spine in head pole in each valve, **Fig. 3.** SEM. Internal view of valve with basal rimoportula, **Fig. 4.** SEM. Narrow valve with rimoportulae in the head pole. Areolae in lines apically as well as transapically, **Fig. 5.** SEM. A basal pole showing slits, no rimoportulae and rounded basal areolae, **Fig. 6.** SEM. An internal view of head rimopor-tula, **Fig. 7.** SEM. Internal view of basal rimoportula opening towards the head pole, **Fig. 8.** SEM. Internal view of head pole with broken rimoportula, **Fig. 9.** SEM. An external view of head pole with rimoportulae. Scale bars = 1 µm (7, 9), 2 µm (5, 6, 8), 5 µm (3, 4), 10 µm (1, 2).

Together, these species represented 2% in June and 5% in July of the total diatom community of Ciervo Island. In Beal wadi this genus contributed 1% in June and 11% in July to the total diatom population. *Licmophora* sp. was the most abundant species, contributing 92% of the cells in the samples, while the other species together (*L. proboscidea, L. debilis, L. tenuis* and *L. flabellata*) only provided 8% of the total abundance.

***Licmophora proboscidea* Mereschkowsky 1901**

Colonies composed of 2 cells on branching stalks were observed in calcinated material (Plate 6 Fig. 1). Valves with an inconspicuous sternum under LM. Spatulate with outstretched and pointed head pole (Plate 6 Figs. 4, 6). Cells 25 – 36 (43) µm long, 2.4 – 3.6 µm wide and (25) 29 – 30 striae in 10 µm in centre of valves, while poles are more densely striated, up to 36 striae in apical pole. Two rimo-phortulae per cell, one in the basal pole pointing towards the head pole (Plate 6 Fig. 7) and the second on the apical pole of the other valve (Plate 6 Fig. 8). One spine at head pole of each valve (Plate 6 Fig. 2). Areolae are arranged in lines apically as well as transapically, 35 – 36 transapical elongate areolae becom-ing rounded toward foot pole. Multiscissura has 5 slits (Plate 6 Fig. 5). Valvocopula has a fairly shallow septum.

Frustules observed in this work have a slightly more dense striation than Hustedt and Honeywill's specimens (24 – 28 striae in 10 µm) (Hustedt 1959, Honeywill 1998).

This species has only previously been found in ex-Yugoslavia (Mereschkowsky 1901), Italy (Alfinito & Zoppini 1982), along the coast of England and Wales (Honeywill 1998), and with doubts in the Mar Menor lagoon (Tomás 1988).

***Licmophora debilis* (Kützing) Grunow in Van Heurck 1881 (= *Podosphenia debilis* Kützing 1844)**

Cells usually in pairs or a few cells on a short stalk (Plate 7 Fig. 11). Valves spathulate with a short at-tenuate base and maximum width in the centre of the valve (Plate 7 Fig. 15). Inconspicuous sternum under LM. Valves 16 – 34.5 µm long, 2.4 – 5.7 µm broad with (26)– 30 – 34 striae throughout most of the valve. Areolae in lines apically as well as transapically. Slightly elongated transapical are-olae along the valve (34)-40-50 in 10 µm become rounded towards basal pole. Two rimoportulae per cell, basal rimoportula opening upward internally towards the head pole and externally with rounded opening (Plate 7 Figs. 13, 14). Multiscissura has 5 slits (Plate 7 Figs. 12, 13). Valvocopula with moder-ately deep septum.

L. debilis and *L. proboscidea* are small diatoms with inconspicuous sternum. It is easy to dis-tinguish between the two species under LM because *L. proboscidea* valves are longer and thinner than those of *L. debilis* and have an attenuated head pole. Moreover, *L. debilis* is more densely striated than *L. proboscidea,* according to Hustedt (1959) and Honeywill (1998).

This species is widespread along European coasts (Witkowski *et al*., 2000) and can support wide ranges of salinity. *L. debilis* has been reported by Tomás (1988) in the hypersaline waters from Almería (40 – 48) and inhabiting salty water (45 – 46) from Catalonia (Clavero 2004). Sullivan (1979) recorded it in Mississippi Sound and Snoeijs & Kasperoviciene (1996) also cited it in water with salinity values between 2 – 25 in Baltic sea.

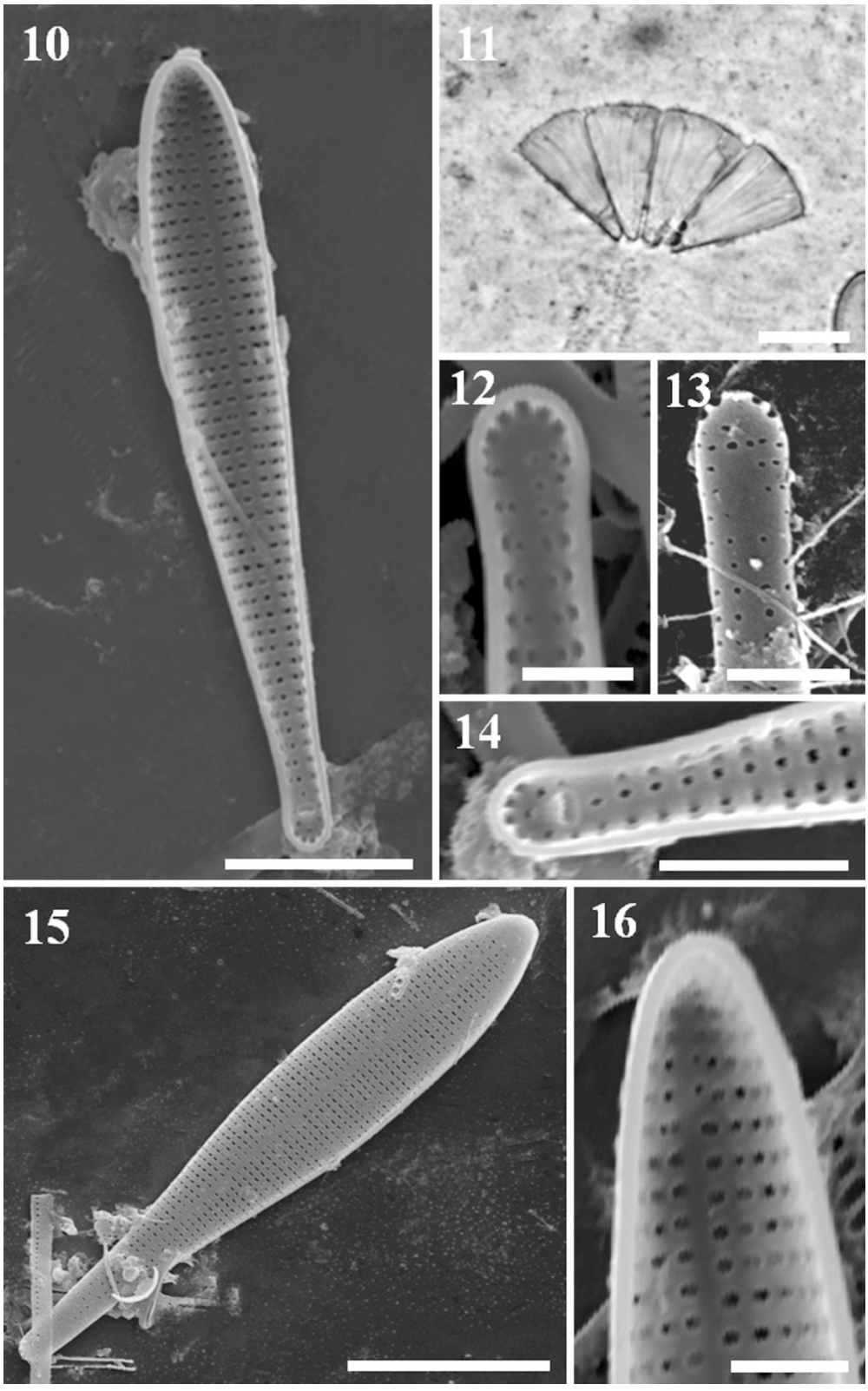

Plate 7. Fig. 10–16. *L. debilis.* **Fig. 10.** SEM. An internal view of basal pole with rimoportula opening towards head pole and slits, **Fig. 11.** LM. A few cells form colonies, **Fig. 12.** SEM. Internal view of basal pole without rimopor-tula, **Fig. 13.** SEM. An external view of basal pole; note pointed foot pole and external rimoportula opening, **Fig. 14.** SEM. An internal view of valve showing basal rimoportula, **Fig. 15.** SEM. Valve spathulate showing short attenuate base, **Fig. 16.** SEM. Internal view of head pole. Scale bars = 1 µm (12, 16), 2 µm (13, 14), 4 µm (10),µm (11, 15).

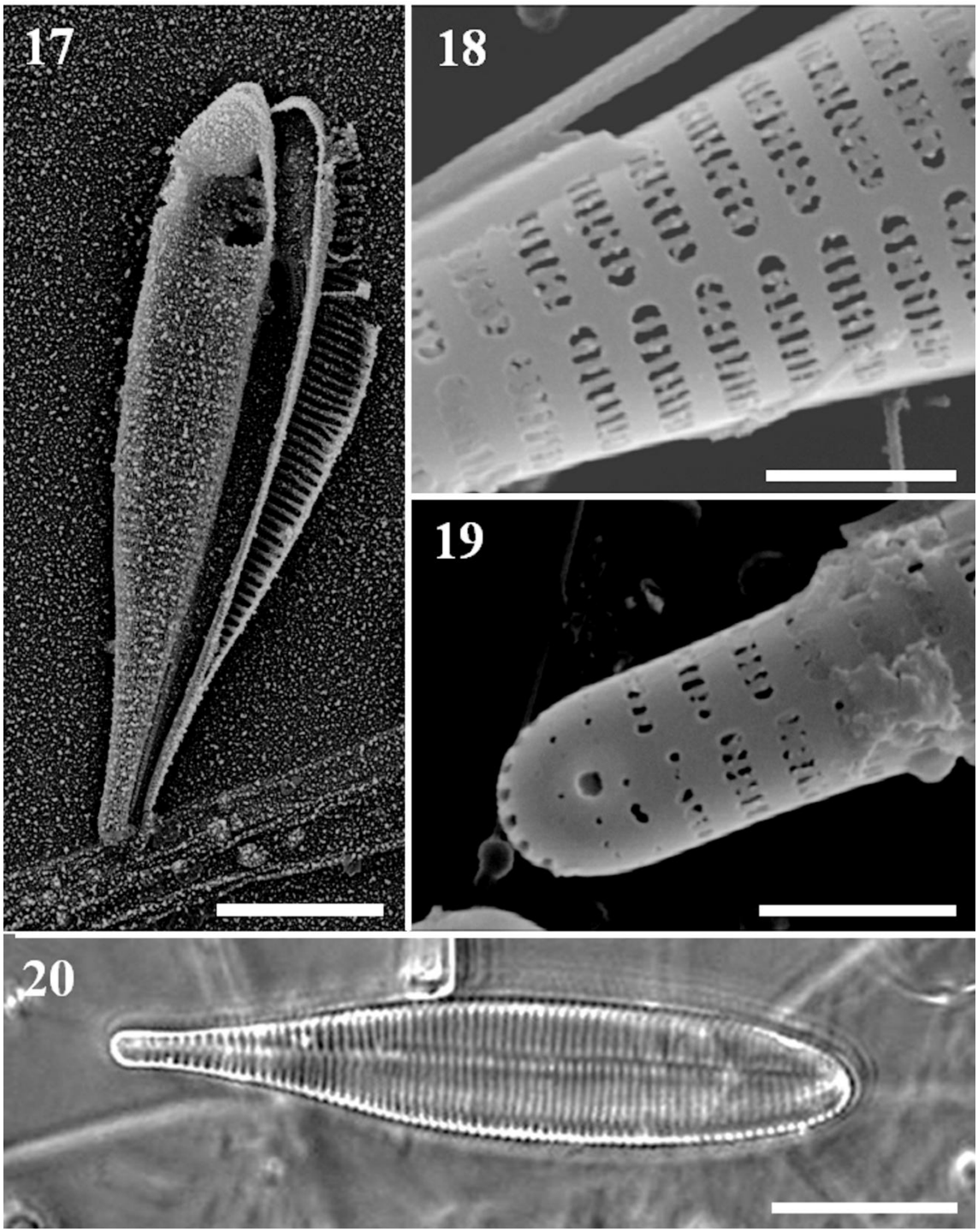

Plate 8. Fig. 17–20. *L. tenuis*. **Fig. 17.** SEM. Valve cuneiform and robust, **Fig. 18.** SEM. Detail of striae with complete vimines, **Fig. 19.** SEM. An external view of basal rimoportula rounded opening surrounded by pores around of this, **Fig. 20.** LM. Valve view of cuneiform and robust valve with coarse striation. Scale bars = 2 µm (18, 19), 10 µm (17, 20).

***Licmophora tenuis* (Kützing) Grunow (= *Podosphenia tenuis* Kützing 1844; *Podosphenia gracilis* W. Smith 1853)**

Single cells attached by mucilage pads. Frustules cuneiform, robust (Plate 8 Fig. 17). Sternum nar-row but distinct (Plate 8 Fig. 20).Valves 39 – 42.4 µm long, 7–7.5 µm broad with 16 –18 striae in 10 µm throughout the valves. Valves have very coarse striae compared with other species of the genus. Elongate areolae in the apical direction, divided by thin and complete vimines, 57 areolae in 10 µm

(Plate 8 Fig. 18). The valves present rounded areolae at the basal pole (Plate 8 Fig. 19). We only observed a rounded external rimoportula opening in the basal pole. Multiscissura has 7 slits (Plate 8 Fig. 19). Val-vocopula has a moderately deep septum.

The morphological characteristics of the specimens agreed with the description provided by Hustedt (1959). The present work reports *L. tenuis* for the first time in the Mar Menor lagoon and provides new information about slits in multiscissura, rimoportulae, areolae, vimines details, mu-cilage stalks and valvocopula septum. Peragallo & Peragallo (1897–1908) and Hustedt (1959) only record valves in girdle view and striation density.

L. tenuis to date known from the northern of Spanish coast, coast of France to Norway and Balearic Islands (Peragallo & Peragallo 1897–1908; Hustedt 1959).

***Licmophora flabellata* (Carmichael) Agardh 1831**

Colonies composed of numerous cells at the tips of long and branching stalks (Plate 9 Fig. 21). Valves narrow spatulate with a rostrate base. 104 –174 µm long, 5.8 –7.4 broad with 30 – 32 striae in 10 µm. One transapical rimoportula at basal pole of one valve (Fig. 25) and a smaller rimoportula at head pole of the other valve, also numerous smaller rimoportulae (7– 9) at irregular intervals along the sternum (Plate 9 Figs. 22, 23). Multiscissura with 30 slits (Plate 9 Fig. 25). Two spines in head pole of both valves (Plate 9 Fig. 24).

L. flabellata was more abundante than *L. tenuis*, *L. proboscidea* and *L. debilis* so it contributed 6% of the 8% represented by the group as a whole. Striae range coincides with valves displayed by Lobban *et al*. (2011), Hustedt (1959) and Witkowski *et al*. (2000), while specimens described by Honeywill (1998) were more densely striated (35 striae in 10 µm).

This is a well-known species reported by several authors (Peragallo & Peragallo 1897–1908, Hustedt 1959, Honeywill 1998, Witkowski *et al*., 2000, Lobban *et al*., 2011). It is common in Eu-ropean coasts. Tomás (1988) reported it in a marsh of Girona (Spain). It can also occur in less salty waters such as river mouths. This study reports it for the first time in the Mar Menor lagoon and confirms the wide ranges of salinity and temperature that this species can withstand.

***Licmophora* sp.**

Wedge-shaped valves, tapering from the apical pole (robust, broad and rounded) to the foot pole (smaller and capitate). Margins slightly concave near the apical pole. *Licmophora* sp. has rounded plastids, distributed throughout three quarters of the cells analyzed (Plate 10 Fig. 28). Single cells or few cell groups attached to long and branching stalks were observed (Plate 10 Fig. 27). Three morphs were observed with varying shape, striation, size, rimoportulae (position, shape and orientation) and number of slits in multiscissura. Variations in rimoportula orientation are clearly visible under LM.

The morphological characteristics of this large species with a high number of slits in multicis-sura do not fit any of the known species and so they are treated as a potentialy new taxon while a deeper study is undertaken.

***Licmophora* sp. morph 1:** Valves clavate (**Plate 10** Fig. 26), 322 – 335 µm long, 20 – 23.5 µm broad with 23 – 24 striae in 10 µm (apical and foot pole). 24 – 26 transapical elongate areolae in 10 µm in the apical pole and 40 rounded areolae in 10 µm in the basal pole. Two rimoportulae per cell, one situated in the apical pole fan-shaped, open labiate, with a variable position and orientation in respect to the valve plane. Apical rimoportulae in the right, left and center of the sternum. Rimoportula orientation can be 35^{o} or parallel to the valve plane (**Plate 10** Fig. 29). The rimoportulae of the basal pole is an elongated opening parallel to the sternum. Multiscissura with 32 – 38 slits (**Plate 10** Fig. 30).

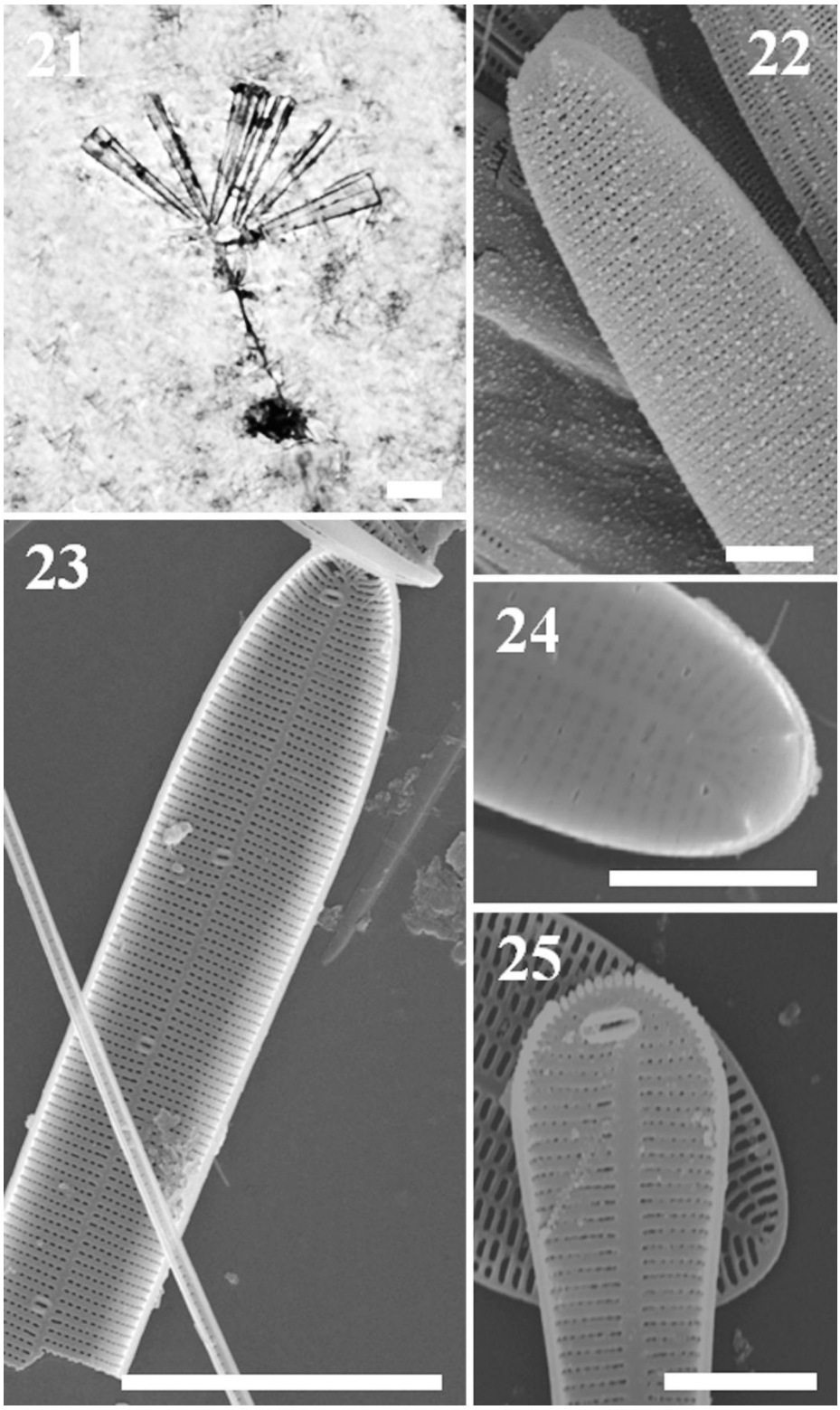

Plate 9. Fig. 21–25. *L. flabellata.* **Fig. 21.** LM. Numerous cells form fans at the end of long stalks (calcinated material), **Fig. 22.** SEM. A valve showing head spines and rimoportulae opening externally, **Fig. 23.** SEM. An internal view of valve showing numerous rimoportulae along the sternum, **Fig. 24.** SEM. Head pole showing the spines and rimoportulae, **Fig. 25.** SEM. An internal view of basal rimoportula. Scale bars = 3 μm (22, 24, 25), 10 μm (23), 40 μm (21).

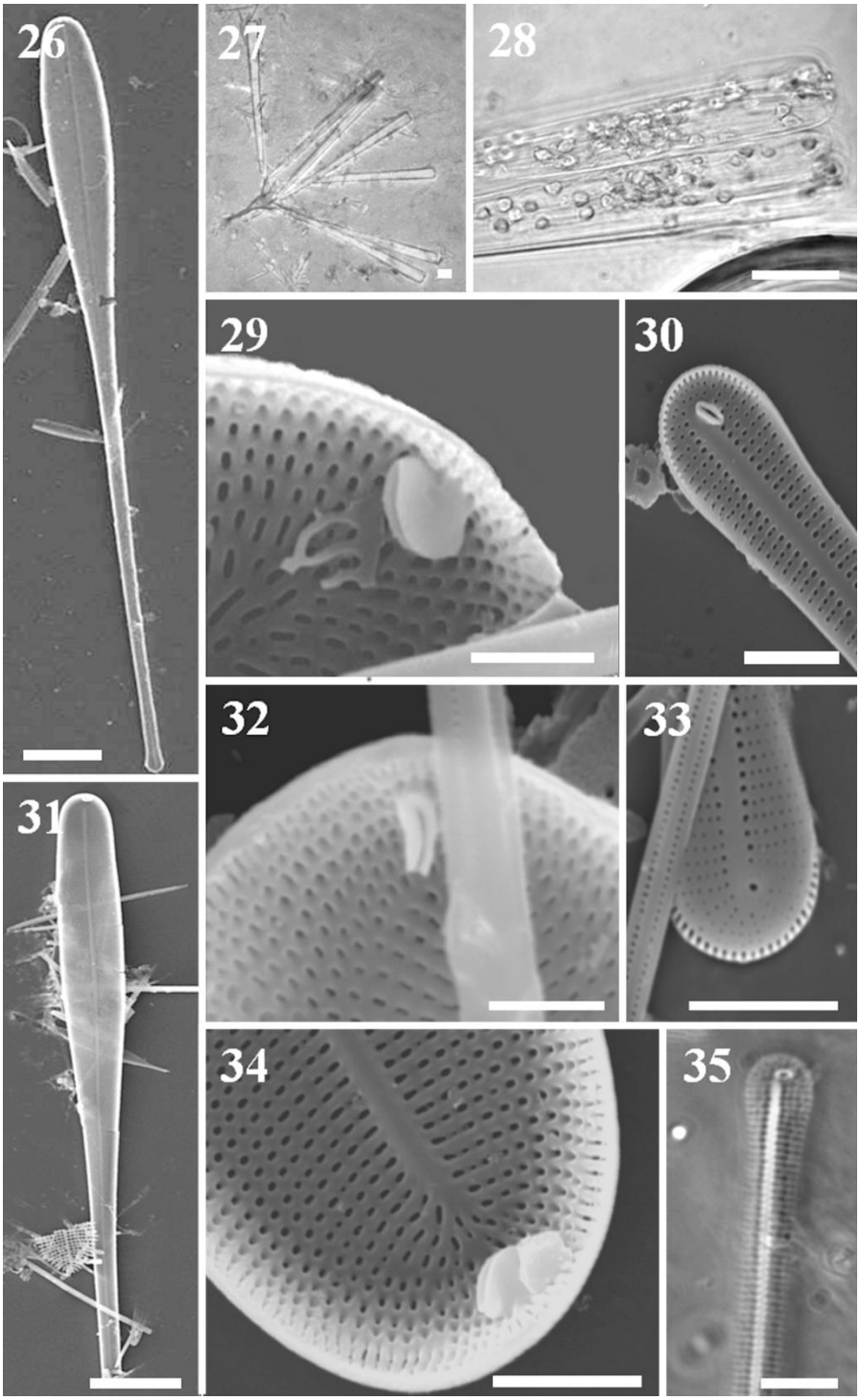

Plate 10. Fig. 26–35. *Licmophora* sp. 26. SEM. Clavate valve of L. sp. morph 1, **Fig. 27**. LM. Colonies of *Licmophora* sp. formed by single cells attached to substratum by a branched stalk; **Fig. 28.** LM. Detail of chloroplasts of Licmophora sp.; **Fig. 29.** SEM. Detail of the rimoportula orientation at 35 ° to the valve plane in the apical pole of Licmophora sp. morph 1**; Fig. 30.** SEM. Detail of the rimoportula of the basal pole of *Licmophora* sp. morph 1, parallel orientation from the sternum; **Fig. 31.** SEM. Internal view of valve spatulate of *Licmophora* sp. morph 3; **Fig. 32.** SEM. Internal view of apical rimoportula orientated at 90 ° plane valve of *Licmophora* sp. morph 2; **Fig. 33.** SEM. Detail of rounded areolae in apical pole of *Licmophora* sp. morph 2; **Fig. 34.** SEM. Detail of double rimoportula in apical pole of Licmophora sp. morph 3; 35. LM. Basal pole rimoportula with perpendicular orientation at sternum of *Licmophora* sp. morph 3. Scale bars = 2 µm (29, 32, 34), 3 µm (30), 5 µm (33, 35), 10 µm (27), 20 µm (26, 28, 31).

***Licmophora* sp. morph 2:** Clavate valve with more rounded and wide apical pole than morph 1, 220 – 255 µm long, 14.5 –18.8 µm wide with 25 – 27 striae in 10 µm (apical and foot pole). 40 transapical rounded double areolae surrounded by visible criba in 10 µm in the apical pole and 28 single round areolae in 10 µm in the basal pole. Two rimoportulae per cell, one with a fan-shape situated in the apical pole, closed labiate internally and elongated opening externally, with an orientation 90 ° to the valve plane (**Plate 10** Fig. 32). The rimoportulae of the basal pole is a rounded opening at the end of the valve. Multiscissura with 28 – 30 slits (**Plate 10** Fig. 33).

***Licmophora* sp. morph 3:** Valve spatulate (**Plate 10** Fig. 31), 177– 281 µm long, 13 –15 µm broad with 25 – 26 striae in 10 µm (apice and foot pole). 21– 23 transapical areolae in 10 µm in the apical pole and 56 rounded areolae in 10 µm in the basal pole. Three rimoportulae per cell: two of them open labiate, situated with a fan-shape in the apical pole of one valve (**Plate 10** Fig. 34) while the third one is smaller, and close to the basal pole of the other valve with perpendicular (90 °) orientation to the sternum (**Plate 10** Fig. 35). Multiscissura with 24 – 28 slits.

In the present work we have provided new information about the great morphological and ecological variability that *Licmophora* species can display in a Mediterranean hypersaline coastal lagoon (Mar Menor). *Licmophora* sp. shows a great morphological variability, especially in the rimoportulae, suggesting the need for further studies with DNA sequences to check if they are a cluster species.

References

Alfinito, S. & Zoppini, A. 1982. Diatoms of the State Salt Works of Tarquinia. Nova Hedwigia 36:423–428.

Barnes, R. S. K. & Mann, K. H. 1982. Fundamentals of Aquatic Ecosystems. Blackwell, Oxford.

Calvín-Calvo, J. C. 1999. El litoral sumergido de la Región de Murcia. Cartografía bionómica y valores ambientales. Consejería de Medio Ambiente, Agricultura y Agua. Región de Murcia.

Clavero, E. 2004. Diatomees d'ambients hipersalins costaners. Ph.D. diss., Universitat de Barcelona, Spain.

Gilabert, J. 2001. Seasonal plankton dynamics in a Mediterranean hypersaline coastal lagoon: the Mar Menor. Journal of Plankton Research, 23(2), pp.207-218.

Honeywill, C. 1998. A study of British *Licmophora* species and a discussion of its morphological fea-tures. Diatom Research. 13:221– 271.

Hustedt, F. 1959. Bemerkungenüber die Diatomeenflora des Neusiedler Sees und des Salzlackengebietes. Landschaft Neusiedler See". Wiss. Arb. aus dem Burgenland, 23:129 –133.

Lloret, J., Marín, A. and Marín-Guirao, L. 2008. Is coastal lagoon eutrophication likely to be aggravated by global climate change?. Estuarine, Coastal and Shelf Science, 78(2), pp.403-412.

Lloret, J., Marin, A., Marin-Guirao, L. and Velasco, J. 2005. Changes in macrophytes distribution in a hypersaline coastal lagoon associated with the development of intensively irrigated agriculture. Ocean & Coastal Management, 48(9), pp.828-842.

Lobban, C. S., M. Schefter & Ruck, E. C. 2011. *Licmophora flucticulata* sp. nov. (Licmophoraceae, Bacillariophyceae) an unusual new flabellate species from Guam and Palau. Phycologia, 50:11– 22.

Marín-Guirao, L., A. Cesar, A. Marín & Vita, R. 2005. Assessment of sediment metal contamination in the Mar Menor coastal lagoon (SE Spain): Metal distribution, toxicity, bioaccumulation and benthic community structure. Ciencias Mararinas. 31:413 –428.

Marín-Guirao, L., J. Lloret, A. Marín, G. García & Fernández, A. J. G. 2007. Pulse-discharges of mining wastes into a coastal lagoon: Water chemistry and toxicity. Chemestry and Ecolology. 23:217– 231.

Mereschkowsky, C. 1901. Etudes sur l'endochrome des diatomees. Memoires de Academie Imperiale des. Sciences de St. Petersbourg 11:1– 40.

Peragallo, H. & Peragallo, M. 1897–1908. Diatomées Marines de France et des Districts Maritimes Voisins. M. J. Tempère (ed.), Grez-sur-Loing, 491 pp.

Pérez Ruzafa, A., J. Gilabert, J. M. Gutiérrez, A. I. Fernánder, C. Marcos & Sabah, S. 2002. Evidence of a planktonic food web response to changes in nutrient input dynamics in the Mar Menor coastal lagoon, Spain. Hydrobiologia 475/476:359 –369.

Ros, M. & Miracle, M. R. 1984. Variación estacional del fitoplancton del Mar Menor y su relación con la de un punto próximo en el Mediterráneo. Limnetica 1: 32–42.

Round, F. E., R. M. Crawford & Mann, D. G. 1990. The diatoms: biology and morphology of the genera.Cambridge Univ. Press. Snoeijs, P. & J. Kasperoviciene (1996): Intercalibration and distribution of diatom species in the Baltic Sea, Vol. 4: The Baltic Marine Biologists Publication No. 16 d, 126 pp.

Sullivan, M. J. 1979. Taxonomic Notes on Epiphytic Diatoms of Mississippi Sound, U.S.A. Nova Hedwigia 64:237, 249.

Sullivan, M. J. 1999. Applied diatom studies in estuaries and shallow coastal environments. In: Stoermer, E. F. & Smol J. P. (eds), The Diatoms: Applications for the Environmental and Earth Sciences, pp. 334 – 351, Cambridge Univ. Press.

Terrados, J. & Ros, J. 1991. Production dynamics in a macrophyte dominates ecosystem: the Mar Menor coastal lagoon (SE Spain). Oecologia Aquatica. 10:25 5–270.

Terrados, J. & Ros, J. 1992. Growth and primary production of *Cymodocea nodosa* (Ucria) Ascherson in a Mediterranean coastal lagoon. Aquatic Botany. 43:63 –78.

Tomás, X. 1988. Diatomeas de las aguas epicontinentales saladas del litoral mediterráneo de la península Ibérica. Ph.D. diss., Universitat de Barcelona, Spain.

Witkowski, A., H. Lange-Bertalot & Metzeltin, D. 2000. Diatom flora of Marine Coasts I. – Iconogr. Diatomol. 7: 925 pp.

Woods, D. C. & Fletcher, R. L. 1991. Studies on the strength of adhesion of some common marine fouling diatoms. Biofouling 3:287– 303.

Chapter 3

Licmophora colosalis sp. nov. (Licmophoraceae, Bacillariophyta), a large epiphytic diatom from coastal waters

Introduction

Diatoms of the araphid genus *Licmophora* C.Agardh contribute to microalgal biofilm communities (Woods & Fletcher 1991); they are common epiphytes of seaweeds (Honeywill 1998; Lobban *et al*., 2011; Belando *et al*., 2012) and they have a cosmopolitan distribution in coastal areas (Round *et al*., 1990). Species of this genus are easily recognized due to their wedge-shaped frustules in both valve and girdle views. Cells usually form colonies attached to branching stalks or mucilage pads (Round *et al*.,1990). Valves have uniseriate striations with elliptical or elongated areolae usually separated by vimines on both sides of the central sternum. Each cell has one rimoportula at the basal pole of one valve and another at the head pole of the opposite valve or at the head poles of both valves. The basal pole has a variable number of slits in the multiscissura (Honeywill 1998).

Mereschkowsky (1901) described several large species of *Licmophora*; however, his observations were only with light microscopy, which made the identification of specimens with dense striation difficult and unreliable. More recent studies have provided morphological information based on scanning electron microscopy (e.g. Honeywill 1998, in a revision of British species of *Licmophora*). Lobban *et al*. (2011) and Lobban & Schefter (2013) also described new large taxa providing extensive scanning electron microscope (SEM) images and applying molecular analyses for *Licmophora flucticulata* Lobban, Schefter & Ruck.

In a previous work Belando *et al*. (2012) reported high morphological variability among large *Licmophora* specimens from the Mediterranean coastal lagoon, Mar Menor in SE Spain, prompting a deeper investigation of the material, and here we provide a description and phylogenetic information for *Licmophora colosalis*, a large new epiphytic species. Morphological characters of *L. colosalis* are compared with three morphologically similar species: *L. remulus* Grunow, *L. gigantea* Mereschkowsky and *L. grandis* (Kützing) Grunow. Phylogenetic analyses were performed using all sequences of the nuclear encoded small subunit ribosomal DNA (SSU rDNA) and the plastidial large subunit of ribulose-1,5-bisphosphate carboxylase/oxygenase (Rubisco) (*rbc*L) available in Genbank for *Licmophora* and *Licmosphenia peragallioides* Lobban due to its close relationship to species of *Licmophora* (Lobban 2013).

Material and Methods

Licmophora colosalis sp. nov. was found in three different geographic areas (Figure 1): the south-east of Spain in the Mediterranean Sea, from Florida Bay (USA) and from the coast of Saudi Arabia in the Red Sea. On the Spanish Mediterranean coast it was recorded from four sites. Three sites are from the hypersaline (salinity 42–47) Mar Menor coastal lagoon (SE Spain):

- Ciervo Island (37º 39´35.7´´ N, 00º 44´26.1´´ W), 0.3-1 m depth.
- Beal wadi (37º 39´58.5´´ N, 00º 48´45.0´´ W), 0.5-1 m depth.
- Los Alcázares (37º 44´19.3´´ N, 00º 50´51.7´´ W), 0.3 m depth.

The fourth site is close to the outlet of the El Estacio channel linking the lagoon to the Mediterranean Sea (Caleta del Estacio, 37º 44´42.9´´N, 00º43´53.9´´W). In all four sites *L. colosalis* was found during the summer (late July–August) spreading rapidly on the leaves of *Cymodocea* nodosa (Ucria) Ascherson, *Cladophora dalmatica* Kützing and *Acetabularia acetabulum* (Linnaeus) P.C. Silva.

Figure 1. Known geographical distribution of *Licmophora colosalis*.

In Florida Bay it was found attached to leaves of the seagrass *Thalassia testudinum* K.D. Koenig, at 1–2 m depth (24–42 salinity) at two locations:

- Rabbit Key Basin (24º58´37.2´´ N, 80º50´20.4´´ W), March 2011 (Matt P. Ashworth, personal communication), HK366/ECT3907 strain.
- Duck Key (25º10´35.4´´ N, 80º29´23.4´´ W), February 2001 (T.A. Frankovich, personal communication).

In the Red Sea it was found in the Obhur area of Jeddah (Kingdom of Saudi Arabia, (21º43´32.1´´ N, 39º06´56.9´´E, Matt P. Ashworth, personal communication). Records are available at http://www.protistcentral.org/Taxa/get/taxa_id/586040 (Jordan *et al*., 2009–2015).

The samples of *Licmophora colosalis* sp. nov. used in this study were collected from filaments of *Cladophora dalmatica* in the vicinity of Ciervo Island from the Mar Menor lagoon in July 2008 and were isolated into culture in July 2013. L. remulus was also collected and cultured in September 2012. In both cases, pieces of filament or leaves containing diatom colonies were placed in Petri dishes with enriched seawater medium f/2 (SAG Göttingen Germany). Diatom cells were then isolated into monoculture using micropipettes. Cultures were maintained at 20 ºC under a 16:8 light regime with an irradiance of 35 μmol photons m^{-2} sec^{-1}.

Macroscopic colonies were identified on macrophyte leaves and photographed in the field using an underwater camera (Intova IC600, Honolulu, Hawaii USA). Colonies and chloroplasts from live cells and cleaned material were examined using light microscopy (LM, Leica DMRB, Wetzlar Germany). Samples from the field and culture material were cleaned of organic matter by boiling in 33% H_2O_2 solution (70 ºC, 2 h), filtered (0.2 μm nylon membrane filter, Millipore, Billerica, Massachusetts USA), washed with distilled water and resuspended in an ethanol solution (96%). For LM observation cleaned material was air dried onto glass coverslips, and permanent slides were mounted using Naphrax (refractive index 1.69). Light micrographs were documented using a Leica DC-500 camera. For SEM analysis, glass coverslips containing cleaned material were mounted on stubs and coated with gold-palladium. Electron micrographs were taken using a scanning electron microscope (JEOL-6100, Oxford Instrument, Abingdon UK) operating at 15 kV. Terminology used in this study is based on Round *et al*. (1990) and Honeywill (1998).

In total, 21 samples representing 18 *Licmophora* strains, *Licmosphenia peragallioides* (which is closely related to species of *Licmophora*; Lobban 2013) and two outgroup taxa were used for phylogenetic analysis (Table Ap2 1). We retrieved 19 SSU rDNA sequences and 10 *rbc*L sequences from Genbank. Only two accessions were sampled by authors (*L. colosalis* LICOL1 and *Licmophora remulus* LIREM1; Table Ap2 1). Species from *Hyalosira*

and *Grammatophora* were selected as outgroup taxa, as used in a similar study for the description of *L. flucticulata* (Lobban *et al*., 2011).

Extraction of DNA from *Licmophora colosalis* and *L. remulus* was performed from pelleted culture material using a cetyltrimethyl ammonium bromide extraction method described by Doyle & Doyle (1987) and stored frozen at -20 ^{o}C until the polylmerase chain reaction (PCR) reaction was carried out. For the phylogenetic analysis, the nuclear encoded SSU rDNA and a chloroplast region, large subunit of Rubisco (*rbc*L), were sequenced. Primers used for the amplification and sequencing were selected from Alverson *et al*. (2007). For SSU rDNA gene, three pairs of primers were used (SSU 1+/568-, 301+/1147- and 1004+/ITS D-), and for *rbc*L gene the pair of primers *rbc*L 66+/*rbc*L 1255- were used. Amplification reactions were conducted in 50 µl volumes containing approximately 20 ng of genomic DNA, 0.2 mM of each dNTP, 2.5 mM $MgCl_2$, 2 units of Taq polymerase (Biotools, Madrid, Spain), the buffer provided by the manufacturer, the combinations of primers at a final concentration of 0.4 mM and ddH_2O to the final volume. Polymerase chain reactions were performed in a thermocycler (Eppendorf mastercycler gradient, Hamburg Germany) using the following program outlined in Alverson *et al*. (2007): 94 ^{o}C for 3:30 min, 35 cycles of 94 ^{o}C for 50 s, 53 ^{o}C for 50 s and 1 min at 72 ^{o}C. A final step of 72 ^{o}C for 8 min was included to terminate amplification products. Finally, 2 ml of the amplification products were visualized on a 1.5% agarose gel, and successful amplifications were cleaned with the GenElute PCR cleanup kit (Sigma-Aldrich, St Louis, Missouri USA). For sequencing, purified PCR products were reacted with the BigDye terminator cycle sequencing ready reaction (Applied Biosystems, Foster City, California USA) using amplification primers.

Sequences were checked for inaccurate base identification using Chromas Lite v2.01 (Technelysium 2002). Consensus sequences of *rbc*L gene fragments were aligned using ClustalX (Thompson *et al*., 1997), and alignments of SSU rDNA sequences were performed using SSU-Align package (Nawrocki 2009; Nawrocki *et al*., 2009). SSU-Align performs secondary structure alignments based on the covariance model (CM; Cannone *et al*., 2002; see diatom examples in Alverson *et al*., 2007; Nawrocki 2009; Theriot *et al*., 2009). The sequences were aligned to the consensus CM model of Eukarya integrated in the SSU-Align package. Alignment columns with low posterior probability (PP), which generally corresponded to large loops for which positional homology and covarying nucleotides were difficult to assign, were removed using the SSU-Mask routine from the SSU-Align package. The total alignment after masking was 1614 nucleotides (nt) long, and a total of 267 nt were masked. Bioedit (Hall 1999) was used for minor manual adjustments of the alignment. Maximum parsimony analyses were conducted using TNT v1.1 (Goloboff *et al*., 2008). Bayesian analyses were performed using MrBayes v3.1 (Ronquist & Huelsenbeck 2003).

For the parsimony analysis, all characters were treated as unordered and equally weighted. The heuristic tree search consisted of 10,000 replicates of Wagner trees (using random addition sequences) followed by Tree Bisection Reconnection (TBR) branch swapping (saving 10 trees per replication). Branch support was calculated using bootstrap resampling (Felsenstein 1985). One thousand bootstrap replicates were performed as a heuristic tree search consisting of 100 replicates of Wagner trees (with random addition sequences) followed by TBR (saving 20 trees per replicate). For the Bayesian analysis, the choice of the model of sequence evolution was performed using the program Modeltest 3.7 (Posada & Crandall 1998). Modeltest returned GTR + I + G (general time reversible model of DNA substitution) as the optimal model of evolution. Two simultaneous runs were initiated starting from random trees. To ensure that the two runs converged onto a stationary distribution, analyses were run until the average standard deviation of split frequencies was 0.01. Convergence was evaluated using the potential scale reduction factor. Five hundred thousand generations were run, sampling every 100th generation using the settings: Nst = 6, rates = invgamma, statefreqpr = dirichlet (1,1,1,1). Burnin (the number of starting generations discarded from further analysis) was set at 100,000 generations after visual inspection of the likelihood values in Excel. A 50% majority rule consensus tree was constructed using the 'sumt' command of MrBayes. The tree was edited using Figtree v1.3. All new sequences for *L. colosalis* LICOL1 and *Licmophora remulus* LIREM1 have been deposited in GenBank (Table Ap2 1).

Table 4. Comparison of characters of *Licmophora colosalis* with other large species.

Character	*L. colosalis*	*L. remulus*	*L. gigantea*	*L. grandis*
Mucilage stalk	extremely long, extensive, dichotomically branched	mucilage pad	-	*extremely long, dichotomously branched stalks
Colony form	arborescent macroscopy colony	rosette-shaped microscopic colony	-	-
Valve shape	spathulate, gradually tapering to a narrow capitate basal pole	spathulate, abruptly narrowed to a long stem	slightly clavate, gradually attenuated to the basal pole	-
Shape in girdle view	cuneate, gradually narrowed to the basal pole	cuneate, abruptly narrowed to the basal pole	cuneate, noticeably narrowed to the basal pole	-
Valve length (µm)	(142-177) 220-335	158-171	277-322	90-180
Valve width at apical pole (µm)	(15-18.8) 23-27	9-13	24-25.6	10-14
Valve width at basal pole (µm)	4.3-5.7	2.7-3.2	-	-
Striae in 10 µm	23-27	31-37	delicate striation	25 head pole/ 20 foot pole
Areolae in 10 µm	21-26	24-30	-	-
No. head rimoportulae per cell	1	1	-	-
Head pole rimoportula	massive, fan-shaped, in the valve mantle, opening externally	Moderate, fan-shaped, in the valve mantle, no external opening	-	-
Basal rimoportulae, angle to apical axis	45º-90º	90º, pointed towards head pole	-	-
Valvocopula septa	shallow	none	small, quite marginal	deep
Number of slits in multiscissura	29-34	13 (15)	-	-
Plastids	discoid	discoid	endochrome granular	-
References	this study	this study	Mereschkowsky (1901)	* Kützing (1844) Hustedt, F. (1959)

Results

Morphological analysis

***Licmophora colosalis* Belando, Aboal & Jiménez sp. nov.**

DIAGNOSIS: Macroscopic arborescent colonies with extremely long dichotomically branched stalks. Discoid chloroplasts occupy three-quarters of the cell length. Cells (142–177) 220–335 µm long, (15–18) 23–27 µm wide at apical poles and 4.3–5.7 µm at basal poles. Spathulate valves with rounded head poles gradually tapering to a narrow basal pole. Striae 23–27 in 10 µm, 21–26 transapical slightly elongate areolae in 10 µm. Massively fan-shaped rimoportula at the apical pole of one valve located in the valve mantle, and other rimoportula on the basal pole of the other valve orientated at 45º (90º) to the apical axis, opening externally through a discrete elongate pore. Valvocopula has a shallow septum. Multiscissura has 29–34 slits.

GENBANK SEQUENCES: KT321974 (SSU rDNA), KT321972 (*rbc*L).

HOLOTYPE: permanent slide MUB-ALGAS (Bacillariophyta) 798 deposited at the Herbarium Universitatis Murcicae-Diatomeas, Spain. Coll. Belando, M.D. in the Mar Menor lagoon (SE Spain), 20 July 2008.

ISOTYPE: permanent slide (deposit is in progress) deposited in the California Academy of Sciences. Coll. Belando, M.D. in the Mar Menor lagoon (SE Spain), 20 July 2008.

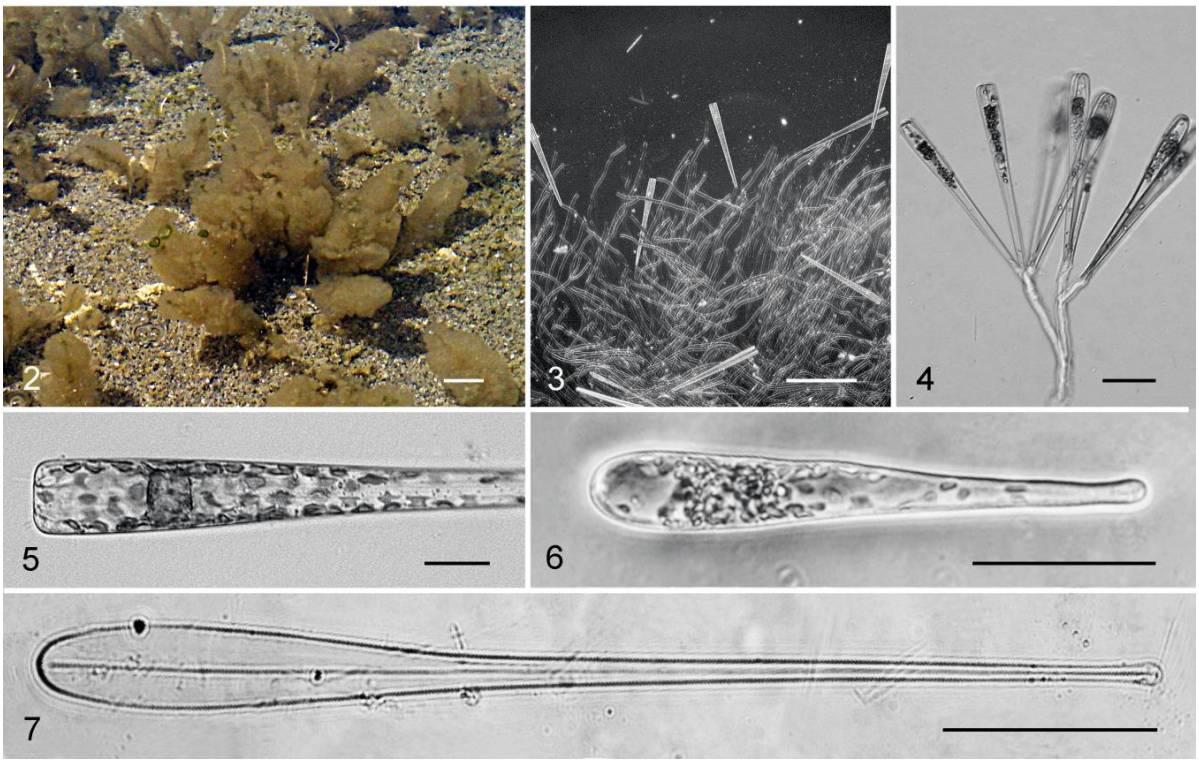

Plate 11. Figs 2 -7 *Licmophora colosalis* sp. nov. live material and light microscope micrographs. All are from the LICOL1 strain (holotype), except Figure 6, which shows the HK366 strain (paratype). **Figure 2**. Underwater photo showing arborescent colonies attach to *Acetabularia* sp. Scale bar = 2 cm. **Figure 3**. Long-branched mucilage stalks forming colonies. Scale bar = 200 μm. **Figure 4.** Detail of mucilage stalk showing dichotomous branching. Scale bar = 50 μm. **Figure 5.** Detail of live cell (in girdle view) showing discoidal plastids. Scale bar = 20 μm. **Figure 6.** Small live cell of L. colosalis (156 μm long). Scale bar = 50 μm. **Figure 7.** Cleaned material showing the valve view of *L. colosalis* cells. Scale bar = 50 μm.

PARATYPE: permanent slide BM 101 805 deposited in the Natural History Museum in London. Coll. Matt P. Ashworth in Florida Bay (Rabbit Key Basin), March 2011.

TYPE LOCALITY: Ciervo Island (37º 39´35.7´´ N, 00º 44´26.1´´ W), epiphyte on *Cladophora dalmatica*, 0.3 m depth.

ETYMOLOGY: from Latin colossus, from Ancient Greek κολοσσός (kolossós, "giant statue"), with reference to the extremely large cells and visible colonies easily recognizable with the unaided eye.

Distribution and field observations

Licmophora colosalis has a wide distribution, including temperate coastal zones in the Mediterranean Sea, the tropical waters of Florida Bay and the arid-subtropical region of the Red Sea (Figure 1). In the Mediterranean sites, populations were extremely dense and formed arborescent colonies that were large enough (3–4 cm) to be visible and recognisable to the unaided eye of the diver (Plate 11 Fig. 2). In the Mar Menor lagoon, the colonies of *L. colosalis* were observed in various years (from 2009 to 2015) spreading rapidly and covering almost the entire surface of macrophyte leaves during summer months (later July–August).

Colony and cells characters

Licmophora colosalis forms macroscopic arborescent colonies (Plate 11 Fig. 2) comprised of extremely long mucilage stalks and numerous cells (Plate 11 Fig. 3). Each cell was individually attached to the substratum through long mucilage stalks that have multiple dichotomous branches (Plate 11 Fig. 4). Most of the cells in situ were 220–335 μm long and 23–27 μm wide but smaller cells were also observed, 142–177 μm long and 15–18

μm wide; these were relatively abundant in the culture (Table 4). In valve view the cells had a rounded apical pole (robust and broad) and gradually tapered to a narrow foot with a capitate pole (Plate 11 Figs. 6-7, Plate 12 Fig. 8, Plate 15 Figs. 27–28), with a pseudosternum visible at LM ×20 magnification (Plate 11 Fig. 7), and striation at ×100 magnification (23–27 striae in 10 μm). The transapical slightly elongate areolae (21–26 in 10 μm) became rounded toward the basal pole. Numerous discoid chloroplasts were distributed for three-quarters of the length of the cell (Plate 11 Fig. 5–6).

One rimoportula was located at the apical pole of one valve and another at the basal pole of the opposite valve, both with variable orientation. The head pole rimoportula was fan shaped and located in the valve mantle, opening both externally and internally (Plate 12 Figs. 9–10). It was relatively large for the genus and had a short stalk (Plate 12 Fig. 10). The basal pole rimoportula of the other valve was orientated at 45º (less frequently at 90º) to the apical axis (Plate 12 Figs. 11–12), opening externally through a discrete elongate pore (Plate 12 Fig. 13). Only sporadically and in deformed cells were three rimoportulae observed per cell, two in one of the valves (one rimoportula in each pole, or joined in the same pole) and another at the basal pole of the opposite valve.

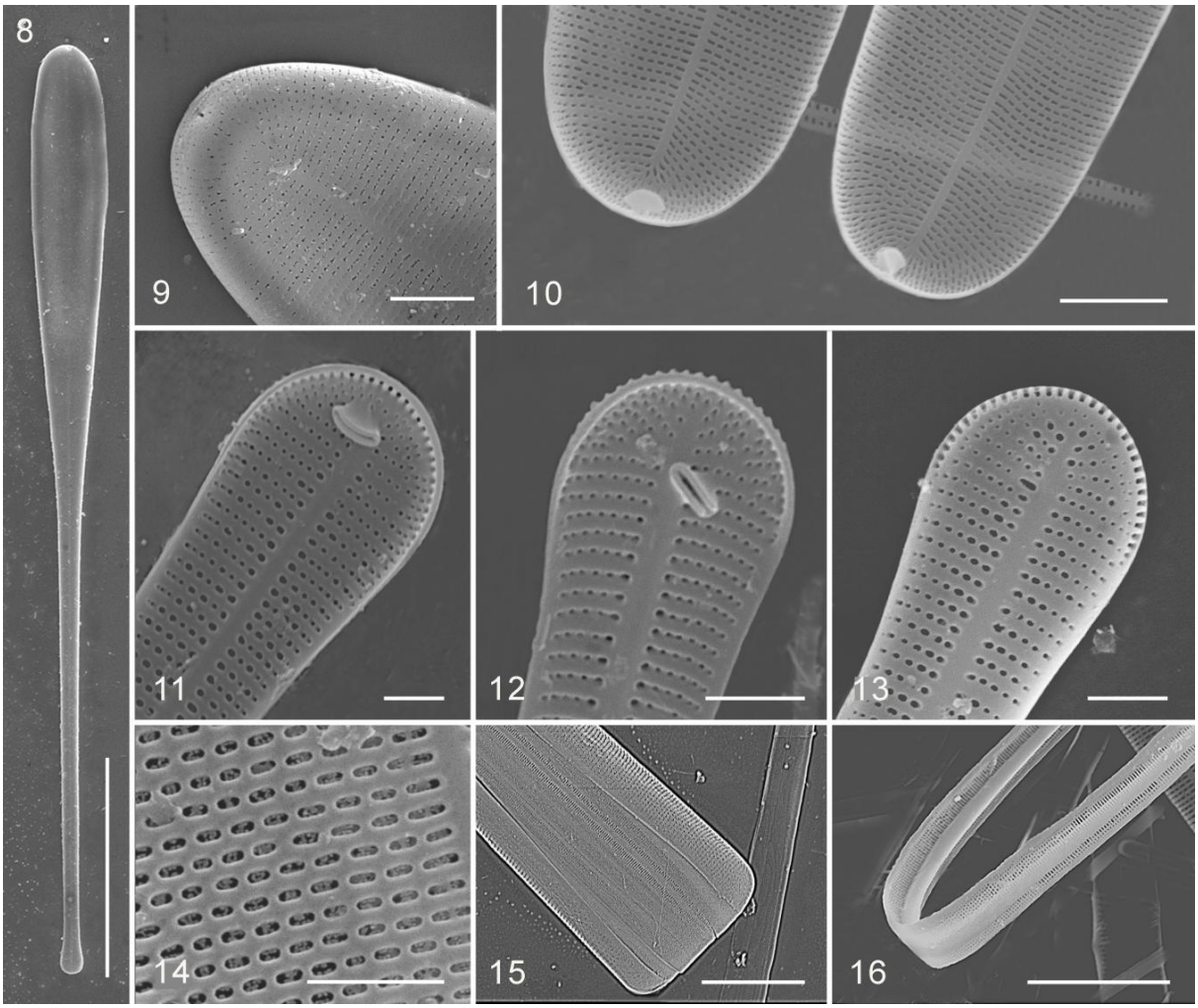

Plate 12. **Figs. 8–16.** *Licmophora colosalis*, SEM micrographs. LICOL1 strain (holotype). **Fig. 8.** Cells gradually tapering toward the basal pole in valve view. Scale bar = 50 μm. **Fig. 9.** Detail of external view of the head pole with rimoportula opening. Scale bar = 5 μm. **Fig. 10.** Internal view of the head pole showing variability in rimoportula orientation. Scale bar = 10 μm. **Figs. 11–12**. Internal view of the basal pole showing variability in rimoportula orientation. Scale bar = 2 μm. **Fig. 13.** External view of the basal pole with the rimoportula's external opening and numerous slits in the multiscissura. Scale bar = 2 μm. **Fig. 14.** Internal view of the valve with detail of areolae, virgae and vimines in the central section of the cell. Scale bar = 2 μm. **Figs. 15–16.** Girdle view of cells on the SEM and detail of girdle bands at the head pole. Scale bar = 10 μm.

Striae were separated by vimines into short and slightly elongate areolae in the transapical direction (Plate 12 Fig. 14) but became rounded toward the basal pole where virgae tended to have radiate patterns (Plate 12 Figs. 11–13). Girdle bands, four or five in number (Plate 12 Fig. 15), had two rows of slits in the wider parts of the cells becoming a line of one pore toward the base (Plate 12 Fig. 16 – Plate 13 Fig. 17). The valvocopula had a shallow septum and an opening at the basal pole (Plate 13 Figs. 18–20).

Phylogeny results

A concatenated alignment of both nuclear and plastid regions from 21 taxa yielded 3087 nucleotide sites (1614 SSU rDNA, 1473 *rbc*L), of which 2528 were constant, 195 variable but parsimony-uninformative and 361 were parsimony-informative. The maximum parsimony analysis (MP) search revealed only one most parsimonious tree (length = 1669 steps; consistency index = 0.600; retention index = 0.591). Both the MP and Bayesian inference searches resulted in trees with similar topology, and the PP/Bootstrap values are therefore provided in the same tree for all analyses (Figure 21).

The phylogeny results supported the assignment of the new species to *Licmophora*, and that clearly separated it from *Licmophora remulus* LIREM1 with high support (1.00/99). *L. colosalis* was grouped in the same clade with the large species *L. flucticulata* and two species that are proposed for renaming (Figure 21). Sequences of the strain HK366 were referred to in the Genbank database as *L. grandis*; however, a revision of morphology of this strain (T.A. Frankovich and Matt P. Ashworth, personal communication) showed its similarity with *L. colosalis*. As both strains were linked in the phylogenetic tree with high bootstrap values (1.00/100), we propose that they are the same species and that strain HK366 should be named *L. colosalis*. Indeed, material of this strain has been proposed as a paratype of *L. colosalis* in this study. On the other hand, the strain HK302 (Table Ap2 1) was referred to as *L. remulus* in the Genbank database. However, the morphological characters of this strain did not match the description of *L. remulus* (M.P. Ashworth, personal communication), and the molecular analysis separated it from *L. remulus* LIREM1. It does not match morphologically with *L. colosalis*, and they have been separated with relatively high support in the phylogenetic tree (0.98/52). Overall these features supported the proposal of this strain as *Licmophora* sp. (Figure 21; Table Ap2 1**¡Error! No se encuentra el origen de la referencia.**) and suggested it needs further investigation.

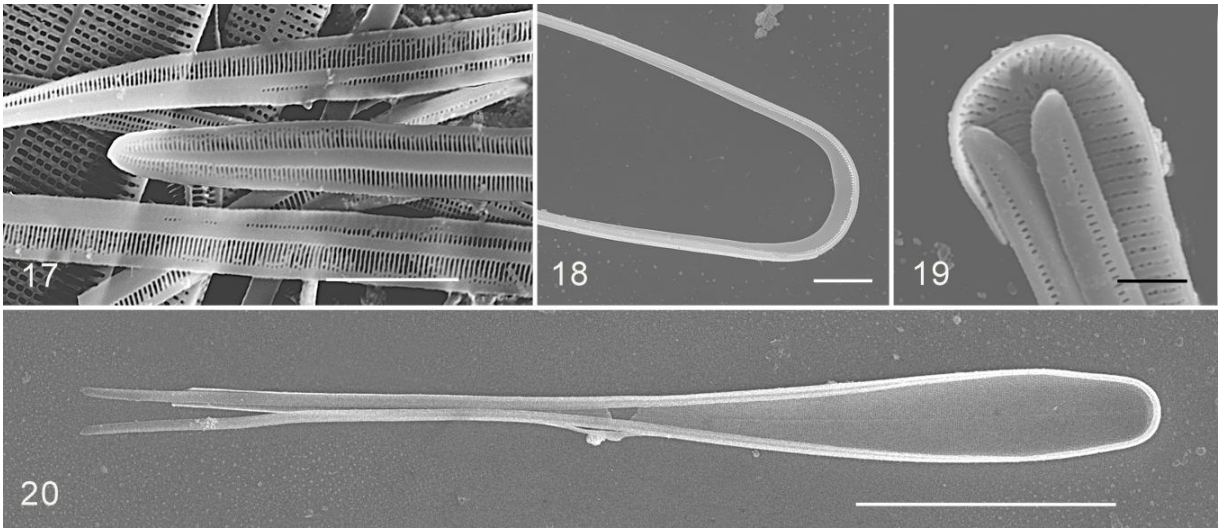

Plate 13. Figs. 17–20. SEM views of girdle bands and valvocopula of *Licmophora colosalis*. **Fig. 17.** Portions of girdle bands with two rows of slits becoming a line of one pore toward the basal pole. Scale bar = 5 μm. **Fig. 18.** Basal pole with open ends of girdle bands. Scale bar = 2 μm. **Fig. 19.** Valvocopula with shallow septum. Scale bar = 5 μm. **Fig. 20.** Internal view of valve showing girdle band opening at the basal pole. Scale bar = 50 μm.

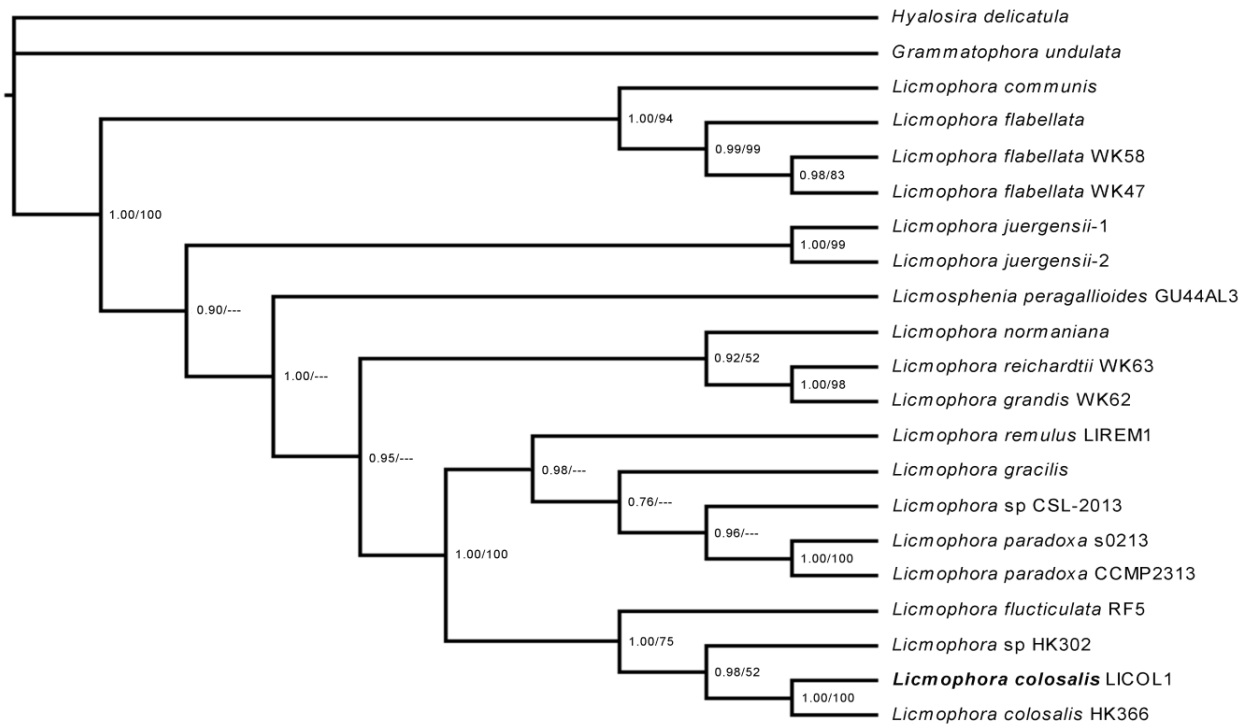

Figure 21. Majority rule consensus tree retrieved by Bayesian phylogenetic analysis of species of *Licmophora*, based on concatenated alignment of two molecular markers, including nuclear markers SSU rDNA and the chloroplast markers *rbcL*. Node support is given on the branches as Bayesian posterior probability/maximum parsimony bootstrap values**.**

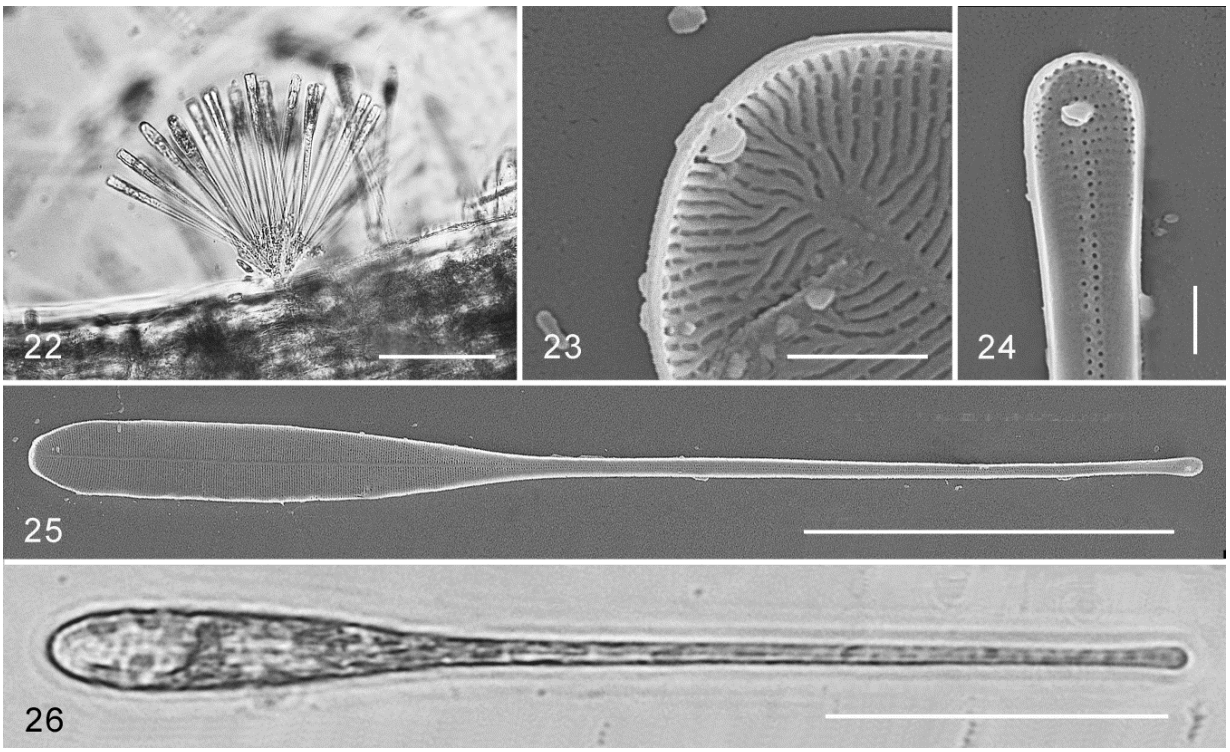

Plate 14. Figs. 22–26. *Licmophora remulus* LIREM1 strain. **Fig. 22**. Live cells forming a rosette-shaped colony that is epiphytic on *Cymodocea nodosa*. Scale bar = 50 μm. **Fig. 23**. Internal view of the apical pole showing rimoportula. Scale bar = 2 μm. **Fig. 24.** Internal view of the basal pole showing rimoportula. Scale bar = 2 μm. **Fig. 25.** Internal view of valve showing an abrupt decrease in width toward the long stem. Scale bar = 50 μm. **Fig. 26.** Living cells showing plastids. Scale bar = 50 μm.

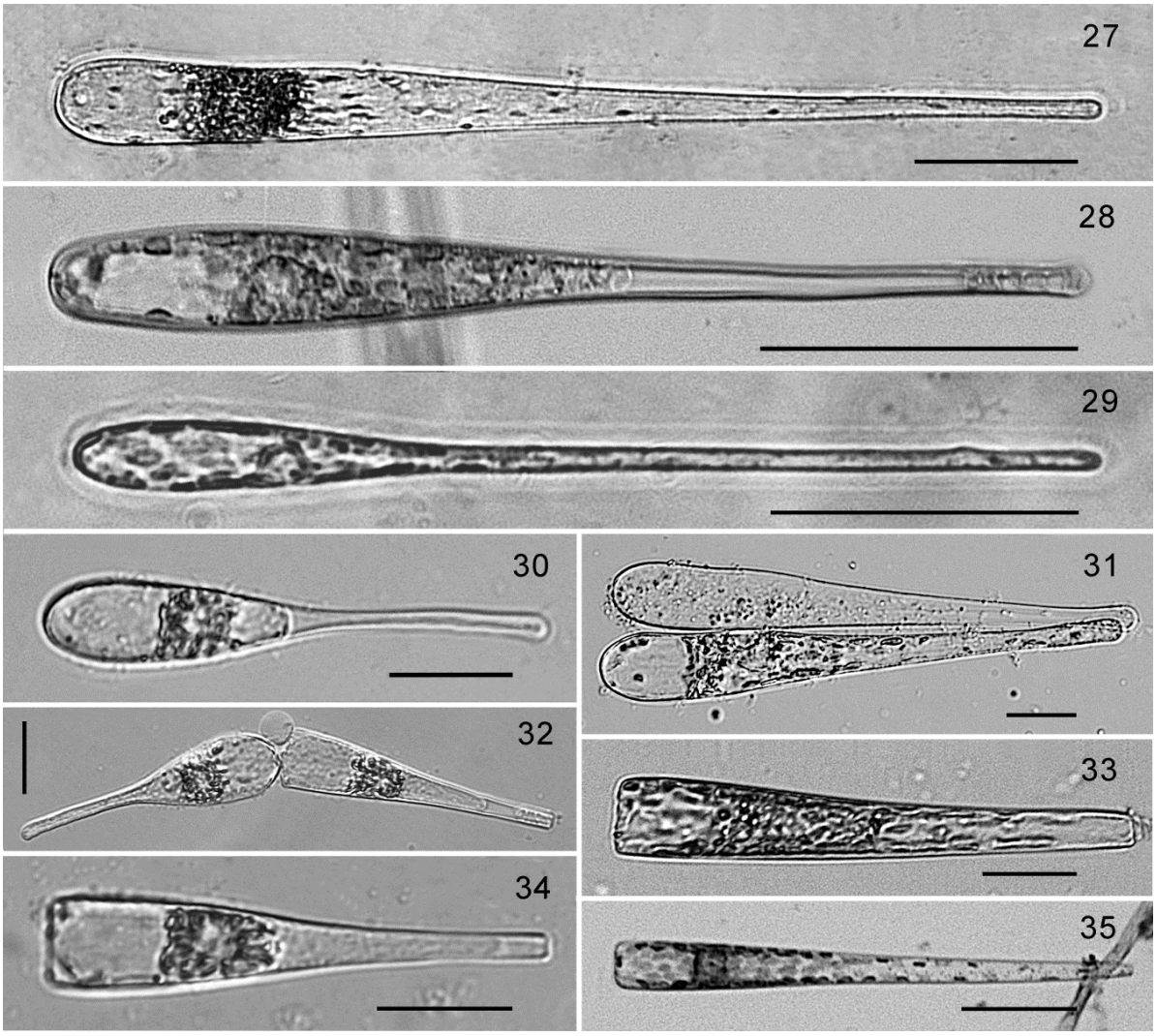

Plate 15. Figs 27–35. Light micrographs of *L. colosalis* and *Licmophora remulus* showing different valve shape. Samples isolated from culture of L. colosalis LICOL1 strain and *L. remulus* LIREM1 strain. **Figs 27–28.** *Licmophora colosalis* valves gradually tapering to a narrow basal pole. Scale bar=50 µm.Fig. 29. *Licmophora remulus* valve abruptly narrowed to a long stem. Scale bar =50 µm. **Fig. 30.** *Licmophora remulus* cell showing abrupt decreasing in valve width from apical to basal pole. Scale bar = 20 µm. **Fig. 31.** *Licmophora colosalis* valves gradually attenuated to the basal pole. Scale bar =20 µm. **Fig. 32.** *Licmophora remulus* cells in valve and girdle view. Scale bar =20 µm. **Fig. 33.** Small cell of *L. colosalis* gradually attenuated toward basal pole in girdle view. Scale bar = 20 µm. **Fig. 34.** *Licmophora remulus* cell showing abrupt attenuation of width in girdle view. Scale bar = 20 µm. **Fig. 35.** *Licmophora colosalis* large cell showing cuneate shape in girdle view. Scale bar =50 µm.

Taxonomic comparisons of species with morphology similar to *L. colosalis*

***Licmophora remulus* Grunow 1867**

Populations of Licmophora remulus from the Mar Menor lagoon were observed as epiphytes on *Cymodocea nodosa* and *Cladophora dalmatica*. They were less abundant than *L. colosalis* in July but highly abundant in September. Cells were attached to the substratum by mucilage pads forming small clusters of cells with a rosette-shaped colony (Plate 14 Fig. 22). Valves had a pronounced spathulate shape with a linear-elliptical upper part that suddenly changed into a very long, narrow stem with a slightly inflated basal pole (Plate 14 Figs. 25–26, 29–30). Cell dimensions are summarized in Table 4. Cells 158–171 µm long but in culture they may be smaller (75–82 µm long, Plate 15 Figs 32, 34). There were two rimoportulae per cell, one in each valve. The head rimoportula in the valve mantle was moderately fan shaped with no external opening and no stalk (Fig.

23). The basal rimoportula was orientated 90º to the apical axis, with a relative large tube pointing toward the head pole (Plate 14 Fig. 24). The multiscissura had 13 (15) slits. There was no septum in the valvocopula.

GENEBANK SEQUENCES: KT321975 (SSU rDNA), KT321973 (*rbc*L).

RECORDS: Fresh material collected and isolated in culture in September 2012. The preserved bulk of cells from the culture (LIREM1 strain) was deposited in the Herbarium Universitatis Murcicae-Diatomeas, Spain. MUB-ALGAS 5815.

***Licmophora gigantea* Mereschkowsky 1901**

The original description for this species did not have an illustration, and some taxonomic characters such as striae density were not mentioned (Table 4). Furthermore, these characteristics cannot be confirmed, as the type material is not available for comparison. Hustedt (1959) did not provide new information about this taxon. Cells had large dimensions, and valvocopula had a marginal septum (Table 4). Valves had delicate striations (not visible in LM) and narrowed abruptly to a basal pole in girdle view (similar to Licmophora remulus).

***Licmophora grandis* (Kützing) Grunow 1880 (=*Riphidophora grandis* var. *arachnoidea* Kützing 1844)**

In the original description, Kützing (1844), depicted this species with extremely long, extensive and dichotomously branched stalks. The morphological description of Licmophora grandis in Hustedt (1959) has been used for comparison in this study and is summarized in Table 4. Peragallo & Peragallo (1897–1908) indicated valves that were 140–160 μm long, with 20–24 striae in 10 μm, with a higher density in the head pole. Honeywill (1998) reported cells that were 40–62 μm long, 9–10 μm wide and with 21–23 striae in 10 μm. The multiscissura had 15–17 slits, and the valvocopula had a deep septum.

Discussion

Licmophora is an easily recognizable genus due to its wedge-shaped cells in valve and girdle views. However, due to incomplete documentation and illustration, it is possible to confuse the identity of several large species of *Licmophora*. For example, *L. colosalis* could be confused with *L. gigantea* Mereschkowsky, which has similar cell dimensions (Table 4). However, Mereschkowsky (1901) noted that cells of L. gigantea had delicate striations (not visible in LM) and an abrupt difference in width between the upper and basal poles of its cells in girdle view, similar to *L. remulus*. Since Mereschkowsky described some species with 24 striae, e.g. *L. proboscidea*, cells of *L. gigantea* probably have a higher stria density than *L. colosalis* (23–27 striae in 10 μm). In addition, specimens of the new species had a moderate narrowing toward the basal pole but not an abrupt narrowing. Tomás (1988) recorded L. gigantea in samples from the Mar Menor but the cell dimensions (254–338 μm long, 16–20 μm broad), striation (21–27 striae in 10 μm) and illustrations seem to correspond to *L. colosalis* as described in this study.

Cells of *Licmophora colosalis* were attached to the substratum by long dichotomously branched stalks similar to those noted in the original description of *L. grandis* (Kützing 1844). Both species have a similar shape in valve view (Hustedt 1959), and small cells of *L. colosalis* could be easily mistaken for *L. grandis* using light microscopy. However, if taxonomic characters are analyzed in detail, both species are clearly different. Cells of *L. colosalis* have larger dimensions (Table 4), with a higher striation density than L. grandis (Peragallo & Peragallo 1897–1908; Hustedt 1959; Honeywill 1998). The valvocopula on *L. colosalis* cells have shallow septa in contrast with the deeper ones described for *L. grandis* (Hustedt 1959; Honeywill 1998). Furthermore, *L. colosalis* has a higher number of slits (29–34) in its multiscissura compared with the 15–17 slits observed in *L. grandis* (Honeywill 1998). Molecular results showed that strain HK366 (referred as *L. grandis* in Genbank database) was closely connected with *L. colosalis* in the phylogenetic tree. Similarly, the morphological revision

of this strain (Matt P. Ashworth and T.A. Franckovich, personal communication) also matched the description of *L. colosalis*. Hence, the strain HK366 is proposed as a paratype of *L. colosalis* in this study. A change of the name of JX401239 (SSU rDNA), JX401257 (*rbc*L) and JX401274 (*psb*C) sequences in GenBank database is in progress.

Molecular results also showed that *Licmophora colosalis* is closely related to *L. flucticulata*, as it is included in the same clade in the phylogenetic tree (Figure 21). Both taxa are among the largest species of *Licmophora* (up to 335 and 850 lm respectively), and they also have massive fan-shaped apical rimoportula located in a valve mantle. The high number of slits in the multiscissura of L. colosalis also match those of *L. flucticulata*, which has 40 slits (Lobban *et al*., 2011). This character is also shared with other species such as *L. flabellata* (Greville) C.Agardh, which has 30–45 (Belando *et al*., 2012; Lobban & Schefter 2013), and *L. comnavmaria*, which has 50 (Lobban & Schefter 2013).

In the field, *Licmophora colosalis* is relatively easy to confuse with *L. remulus*, and they can be found together in epiphytic communities. In the laboratory, both species can be difficult to separate even with light microscopy. The clearest taxonomic characters separating them are the macroscopic arborescent colonies that are formed by the long stalks of L. colosalis, which are easily recognised by the unaided eye. In contrast, the rosette-shaped colonies formed by *L. remulus* are microscopic. Cells of *L. colosalis* in the valve view are wider at both their apical and basal poles and have less dense striation (23–27) than *L. remulus* (31–37). Valves of *L. colosalis* are not abruptly narrowed toward their basal pole (Plate 15 Figs. 27–35) and have higher numbers of slits in the multiscissura (29–34) than *L. remulus* (13–15). Phylogenetically, both species were in separate clades with high support, corroborating the morphological and molecular differences between them.

Licmophora colosalis has a wider geographical distribution and seems to tolerate a high range of salinity: Florida Bay (24–42), the Mediterranean Sea (37), the Mar Menor lagoon (42–47) and the Red Sea (40). In the Mar Menor lagoon *L. colosalis* spreads rapidly in summer months forming macroscopic arborescent colonies and covering great areas of the bottom attached to macrophytes. It has been found colonising Acetabularia acetabulum, *Cladophora dalmatica* and the seagrasses *Cymodocea nodosa* and *Thalassia testudinum*.

REFERENCES

Alverson, A.J., Jansen, R.K. and Theriot, E.C. 2007. Bridging the Rubicon: phylogenetic analysis reveals repeated colonizations of marine and fresh waters by thalassiosiroid diatoms. Molecular Phylogenetics and Evolution, 45(1), pp.193-210.

Belando, M.D., Marín, A. & Aboal, M. 2012. *Licmophora* species from a Mediterranean hypersaline coastal lagoon (Mar Menor, Murcia, SE Spain). Nova Hedwigia 141: 275–288.

Cannone, J.J., Subramanian, S., Schnare, M.N., Collet, J.R., D'Souza, L.M., Du, Y.S., Feng, B., Lin, N., Madabusi, L.V., Muller, K.M., Pande, N., Shang,Z.D., Yu,N., & Gutell, R.R. 2002. The Comparative RNA Web (CRW) Site: an online database of comparative sequence and structure information for ribosomal, intron, and other RNAs. Bmc Bioinformatics 3.

Doyle, J.J. & Doyle, J.L. 1987. A rapid DNA isolation procedure for small quantities of fresh leaf tissue. Phytochemical Bulletin 19: 11–15.

Felsenstein, J. 1985. Confidence limits on phylogenies: an approach using the bootstrap. Evolution 39: 783–791.

Goloboff, P.A., Farris, J.S. and Nixon, K.C., 2008. TNT, a free program for phylogenetic analysis. Cladistics, 24(5), pp.774-786.

Hall, T.A. 1999. BioEdit: a userfriendly biological sequence alignment editor and analysis program for Windows 95/98/NT. Nucleic Acids Symposium Series 41: 95–98.

Honeywill, C. 1998. A study of British *Licmophora* species and a discussion of its morphological features. Diatom Research 13: 221–271.

Hustedt, F. 1959. Die Kieselalgen Deutschlands, Österreichs und der Schweiz unter Berücksichtigung der ubrigen Länder Europas sowie der angrezenden Meeresgebiete. 2 Teil. In: Kryptogamen-Flora von Deutschland, Österreich und der Schweiz (Ed. By L. Rabenhorst). Akademische Verlagsgesellschaft, Leipzig, 845 pp.

Jordan, R.W., Lobban, C.S. & Theriot, E.C. 2009-2015. Western Pacific Diatoms Project. ProtistCentral. http://www.protistcentral.org/index.php/Project/get/project_id/17; searched on december 2015.

Kützing, F.T. 1844. Die kieselschaligen Bacillarien oder Diatomeen. W. Köhne. Nordhausen. 152 pp.

Lobban, C.S. 2013. The marine araphid diatom genus *Licmosphenia* in comparison with *Licmophora*, with the description of three new species. Diatom Research 28: 185–202.

Lobban, C.S. and Schefter, M. 2013. *Licmophora comnavmaria* sp. nov.(Licmophorales, Bacillariophyta), a new diatom with intercalary rimoportulae. Marine Biodiversity Records, 6.

Lobban, C.S., Schefter, M. & Ruck, E.C. 2011. Licmophora flucticulata sp. nov. (Licmophoraceae, Bacillariophyceae), an unusual flabellate species from Guam and Palau. Phycologia 50: 11–22.

Mereschkowsky, C. 1901. Diagnosis of new Licmophorae. Nuova Notarisia Series 12: 141–153.

Nawrocki, E.P. 2009. Structural RNA homology search and alignment using covariance models. PhD thesis. Washington University, St Louis, Missouri. 266 pp.

Nawrocki, E.P., Kolbe, D.L. and Eddy, S.R. 2009. Infernal 1.0: inference of RNA alignments. Bioinformatics, 25(10), pp.1335-1337.

Peragallo, H. & Peragallo, M. 1897–1908. Diatomées marines de france et des districts maritimes voisins. J. Tempère, Grezsur-Loing, France. 491 pp.

Posada, D. and Crandall, K.A. 1998. Modeltest: testing the model of DNA substitution. Bioinformatics (Oxford, England), 14(9), pp.817-818.

Ronquist, F. and Huelsenbeck, J.P. 2003. MrBayes 3: Bayesian phylogenetic inference under mixed models. Bioinformatics, 19(12), pp.1572-1574.

Round, F.E., Crawford, R.M. and Mann, D.G., 1990. Diatoms: biology and morphology of the genera. Cambridge University Press, Cambridge. 747 pp.

Theriot E.C., Cannone J.J., Gutell R.R. & Alverson A.J. 2009. The limits of nuclear-encoded SSU rDNA for resolving the diatom phylogeny. European Journal of Phycology 44: 277–290.

Thompson, J.D., Gibson, T.J., Plewniak, F., Jeanmougin, F. and Higgins, D.G. 1997. The CLUSTAL_X windows interface: flexible strategies for multiple sequence alignment aided by quality analysis tools. Nucleic acids research, 25(24), pp.4876-4882.

Tomás, X. 1988. Diatomeas de las aguas epicontinentales saladas del litoral mediterráneo de la Península Ibérica. PhD thesis. Universitat de Barcelona, Spain. 687 pp.

Woods, D.C. and Fletcher, R.L. 1991. Studies on the strength of adhesion of some common marine fouling diatoms. Biofouling, 3(4), pp.287-303.

Chapter 4

Interactive effects of temperature and nutrient stoichiometry on population dynamics and stalk production of *Licmophora colosalis* (Bacillariophyta): perspective in a climate change scenario

Introduction

Marine ecosystems are one the areas primarily affected by global climate change given its effects on the sea level rise, increased frequency and intensity of storms, and warmer ocean temperatures (IPCC 2007). Coastal ecosystems are considered one of the most vulnerable marine environments to face such changes and their effects (IPCC 2007, LLoret et al., 2008) given their confined nature compared with open seas. Moreover, they are subjected to high variety of pressure derived from the human activity (e.g., delivery of nutrients from surrounding areas), that may exacerbate climate-driven impacts (LLoret *et al*., 2008). Mediterranean regions have been identified as one of the most prominent "Hot spots" in future climate change predictions (Giorgi, 2006), where climate anomalies have exponentially increased in recent decades (Danovaro et al., 2009). Predictions of rises in temperature effects indicate changes in species distribution/abundance according to thermal tolerances and the ability to adapt (Harley et al., 2006, and reference therein). In the last few decades, several mucilage overproduction episodes, of both planktonic and benthonic types, have already been observed on eastern Mediterranean coasts (e.g., De Philippis et al., 2005; Schiaparelli et al., 2007; Sartoni et al., 2008), which have been related to episodes of extremely high temperatures and anomalous increases in seawater temperatures (Danovaro et al., 2009; Mangialajo et al. 2011; Aktan et al., 2011).

This mucilaginous snow mainly consists in macroalgal and microscopic organs, mainly diatoms and cianobacteria, embedded in a matrix of extracellular polymeric substances (EPS) (De Philippis et al., 2005). Most empirical studies have focused on the linkage between EPS overproduction and nutrient supply, but the role of increasing temperature has scarcely been investigated. In this sense, several works have already indicated that nutrient-limited conditions favour the release of EPS in many phytoplankton (e.g. Myklestad 1995) and epipelic species (Alcoverro et al., 2000; Staats et al., 2000,) and benthic intertidal diatoms (Smith & Underwood 2000; Underwood et al., 2004). It has also been proven that nutrient ratios, mainly the N:P ratio of water, can influence EPS production (Myklestad et al., 1972; Myklestad 1995), but the response to high or low N:P ratios can differ among species.

These EPS may play a relevant ecological role for benthic diatom species as this excretion is essential for their motility, and it may also be primarily the component in the attachment of cells with the substratum (Daniel et al., 1987). Specifically in most stalked species, as the complex structure of attachment is constituted mainly by extracellular polymeric substances (Daniel et al., 1987). Some trade-based approaches have pointed out that stalked diatoms are good candidates to discriminate different trophic statuses in freshwater ecosystems (Berthon et al., 2011; Passy 2007). More specific approaches, mainly based on the response of *Didymosphenia geminata* to nutrient environmental conditions, have indicated that phosphorus limitation is the main factor to induce reduced growth, and subsequently to stalks overproduction (e.g. Kilroy & Bothwell 2011; Kilroy & Bothwell 2012). In marine ecosystems, this relationship has been investigated only for stalked diatoms *Licmophora flabellata* (Ravizza & Hallegraeff 2015). These authors indicated that high light intensity was the factor that stimulated stalk formation in *L. flabellata.* The variability in response between these two different species from marine and freshwater environments makes the prediction of occurrences of mucilaginous benthic blooms under changing nutrient and temperature conditions very difficult.

In the global climate change context, for marine unicellular organism the prediction of rising temperature impacts has generally focused on the relationship with changes in the cell size of phytoplankton communities (e.g., Adams et al., 2013; Peter & Sommer 2015). Indeed it is universally assumed that warming will shift the distribution of phytoplankton size towards smaller individuals (Olson et al., 1986, Peter & Sommer 2012). However, this has led to controversy as some studies have either indicated the contrary (Durbin 1977; Thompson et al., 1992) or shown no clear trends (Yoder 1979; Verity 1981). It has also been suggested that other factors, such as nutrients, may even play a more relevant role in cell size change than the direct effect of temperature (Peter & Sommer 2012; Deng et al., 2014; Peter & Sommer 2015), but further research along these lines is recommended. In the light of these facts, predictions of global warming on benthic communities are still difficult in coastal environments, where multiple interactions with other stressors, such as nutrients,

may lead to final impacts on biological communities.To investigate the potential interactive effects of warming and N:P stoichiometry of waters on benthic microalgal species, we selected a stalked benthic diatom, *Licmophora colosalis* Belando, Aboal & Jiménez. It is a widely distributed species from temperate to subtropical waters (Belando et al., 2016), which grows exponentially in summer in the coastal Mar Menor lagoon (Mediterranean Sea), and attaches to the leaves of macrophytes to cover large areas at the bottom. Some *Licmophora* species are also common fouling components in fish farm netting in Australia (Ravizza & Hallegraeff 2015), and are among the dominant diatoms that constitute the benthic mucilaginous aggregates in the Tyrrhenian Sea (De Philippis et al., 2005).

The main aim of the study was to assess the interactive effects of temperature and nutrient limitation on populations of a marine stalked-forming diatom, and to evaluate the suitability of stalks overproduction as an indicator of unbalanced N:P stoichiometry. The population dynamics of *L. colosalis* (cell growth, mortality rate, cell size, biovolume), and the production of stalks and carbohydrates accumulation, were monitored at different N:P stoichiometries (5, 10, 16, 21, 42) and at three temperatures (26 °C, 31 °C, 36 °C) to evaluate current heat episodes and the maximum temperatures predicted for global warming from a Mediterranean coastal lagoon. We hypothesised that N:P ratios interfere with temperature, and that nutrients limitation could become relevant at optimal temperature. Otherwise increasing temperatures could have a stronger impact by promoting carbohydrates overproduction and stalks formation, probably through reduced growth, and that heat stress on the currently maximum (around 31 °C) could even prove drastic for the survival of this species.

Material and methods

Organisms and habitat

To develop the experimental design of this study, we took the temperature variations of the temperate Mar Menor lagoon (SE Spain) as a model. It is one of the biggest coastal lagoons in the Mediterranean Sea, and is highly sensitive to environmental changes as it is a semi-enclosed system subjected to several pressures that derive from human activity. One of the major problems is the delivery of vast quantities of nutrients (mainly nitrates) from surrounding agriculture practices (Pérez-Ruzafa et al., 2005; Velasco et al., 2006) that promote the N:P stoichiometry of water to go above 16, and promoted the eutrophication of the lagoon in 2015 . The temperature of its water varies between 10 °C in January to 31 °C in summer, and it can undergo variations of 5 °C on a daily basis (Terrados 1991). For several years, at least from 2008-2015, and prior to eutrophication, in 2015, we observed that the large epiphytic diatom *L. colosalis* appeared as an epiphyte early in summer (June) when the temperature in the lagoon was around 25 °C (Belando et al., 2016). Later it grew exponentially with increasing temperature (Figure 1.) until approximately the end of August, when temperatures can reach 31 °C, and these populations rapidly declined.

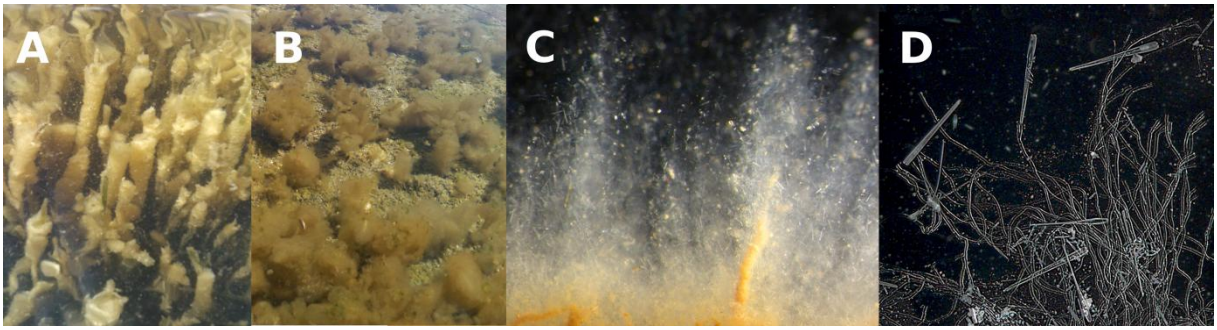

Figure 1. Macroscopic and microscopic view of epiphytic mats of Licmophora colosalis during summer months in the Mar Menor lagoon. **A**. Macroscopic colonies on leaves of *C. nodosa* in august 2015, **B.** Macroscopic proliferations of *L. colosalis* upon *Acetabularia* sp. in June 2015. **C.** Micrographs displayed by a binocular loupes of macroscopic arborescent colonies attached on slides in July 2008, cells are indicated by white arrows. **D.** Optic micrographs showing a detail of the colonies and the large stalks of *L. colosalis.*

Culture conditions and experimental design

Clonal cultures of *L. colosalis* were isolated from the natural populations of the Mar Menor lagoon in June 2015. According to its intrinsic benthic nature, the strain was cultivated in glass Petri dishes (14 cm in diameter) to allow growth on the bottom surface. Initially one diatom cell was added to a Petri dish with f/2 culture (SAG Göttingen, Germany) using a micropipette to ensure monoclonality. Cells were grown in modified f/2 medium at N:P=16, salinity at 44, pH = 8, in an incubation chamber at 25 °C with a 16:8 light:dark cycle (75 µmol photons-m^{-2}.s^{-1} PAR incident light) in an attempt to simulate early summer conditions. Cells were harvested in the exponential phase (when they remain isolated and no formation of aggregates or stalks was observed) to be incubated with the different treatments. Harvesting was done by removing cells from the bottom of the dish with a scraper, and a pellet of cells was obtained by sedimentation. A subsample of the pellet (2 ml) was inoculated in 50 ml of modified f/2 medium for each replicate, which had an initial concentration of 698±190 cells · ml^{-1}.

We conducted factorial short-term nutrient and temperature experiments to test the individual and interactive effects of nutrient limitation (nitrogen and phosphorus) and the increase in temperature on population dynamics (cell growth, mortality rate, cell size, biovolume), production of stalks and carbohydrates accumulation. Nutrient treatments consisted in cultures of modified f/2 medium with a gradient of N:P ratio, including different levels of nitrogen and phosphorus limitation. Five nutrient treatments were applied: highly nitrogen-limited (HNlim, N:P=6), nitrogen-limited (Nlim, N:P=10), balanced (Bal, N:P=16), phosphorus-limited (Plim, N:P=21) and highly phosphorus-limited (HPlim, N:P=42). To obtain the specific N:P ratio for each treatment, the total nitrogen (NT) and total phosphorous (PT) concentrations of the f/2 medium were modified by using different combinations of NaH_2PO_4 (1.6-3.03 mg·L^{-1}) and $NaNO_3$ (10.61-67.7 mg·L^{-1}). The NT and PT concentrations were checked at the beginning and the end of the experiment.

The five levels of N:P treatments were combined with three temperature regimes (26, 31 and 36 °C) in a full factorial design, which resulted in 15 treatment combinations. The coldest temperature (26 °C) simulated the beginning of summer at the Mar Menor lagoon. The 31°C temperature was the maximum value currently observed in the lagoon, and that of 36°C simulated the increase of 4.5 °C following the climate global change prediction (Pascalis et al., 2012). The cultures incubated at 26°C were used as a control, and two different warm treatments were applied. The first, hereafter called the 31°C treatment, consisted in an increase of 5 °C (from 26 °C to 31 °C) on the first day of the experiment. In the second, hereafter called the 36°C treatment, 5 °C was increased on the first day (from 26 °C to 31 °C) and also on the third day (from 31 °C to 36 °C). Three different incubation chambers were used, and the increase in temperature in the warm treatments was gradually applied for 8 h during the light period of each treatment day. All the treatments were checked on each day of the experiment, which finished when stalk production and/or cell death was/were observed. The 31 °C treatment lasted 9 days. It was removed when stalk production was observed in any nutrient treatments (to ensure that this response was related with treatment and not with the limitation of nutrients with time). The 36 °C treatment lasted 5 days as drastic cell death was observed on day 4 of the experiment. The two warm treatments were replicated 5 times, and the control cultures (26 °C) 10 times, because the experiment was sequentially removed (the total number of cultures was 100).

Sampling and analysis

Population dynamics analysis: Morphometric measures and counts.

At the beginning and end of the experiments, counts and morphometric measures of cells and stalks were uninvasively taken by an image analysis of at least 15 images of 1.21 mm^2 per replicate. Image acquisition was systematically recorded with an inverted microscope (Eclipse TE2000-U, Nikon Instruments Europe B.V.) and a camera (Nikon DS-5M). Counts and measures of cells and stalk size were done using the Image J software.

For each replicate treatment, all the cells per image were counted with a mean of 431 cell per replicate and a maximum of 1372 cells per replicate. Fewer cells were counted in some cases (minimum of 100 cells per replicate) where densities were low. Then cell growth was obtained by

$$\text{Growth} = \frac{\text{nº cell}_{t1} - \text{nº cell}_{t0}}{t1 - t0}$$

where nº cell was the number of cells· mL^{-1} and *t* was the time at which the measures were taken. Living and dead cells were also differentiated to calculate the mortality rate (%).

Cell dimensions were displayed for all the cells counted in each replicate, and the total biovolume was calculated by following the ghomphonemoid shape of the geometric models proposed by Sun and Liu (2003). Length and width of cells were directly measured on the captured images, and thickness (transapical view) was obtained from the scanning electron micrographs (scanning electron microscope, JEOL-6100, Oxford Instrument) of the extra cultivated material. Since the warm treatments were removed at different experimentation times, two different stalk development stages were distinguished. Due to the short time that the 36 °C treatments lasted, stalks were found mainly in an incipient development stage in the form of pads, and were only counted, while length could not be measured (Figure 2.1). In the 31 °C treatments, long stalks with a clear entity were observed, which were counted and length was measured (Figure 2.1). Responses related with population dynamics, such as cell growth, mortality and accumulated carbohydrates, were referred to the total of cells. As the mortality rate was high in some treatments, the metrics related with the characteristics of individuals, such as cell size, biovolume and proportion of stalks, corresponded to the responses of live cells.

Carbohydrate pool analysis.

At the end of the experiments cells were scraped from the bottom of the dish, and the resultant cell solution was filtered with GF/F filters precombusted for 1 h at 500 °C. Five filters were used to analyse the total accumulated carbohydrate per treatment, which included cell particulate carbohydrates, extracellular polymeric substances (EPS) and total dissolved carbohydrates. The total concentration was determined following the modified phenol-sulphuric acid method (Pacepavicius et al., 1997). Filters was digested using a mixture of water, phenol 10% and sulphuric acid (1:1:3, v:v:v). Then samples were centrifuged and the carbohydrates in the solution were spectrophotometrically determined, expressed as pg of glucose equivalents per cell (pg glu-equiv. · cel^{-1}).

Statistical analysis.

The effects of the two warm treatments, 31 °C and 36 °C, were independently compared with their controls due to the differential experimentation time. A two-way ANOVA (two factors: N:P ratio and temperature) was performed to assess the global effect of temperature, nutrient limitation, and the interaction of both factors on cell size and accumulated carbohydrate. All the other data sets were analysed using GzLMs with a quasi-Poisson distribution of errors (Zuur et al., 2009). If the N:P ratio x temperature interaction was not significant, a one-way GzLM was, or ANOVA analyses, were performed which each factor independently. Model checking included the visual inspection of the variance-to-mean relationship and linearity of predictors. If the homoscedasticity and normality of model residuals were not met, a more conservative approach was employed using a p-value of 0.01 for the global analysis and *post hoc* analyses with Bonferroni correction to identify the significant differences among treatments (Underwood 1997; Rutherford 2001). The ANOVAs and GzLMs were performed with the R statistical software (R Core Team, 2015).

Table 5. Two-way GzLM and ANOVA results for the effects of the N:P ratio and temperature on all parameters related with the populations dynamics, proportion of stalked cells (stalks) and total carbohydrates (TCH).

Independent variables		Dependent variables					
		Growth	Mortality	Cell size	Stalked cells	Biovolume	Carbohidrates
Main test							
N:P		<0.001	<0.001	<0.001	<0.001	<0.001	<0.001
Temp.		<0.001	<0.001	<0.001	<0.001	<0.001	<0.001
N:P X Temp.		<0.05	<0.001	<0.001	0.15	<0.001	<0.001
Pair wise (factor level)							
N:P fixed		**Chisq/p-value**	**Chisq/p-value**	**Chisq/p-value**	**Chisq/p-value**	**Chisq/p-value**	**Chisq/p-value**
NP=5	26 °C x 31 °C	47.28/<0.001	187.1/<0.001	31.1/<0.001	n.s.	36.7/<0.001	23.61/<0.001
NP=10	26 °C x 31 °C	31.77/<0.001	362.9/<0.001	35.6/<0.001	12.1/<0.01	47.4/<0.001	n.s.
NP=16	26 °C x 31 °C	61.3/<0.001	127.9/<0.001	n.s.	8.1/<0.05	42.1/<0.001	n.s.
NP=21	26 °C x 31 °C	59.4/<0.001	272.1/<0.001	73.1/<0.001	21.3/<0.001	61.6/<0.001	18.3/<0.001
NP=42	26 °C x 31 °C	49.85/<0.001	335.5/<0.001	23.3/<0.001	34.9/<0.001	58.4/<0.001	19.9/<0.001
Temp. fixed	**N:P values**						
26 °C	16 X 5	46.2/<0.001	n.s.	n.s.	n.s.	12.4/<0.01	n.s
	16 X 10	65.2/<0.001	n.s.	n.s.	n.s.	n.s.	n.s
	16 X 21	10.2/<0.05	n.s.	n.s.	n.s.	n.s.	n.s
	16 X 42	49.3/<0.001	n.s.	n.s.	62.2/<0.001	n.s.	n.s
	5 x 10	n.s.	n.s.	n.s.	n.s.	n.s.	n.s
	20 x 41	15.7/<0.01	n.s.	n.s.	n.s.	n.s.	n.s
31 °C	16 X 5	37.6/<0.001	146.6/<0.001	27.1/<0.001	n.s.	13.4/<0.01	65.9/<0.001
	16 X 10	23.4/<0.001	176.5/<0.001	35.4/<0.001	n.s.	12.4/<0.01	46.9/<0.001
	16 X 21	17.37/<0.001	184.9/<0.001	64.3/<0.001	12.5/<0.01	n.s.	54.2/<0.001
	16 X 42	45.4/<0.001	145.8/<0.001	31.2/<0.001	20.1/<0.001	22.22/<0.001	81.7/<0.001
	5 x 10	n.d.	n.s.	n.s.	n.s.	n.s.	n.s
	20 x 41	10.1/0.046	n.s.	n.s.		10.7/<0.05	n.s

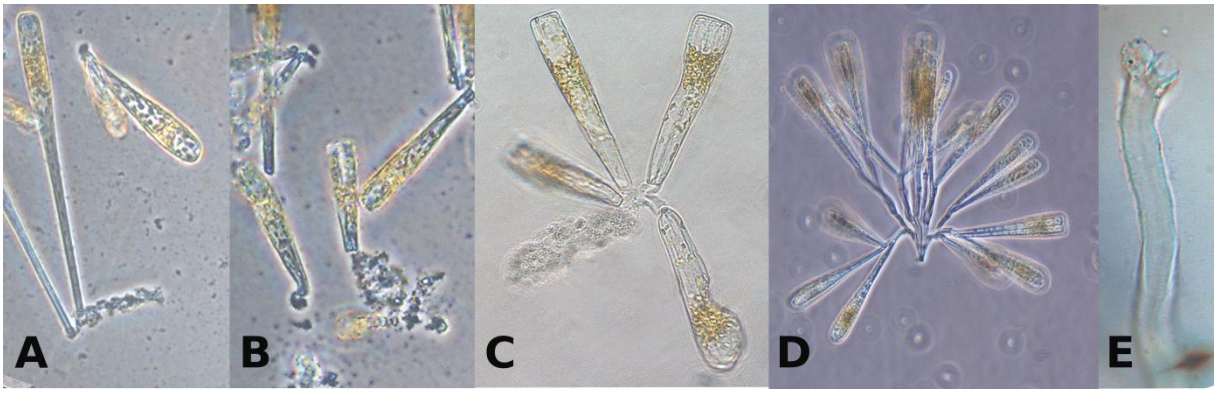

Figure 2. Micrographs of cultures of *L. colosalis*. **A, B.** Amorphous mucilage and incipient stage of stalks excreted by an apical pole of cells. *C. Amorphous mucilage* and stalks, **C.** Colony attached to the substratum by numerous long stalks, **D.** Detail of a upper part of stalks.

Results

The results of GlzMs and ANOVAs showed that the N:P ratio and temperature significantly modified all the analysed variables. Both factors gave a significant interaction when the 31 °C treatment was analysed (Table 5), but this was not the case of the 36 °C treatment, as 100% of the cells died after 24 h. In general, increasing temperature up to 31 °C significantly modified the responses to the gradient of the N:P ratios (Table 5), except for cell growth and stalks production, which showed similar patterns to the control treatments (Figure 3.). With the higher heat stress up to 36 °C, nutrient limitation and temperature significantly modified cell growth and accumulated carbohydrates, while the mortality rate was only statistically altered by temperature. All the cells died within 24 h of reaching 36 °C. Therefore, it was not possible to measure all the parameters related with live cells (cell size, biovolume, stalked cells) in this treatment. Interesting metrics (e.g., number of incipient stalks) were measured and referred to the total of cells. The remarkable findings are indicated in the paragraphs below. The graphs are showed in the supporting information section (Figure Ap 3 1).

Population dynamics: morphometrics measures and counts.

In general cell growth was greater in balanced N:P treatments than under nutrient-limited conditions (Figure 3.). At 26 °C maximum growth corresponded to the balanced treatment, which significantly reduced in the N-limited (HNlim, Nlim) and HPlim treatments (Table 5). The increase of 5 °C significantly reduced cell abundance in all cases, but the patterns of variation among the different nutrient treatments remained similar (Bal=Plim> HPlim=Nlim=HNlim). In the 36 °C treatments, only the cultures grown under the balanced N:P conditions increased in abundance (181±76 cells .ml-1 , mean±SD).

The two warm treatments significantly increased the percentage of dead cell as regards the cultures grown at 26 °C (Table 5). The increase of 5 °C induced higher mortality rates in the nutrient-limited treatments (59-83%) than in the balanced treatments (21%, Figure 3.). The increase of temperature up to 36 °C promoted drastic cell death (100%) after 24 h, while only 4% of the total cells died in its control.

The unique significant change in cell size was observed as a response to the increase of 5°C under nutrient-limited conditions (Figure 3, Table 5). After the increase to 31°C, cell length increased significantly in the nutrient-limited treatments (195±7 µm) compared with the balanced treatments (127±8.9). All the cells treated with 36 °C or the control at 26 °C were similar in length (120.5±4.9 µm long, mean±SD).

The highest total biovolume (um3) was observed in the balanced N:P treatments at 26°C and tended to decrease under the nutrient-limited conditions (Figure 3), but significantly reduced in the HNlim treatment. The increasing temperature up to 31 °C significantly reduced the total biovolume in all cases compared with the cultures grown at 26 °C (Table 5).

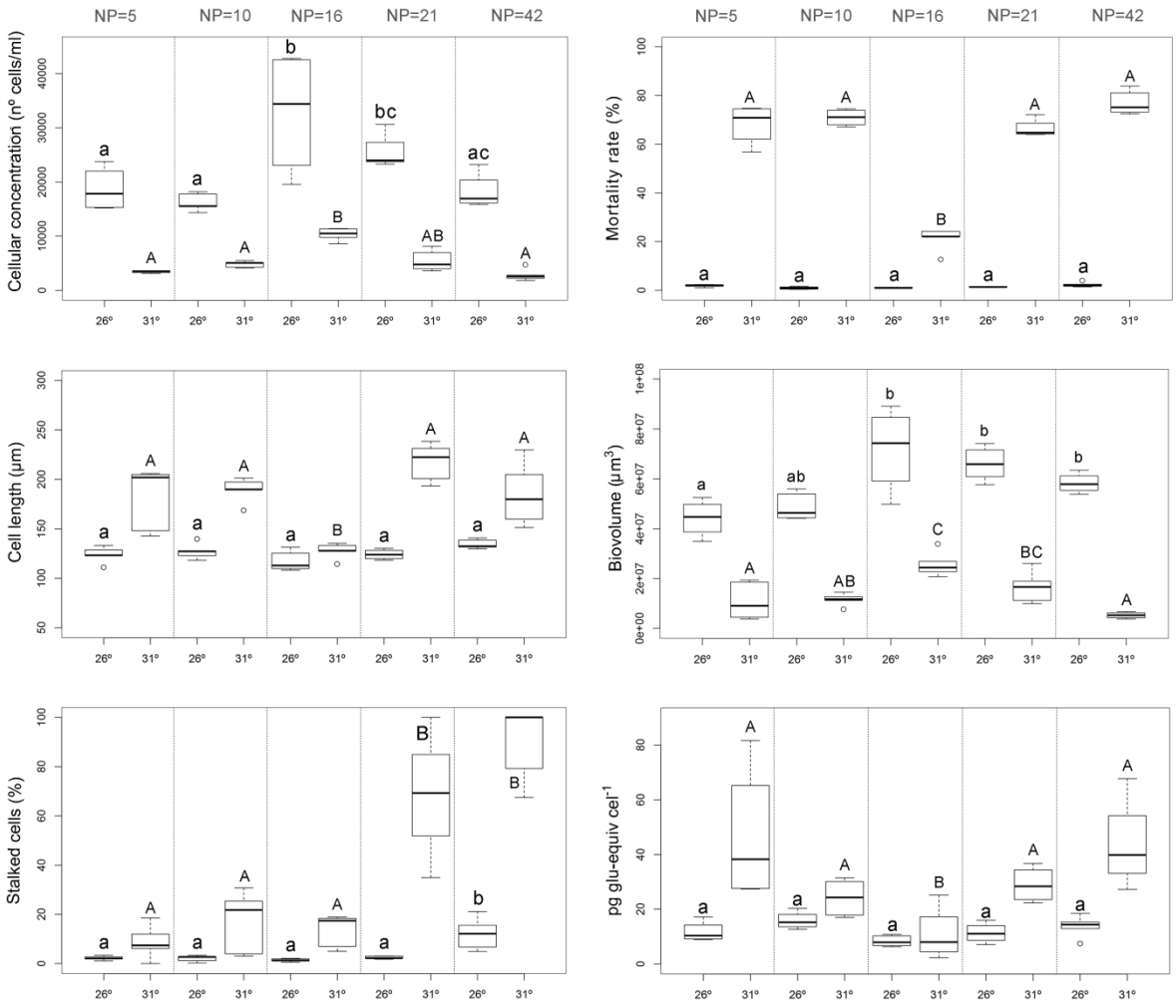

Figure 3. *L. colosalis* responses to the gradient of N:P ratios at 26 and 31 °C. Capital letter indicates significant differences among N:P treatments at 31 °C, and regular letter at 26 °C.

The percentage of cells attached to stalks showed the same response patterns to the N:P treatments at the three analysed temperatures. In general, the percentage of stalked cells remained similar in the treatments with N:P values of 16 or below, while the P-limited treatments promoted a significant increase in stalk production. At 26 °C only the HPLim treatment induced a significant increase in the percentage of stalked cells compared with all the other N:P treatments (Figure 3). The increase of 5 °C significantly stimulated stalk production in all the N:P treatments as regards the 26 °C treatments, except for the HNlim treatment. Besides, both Plim and HPLim treatments led to a significantly increase in the percentage of stalked cells compared to all the other N:P treatments at this temperature. Despite drastic cell death occurring at 36 °C, we observed numerous stalks in an incipient phase (pads, Figure Ap 3 1), and we found consistent responses over the gradient N:P treatments. The higher percentage of stalked cell was also observed in HPlim (3%) compared to all the other treatments (<1%).

Accumulated carbohydrate pool. The concentration of total carbohydrates (TCH) showed the same patterns of response at the three temperatures, and tended to increase from the balanced N:P ratios under the nutrient-limited conditions (N and P), but the significant differences observed among treatments (Figure 3, Table 5) were observed only after the increase of 5 °C (at 31 °C). At a higher N or P limitation level, more TCH accumulated, but not significantly. Despite the responses being consistent in the cultures incubated at 36°C, the response was less evident due to the short experimentation time (Figure Ap 3 1).

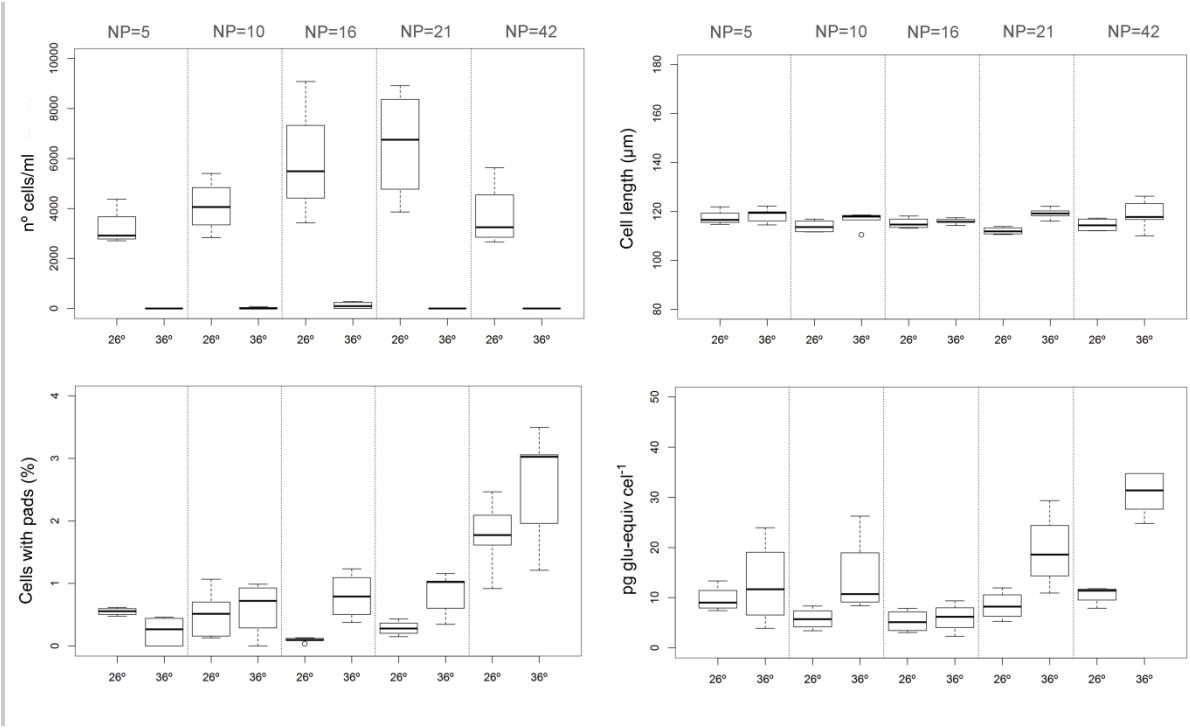

Figure 4. Summary of responses to the gradient of N:P ratios at 26 and 36ºC. Grey box correspond to responses at 36ºC treatment and white box at 26ºC. Capital letter indicates significant differences among N:P treatments at 31ºC, and regular letter at 26ºC.

Discussion

The results of this study can help to understand epiphytes proliferation dynamics in temperate marine ecosystems during the warm season, and also highlight the drastic negative effect of global warming on the large diatoms that grow in environments with an unbalanced N:P stoichiometry.

Based on all the responses of *Licmophora colosalis*, we found that its optimal growth temperature came close to 26 °C, and that increasing temperature generally had a deleterious effect on this species' fitness, which was lethal at 36 °C. We detected that at its optimal growth temperature, *L. colosalis* could live within a wide range of N:P stoichiometries as mortality was not observed in any N:P treatment. However, it seemed to better adapt to the environments with an N:P stoichiometry between 16 and 21 as its growth and biolovolume was negatively affected when it grew in the medium with N:P ratios beyond this range. The strongest impacts were observed under N-depleted conditions. These responses may explain why *L. colosalis* is highly abundant in early summer months when temperatures come close to 26 °C, or go slightly higher ≈28.5 °C in July, in the nitrate-enriched waters of the Mar Menor lagoon.

The main effect of an increasing temperature of 5 °C, but below the lethal temperature, was a reduction in abundance and biovolume due to decreased growth and the mortality of a high percentage of individuals. However, the effects of warming were also modulated by the N:P stoichiometry of water, which promoted higher mortality rates at unbalanced N:P ratios (58-82%) than when grown under balanced conditions (20%). These responses could explain why a population of *L. colosalis* tended to disappear in August when the shallow Mar Menor lagoon water may reach 31 °C, and highlight that the continuous heat waves linked to global climate change could alter the populations dynamics of this species and of similar ones, which might may be at risk of disappearing in the future.

The declining biovolume that accumulated with increasing temperature was consistent with the biomass responses of phytoplankton (Peter & Sommer 2012; Peter & Sommer 2015) and some benthic diatom communities (Svensson & Snoeijs 2014). This response is generally related with a reduced cell size of the constituting diatom species, and with decreasing abundance. In line with this, Peter & Sommer (2012) also highlighted that large species can be at a greater disadvantage when it comes to coping with heat stress than smaller species, and suggested that the body size of large diatoms could decrease more. Our results confirmed that when heat stress went above its optimal temperature, it could have strong deleterious effects on the abundance of populations of the large diatom *L. colosalis*, and we also detected that size changes seemed strongly modulated by the N:P stoichiometry of water. Indeed body size changed only when temperature was combined with nutrient limitation, and the response was an enlarged cell size, which remained constant under balanced conditions. The bath cultures used in this study had minimum values (129±8.9 µm) within the cell size range of this species (maximum 335 µm), therefore we expected heat stress to not affect cell size. Since cell enlargement only occurred when the growth rate was strongly limited, the increase in the size of live individuals could be interpreted as a strategy to enhance S/V ratios, which could benefit their nutrient capitation ability and, therefore, a survival strategy in highly stressed environments. Overall, these responses first suggested that: changes in body size with increasing temperature may vary among species, which is consistent with the varied responses cited in previous studies (e.g. Verity 1981; Olson et al., 1986; Thompson et al., 1992; Peter & Sommer 2012). Secondly, shifts in body size was driven more by the joint temperature+nutrient limitation effects than by the direct effects of temperature, which agrees with what has been indicated for phytoplankton species (Peter & Sommer 2012; Peter & Sommer 2015). These results do not contradict reduced mean size of whole communities with increasing temperature, but highlight the variability in response that can be found between small and large species, and could help to better interpret the global climate change effects on benthic communities.

In general, the overall responses related with populations dynamics indicated that temperature could have a stronger impact when growth was also nutrient-limited. Consequently, L. colosalis accumulated the largest amount of carbohydrates when growth was strongly disrupted by both nutrient deprivation and heat stress. It is well-known that nutrient depletion favours the release of extracellular polymeric substances in diatoms (e.g., Myklestad et al., 1972; Myklestad 1995, Obernosterer et al., 1995; Alcoverro et al., 2000; Staats et al., 2000; Abdullahi et al., 2006). This phenomenon is understood as a manifestation of photosynthetic overflow production when insufficient nutrients are available to sustain cell division and light levels favour photosynthetic activity (Staats et al., 2000). Under these conditions a slower growth rate means more carbon than that needed would be available, which is used for the synthesis of extracellular polymeric substances (Staats et al., 2000; Underwood & Paterson 2003). The responses of *L. colosalis* seemed to follow these patterns as the amount of carbohydrates was always larger under the N- or P-limited conditions than at a balanced N:P ratio, and was larger with lower growth rates. The fact that an increase in temperature from 26 to 31 °C amplified carbohydrates production highlighted the strong impact that global warming could have on the overproduction of benthic mucilaginous aggregates. Indeed the proliferation of benthic aggregates composed of macroalgae and diatoms has already been observed in some areas of the Mediterranean sea ig spring-summer months (e.g. De Philippis et al., 2005; Sartoni et al., 2008). *Licmophora colosalis* did not produce extracellular polymeric substances to coat its frustules in the forms of sheaths or capsules, which agrees with what has been indicated for other species of Licmophora, which form benthic mucilage aggregates in the Tyrrhenian Sea (De Philippis et al., 2005). However, it excreted amorphous mucilage though the basal pole by which it was attached to the substratum (Figure 2). We observed that the substratum surface occupied by this excretion was maximum under nutrient depletion at 31 °C (data not shown), and followed similar carbohydrates overproduction patterns at these temperatures. This amorphous excretion was observed mainly under nutrient-depleted conditions and it was noted before stalks formation in some cases (Figure 2). This finding suggested that extracellular metabolism overflow production could be excreted in this manner, but further research is required to confirm this.

Some studies, which have essentially focused on stalked freshwater species, have already suggested that under unfavourable growth conditions, photosynthetic EPS are channelled in the form of polysaccharide stalk material (Perkins 2010; Kilroy & Bothwell, 2011). As far as we know, in marine systems the linkage of nutrient and stalk production has been essentially investigated for *Licmophora flabellata* (Ravizza & Hallegraeff 2015). In this case stalk formation was essentially stimulated by high light intensity (233 µmol photons m^{-2} s^{-1}, similarly to our study), whereas nutrients or temperature did not influence growth rates or stalk formation/length. These results did not match the responses of *L. colosalis* or those of other marine and freshwater stalked-diatoms (Lewis et al., 2002; Bothwell & Kilroy, 2011; Perkins 2010). *L. colosalis* clearly produced the largest amounts of stalks when cell division rates were limited by phosphorus. The linkage between the number of stalked cells and P-limited growth was consistent at all temperatures, and became even more evident when the growth rate significantly lowered at 31 °C. The amplified responses with heat stress were detected at both levels; the number of stalks reached 85-100% of the stalked cells, and increased sensitivity no matter what the level of low or high P-limitation. Heat stress also favoured the formation of larger stalks as regards the control at 26 °C, which has been previously found for other freshwater benthic diatoms, like *Gomphonema* sp and *Didymosphenia* (Perkins 2010). However, we found no clear relationship of stalk length with nutrients depletion or cell density, as indicated for *Didymosphenia* (Kilroy & Bothwell 2011) and *Achnanthes* (Lewis et al., 2002), respectively. As our study ended immediately after detecting stalk formation after 9 days, our findings only allow us to indicate that in the initial stalk formation stage of formation, stalk length seems inversely related with the number of stalked cells. Probably more prolonged exposure times could allow stalks enlargement and clearer results could be elucidated.

Our findings agree with stalks formation patterns of *Didymosphenia geminata.* It forms blooms in oligotrophic rivers, where it has been proven that stalks overproduction is linked to the growth P-depleted conditions of overlying waters (Bothwell & Kilroy 2011; Kilroy & Bothwell 2011; Kilroy & Bothwell 2012). This proliferations consists mainly in stalk material (Bray, 2014), which has been interpreted as an adaptation mechanism to maximise the phosphate supply under chronic phosphorus-limited environments (Bray et al., 2017) . In this species, phosphatase activity has been localised on or within stalks (Ellwood & Whitton 2007; Aboal et al., 2012,) by means of cells that can uptake organic phosphate; e.g. from the surrounding mucilage matrix, it is hydrolyzed in the tubular structure and is then passed to cells in its inorganic forms (Kirkwood et al., 2007; Aboal et al., 2012).

Since the stalks structure of *Licmophora colosalis* (Figure 2) seems similar to those of *D. geminata* (Aboal et al., 2012), and the high percentage of mucilaginous mass consisted in stalk material in both species (Bray 2014, Figure 1), our findings seem to generally indicate that the stalks of *L. colosalis* could also perform a significant function to live in marine coastal systems with a high N:P stoichiometry of water. All our findings indicate that this species might also possess the phosphatase activity located in stalks, but further research is needed to confirm this hypothesis.

We conclude that the effects of rising temperature on *L. colosalis* populations are modulated by the stoichiometry N:P ratio of the environment. This species seem to be adapted to environments with N:P ratios that fall within the 16-21 range, and the optimal growth temperature comes close to 26 °C, but it will better overcome the increasing temperature under balanced conditions. The increase of 5 °C could have strong impacts on the populations that live in waters with an unbalanced N:P stoichiometry as it could reduce cell growth and promote high mortality rates. The strong reduction in growth under these conditions is reflected in EPS overproduction under nutrient-limited conditions (N or P), and by the high stalks production only in environments with P-limited conditions. The stimulation of stalks production of by P-limited conditions was consistent at both 26 °C and 31 °C, which indicates its suitability as an indicator of high N:P stoichiometry of water, which is related with nutrients contamination. Hence this species could be ideal for monitoring nutrient contamination in marine coastal systems.

In addition, effects of global warming on the body size of this large benthic microalgae are driven more by the combined effects of temperature and stoichiometry of water than by a direct effect of temperature, which at least promotes short-term body size enlargement, probably as a strategy to increase the capacity to capture nutrients. This could help to better understand the universal trends of the decreasing mean size of microalgal communities with global climate change.

By extrapolating our results to the real Mar Menor lagoon scenario, *L. colosalis* already comes close to its thermal tolerances in summer, and if global climate change predictions come true, population dynamics and seasonal patterns can strongly alter, at least in the lagoon shallow areas where temperature will possibly reach 36 °C. These results have important ecological implications as *L. colosalis* is a widely distributed species and its drastic death with increasing temperature could have major impacts on the functioning of shallow coastal systems.

References

Abdullahi, A. S., Underwood, G. J., & Gretz, M. R. 2006. Extracellular matrix assembly in diatoms (Bacillariophyceae). V. Environmental effects on polysaccharide synthesis in the model diatom, Phaeodactylum tricornutum. Journal of Phycology, 42(2), 363-378.

Aboal, M., Marco, S., Chaves, E., Mulero, I. and García-Ayala, A. 2012. Ultrastructure and function of stalks of the diatom *Didymosphenia geminata*. Hydrobiologia, 695(1), pp.17-24.

Adams, G.L., Pichler, D.E., Cox, E.J., O'gorman, E.J., Seeney, A., Woodward, G. and Reuman, D.C. 2013. Diatoms can be an important exception to temperature–size rules at species and community levels of organization. Global change biology, 19(11), pp.3540-3552.

Aktan, Y. & Topaloğlu, B. 2011. First record of *Chrysophaeum taylorii* Lewis & Bryan and their benthic mucilaginous aggregates in the Aegean Sea (Eastern Mediterranean). Journal of Black Sea/Mediterranean Environment, 17(2).

Alcoverro, T., Conte, E. and Mazzella, L. 2000. Production of mucilage by the Adriatic epipelic diatom *Cylindrotheca closterium* (Bacillariophyceae) under nutrient limitation. Journal of Phycology, 36(6), pp.1087-1095.

Belando, M.D., Aboal, M., Jiménez, J.F. and Marín, A. 2016. *Licmophora colosalis* sp. nov.(Licmophoraceae, Bacillariophyta), a large epiphytic diatom from coastal waters. Phycologia, 55(4), pp.393-402.

Berthon, V., Bouchez, A. and Rimet, F., 2011. Using diatom life-forms and ecological guilds to assess organic pollution and trophic level in rivers: a case study of rivers in south-eastern France. Hydrobiologia, 673(1), pp.259-271.

Bothwell, M.L. and Kilroy, C. 2011. Phosphorus limitation of the freshwater benthic diatom *Didymosphenia geminata* determined by the frequency of dividing cells. Freshwater Biology, 56(3), pp.565-578.

Bray, J. P. 2014. The invasion ecology of *Didymosphenia geminata.* Ph.D. Thesis, University of Canterbury,195 pp.

Bray, J., O'Brien, J. and Harding, J.S. 2017. Production of phosphatase and extracellular stalks as adaptations to phosphorus limitation in *Didymosphenia geminata* (Bacillariophyceae). Hydrobiologia, 784(1), pp.51-63.

Daniel, G. F., Chamberlain, A. H. L., & Jones, E. B. G. 1987. Cytochemical and electron microscopical observations on the adhesive materials of marine fouling diatoms. British phycological journal, 22(2), 101-118.

Danovaro, R., Umani, S.F. and Pusceddu, A. 2009. Climate change and the potential spreading of marine mucilage and microbial pathogens in the Mediterranean Sea. PLoS One, 4(9), p.e7006.

De Pascalis, F., Pérez-Ruzafa, A., Gilabert, J., Marcos, C. and Umgiesser, G. 2012. Climate change response of the Mar Menor coastal lagoon (Spain) using a hydrodynamic finite element model. Estuarine, Coastal and Shelf Science, 114, pp.118-129.

De Philippis, R., Faraloni, C., Sili, C. and Vincenzini, M. 2005. Populations of exopolysaccharide-producing cyanobacteria and diatoms in the mucilaginous benthic aggregates of the Tyrrhenian Sea (Tuscan Archipelago). Science of the total environment, 353(1), pp.360-368.

Deng, J., Qin, B., Paerl, H.W., Zhang, Y., Wu, P., Ma, J. and Chen, Y. 2014. Effects of nutrients, temperature and their interactions on spring phytoplankton community succession in Lake Taihu, China. *PloS one, 9*(12), p.e113960.

Durbin, E.G. 1977. Studies on the autecology of the marine diatom *Thalassiosira nordenskioeldii*. II. The influence of cell size on growth rate, and carbon, nitrogen, chlorophyll a and silica content. Journal of phycology, 13(2), pp.150-155.

Ellwood, N.T.W. and Whitton, B.A. 2007. Importance of organic phosphate hydrolyzed in stalks of the lotic diatom Didymosphenia geminata and the possible impact of atmospheric and climatic changes. Hydrobiologia, *592* (1), pp.121-133.

Giorgi, F. 2006. Climate change hot-spots. Geophysical research letters, 33(8).

Harley, C.D., Randall Hughes, A., Hultgren, K.M., Miner, B.G., Sorte, C.J., Thornber, C.S., Rodriguez, L.F., Tomanek, L. and Williams, S.L. 2006. The impacts of climate change in coastal marine systems. Ecology letters, *9*(2), pp.228-241.

IPCC, 2007: Climate Change 2007: Impacts, Adaptation and Vulnerability. Contribution of Working Group II to the Fourth Assessment Report of the Intergovernmental Panel on Climate Change, M.L. Parry, O.F. Canziani, J.P. Palutikof, P.J. van der Linden and C.E. Hanson, Eds., Cambridge University Press, Cambridge, UK, 976pp.

Kilroy, C. & Bothwell, M.L. 2012. *Didymosphenia geminata* growth rates and bloom formation in relation to ambient dissolved phosphorus concentration. Freshwater Biology, *57*(4), pp.641-653.

Kilroy, C. & Bothwell, M. L. 2011. Environmental control of stalk length in the bloom-forming, freshwater benthic diatom *Didymosphenia geminata* (Bacillariophyceae). Journal of Phycology, *47*(5), pp.981-989.

Kirkwood, A.E., Shea, T., Jackson, L.J. and McCauley, E. 2007. *Didymosphenia geminata* in two Alberta headwater rivers: an emerging invasive species that challenges conventional views on algal bloom development. Canadian Journal of Fisheries and Aquatic Sciences, *64*(12), pp.1703-1709.

Lewis, R.J., Johnson, L.M. and Hoagland, K.D. 2002. Effects of cell density, temperature, and light intensity on growth and stalk production in the biofouling diatom *Achnanthes longipes* (Bacillariophyceae). Journal of Phycology, 38(6), pp.1125-1131.

Lloret J, Marin A, Marin-Guirao L. Is coastal lagoon eutrophication likely to be aggravated by global climate change? Estuarine Coastal and Shelf Science 2008; 78: 403-412.

Mangialajo, L., Ganzin, N., Accoroni, S., Asnaghi, V., Blanfuné, A., Cabrini, M., Cattaneo-Vietti, R., Chavanon, F., Chiantore, M., Cohu, S., Costa, E., Fornasaro, D., Grossel, H., Marco-Miralles, F.,Masó, M., Reñé, A., Rossi, A.M., Sala, M.M., Thibaut, T., Totti, C., Vila, M., Lemée, R. 2011. Trends in *Ostreopsis* proliferation along the Northern Mediterranean coasts. Toxicon 57:408–20

Myklestad, S., Haug, A. & Larsen, B. 1972. Production of carbohydrates by the marine diatom *Chaetoceros affinis* var. *willei* (Gran) Hustedt. II. Preliminary investigation of the extracellular polysaccharide. Journal of Experimental Marine Biology and Ecology, 9(2), pp.137-144.

Myklestad, S.M. 1995. Release of extracellular products by phytoplankton with special emphasis on polysaccharides. Science of the total Environment, 165(1), pp.155-164.

Obernosterer, I. and Herndl, G.J. 1995. Phytoplankton extracellular release and bacterial growth: dependence on the inorganic N: P ratio. Marine ecology progress series. Oldendorf, 116(1), pp.247-257.

Olson, R.J., Vaulot, D. and Chisholm, S.W. 1986. Effects of environmental stresses on the cell cycle of two marine phytoplankton species. Plant Physiology, *80*(4), pp.918-925.

Pacepavicius, G., Lau, Y.L., Liu, D., Okamura, H., Aoyama, I. 1997. A rapid biochemical method for estimating biofilm mass. Environ. Toxic. Water 12: 97-100.

Passy, S.I., 2007. Diatom ecological guilds display distinct and predictable behavior along nutrient and disturbance gradients in running waters. Aquatic Botany. 86: 171-178.

Pérez-Ruzafa, A., Fernández, A.I., Marcos, C., Gilabert, J., Quispe, J.I. and García-Charton, J.A., 2005. Spatial and temporal variations of hydrological conditions, nutrients and chlorophyll a in a Mediterranean coastal lagoon (Mar Menor, Spain). Hydrobiologia, *550*(1), pp.11-27.

Perkins, K. 2010. Diatom fouling in Tasmanian Hydro Canals. Unpublished Ph.D. Thesis, University of Tasmania, Hobart, 118 pp.

Peter, K.H. & Sommer, U. 2012. Phytoplankton cell size: intra-and interspecific effects of warming and grazing. PloS one, *7*(11), p.e49632.

Peter, K.H. & Sommer, U. 2015. Interactive effect of warming, nitrogen and phosphorus limitation on phytoplankton cell size. Ecology and evolution, 5 (5), pp.1011-1024.

R Core Team, 2015. R: A language and environment for statistical computing.

Ravizza, M. & Hallegraeff, G. 2015. Environmental conditions influencing growth rate and stalk formation in the estuarine diatom *Licmophora* flabellata (Carmichael ex Greville) C. Agardh. Diatom research, *30* (2), pp.197-208.

Rutherford, A., 2001. Introducing ANOVA and ANCOVA a GLM Approach. SAGE Publications, London, U.K.

Sartoni, G., Urbani, R., Sist, P., Berto, D., Nuccio, C. and Giani, M., 2008. Benthic mucilaginous aggregates in the Mediterranean Sea: Origin, chemical composition and polysaccharide characterization. Marine Chemistry, 111(3), pp.184-198.

Schiaparelli, S., Castellano, M., Povero, P., Sartoni, G. and Cattaneo-Vietti, R., 2007. A benthic mucilage event in North-Western Mediterranean Sea and its possible relationships with the summer 2003 European heatwave: short term effects on littoral rocky assemblages. Marine Ecology, 28(3), pp.341-353.

Smith, D.J. and Underwood, G.J. 2000. The production of extracellular carbohydrates by estuarine benthic diatoms: the effects of growth phase and light and dark treatment. Journal of Phycology, 36(2), pp.321-333.

Smith, D.J. and Underwood, G.J. 2000. The production of extracellular carbohydrates by estuarine benthic diatoms: the effects of growth phase and light and dark treatment. Journal of Phycology, 36(2), pp.321-333.

Staats, N., Stal, L.J. and Mur, L.R. 2000. Exopolysaccharide production by the epipelic diatom *Cylindrotheca closterium*: effects of nutrient conditions. Journal of Experimental Marine Biology and Ecology, 249(1), pp.13-27.

Svensson, F., Norberg, J. and Snoeijs, P. 2014. Diatom cell size, coloniality and motility: trade-offs between temperature, salinity and nutrient supply with climate change. PloS one, 9(10), p.e109993.

Terrados, J. 1991. Creciniento y producción de las praderas de macrófitos del Mar Menor, Murcia. Ph.D. thesis, University of Murcia, 229 pp.

Thompson, P.A., Guo, M.X. and Harrison, P.J. 1992. Effects of variation in temperature. I. On the biochemical composition of eight species of marine phytoplankton. Journal of Phycology, *28*(4), pp.481-488.

Underwood, A.J. 1997. Experiments in Ecology: Their Logical Design and Interpretation Using Analysis of Variance. Cambridge University Press, Cambridge, U.K.

Underwood, G.J., Boulcott, M., Raines, C.A. and Waldron, K. 2004. Environmental effects on exopolymer production by marine benthic diatoms: dynamics, changes in composition, and pathways of production. Journal of Phycology, 40(2), pp.293-304.

Velasco, J., Lloret, J., Millán, A., Marin, A., Barahona, J., Abellán, P. and Sánchez-Fernández, D., 2006. Nutrient and particulate inputs into the Mar Menor lagoon (SE Spain) from an intensive agricultural watershed. Water, Air, & Soil Pollution, *176*(1), pp.37-56.

Verity, P.G. 1981. Effects of temperature, irradiance, and daylength on the marine diatom Leptocylindrus danicus Cleve. I. Photosynthesis and cellular composition. Journal of Experimental Marine Biology and Ecology, 55(1), pp.79-91.

Yoder, J.A., 1979. Effects of temperature on light-limitatin growth and chemical composition of Skeletonema costatum (Bacillariophyceae), Journal of Phycology, 15 (4), pp. 362-370.

Zuur, A.F., Ieno, E.N., Walker, N., Saveliev, A.A., Smith, G.M. 2009. Mixed Effects Models and Extensions in Ecology with R. Springer.

Chapter 5

Combined in situ effects of metals and nutrients on marine biofilms: Shifts in the diatom assemblage structure and biological traits

Introduction

Biofilms are ubiquitous aggregates of organisms composed mainly of bacteria and microalgae embedded in an extracellular polymeric substance (EPS) matrix. In estuarine and shallow systems, diatoms dominate these microalgae benthic communities, which occupy vast extensions of soft-bottom substrates. They play a fundamental role in total primary production (Cahoon 2006), providing food for other organisms and contributing substantially to geochemical cycles (Blanchard *et al*., 2000). Biofilms can integrate environmental conditions over long time periods (Dorigo *et al*., 2010), and the short life cycles of most benthic algal result in a rapid response to environmental pollution, which can be reflected in structural changes to biofilm in a few weeks (Sabater *et al*., 2007). Of all benthic algae, diatoms are known to be excellent biological indicators and are routinely used to assess pollution impacts (e.g., metals and nutrients) in freshwater systems (i.e., Ivorra *et al*., 2002; Navarro *et al*., 2002; Morin *et al*., 2008b; Tlili *et al*., 2010, 2011).

Under natural conditions, the responses of the benthic microalgae communities to environmental pollution vary greatly because they depend on the environmental factors and inherent characteristics of biofilms (Navarro *et al*., 2002). The initial community composition and species interactions can control biofilm responses to individual and mixture of various stressors (Guasch *et al*., 1998; Breitburg *et al*., 1999). The wide range of sensitivities among species can generate varied responses to different anthropogenic pressures (Barranguet *et al*., 2002). Thus, a given toxicant can eliminate or hamper the suc-cess of sensitive species and may benefit more tolerant ones through the production of toxicant-induced succession (TIS), which can be observed as changes in the community structure (Blanck 2002). Nevertheless, natural systems are usually subjected to many human-derived pressures, making it very difficult to predict the impacts of a given toxicant because its effects can be modulated by mul-tiple factors; e.g., the presence of nutrients (e.g., Guasch *et al*., 2004; Serra *et al*., 2010). Previous studies have reported different interactive effects of nutrients and toxicants, depending on the type of tox-icant. For example, phosphorus (P) can modulate the effects of copper (Cu) on autothrophic communities (Guasch *et al*., 2004; Serra *et al*., 2010) but not those of diuron (Tlili *et al*., 2010). The mixture of substances should also be considered. P compensates for the toxic effects of zinc (Zn) or Cu but not the toxic effects of both metals together (Ivorra *et al*., 2002). The measured parameters can also provide different interactive results, e.g., functional or structural responses (Tlili *et al*., 2010; Sundbäck *et al*., 2007), which can vary among the study system. Most studies on freshwater systems have noted that nutrients can overcompensate metal effects (e.g., Morin *et al*., 2008a; Guasch *et al*., 2004; Serra *et al*., 2010), whereas in marine systems, toxicant impacts seemed to be more evident under nutrient-enriched conditions (Breitburg *et al*., 1999; Larson *et al*., 2007). The growth form of species and their microdistribution within biofilms can also determine the responses of benthic communities to metals and nutrients (Ivorra *et al*., 2002). However, its suitability as an indicator of environmental pollution has been predominantly investigated in freshwater systems for pesticides and other organic pollutants (e.g., Berthon *et al*., 2011; Rimet & Bouchez 2011).

Most studies on marine environments have assessed the responses of benthic communities to antifouling biocides (e.g., Blanck *et al*., 2009; Dahl & Blanck 1996a), which have shown substance-dependent patterns in community changes (Ohlauson and Blanck, 2014). A few studies have also indicated that metals (Cunningham *et al*., 2005; Cunningham *et al*., 2003) or nutrients can modify diatom species composition (e.g., Wachnicka *et al*., 2011; Armitage *et al*., 2006; Frankovich *et al*., 2006). However, very little has been done to study the combined effects of toxicants and nutrients (Larson *et al*., 2007; Sundbäck *et al*., 2007) or the ecologic preferences of most species, which precludes the development of biological indicators or tools for biomonitoring in coastal environments (Desrosiers *et al*., 2013).

The aim of this study was to assess the responses of coastal biofilm communities to pulse exposures of metals and nutrients and their interaction, as well as to investigate the response of biofilms from sites with distinct exposure histories. Biofilms grown in a reference and a historically contaminated site were exposed in situ to metals (100 mg $Zn \cdot L^{-1}$ plus 50 mg $Pb \cdot L^{-1}$), and nutrients (80 µmol $NO_3^- \cdot L^{-1}$ plus 5 µmol $PO_4^{3-} \cdot L^{-1}$), singly and in combination, simulating the patterns of inputs observed in the study area. The responses of biofilms were

investigated on the microalgae community level (diatom community structure and growth form of species) and the changes in the biofilms' chemical composition were assessed by quantifying the metal, chlorophyll *a* and polysaccharide contents. We hypothesised that nutrient enrichment could amplify metals' effects on reference biofilms, whereas the biofilms at the contaminated site will resist metal and nutrient exposure.

Materials and methods

Study area and experimental sites

The Mar Menor lagoon (SE Spain) is one of the largest hypersaline coastal lagoons in the Mediterranean Sea. Benthic macrophytes are the main primary producers, but the contribution of microphytobenthos is significant and has been estimated to account for up to 11% of total primary production (Terrados and Ros, 1991). The ephemeral streams (wadis) located on the southwest side of the lagoon pour freshwater with large quantities of metals and nutrients derived from former mining activity and agriculture into the surrounding areas (Velasco *et al*., 2006; Marín-Guirao *et al*., 2007). A manipulative experiment was carried out at two sites with similar depths of 1.5 m, located in the southern basin of the lagoon (Figure 1., Figure 7. in General Introduction). The "contaminated site" was located in the El Beal wadi outlet, which is subjected to metals and nutrients loads, as previous analyses of the nitrogen stable isotopes and metals in the lagoon's food webs evidenced (Marín-Guirao *et al*., 2008). The wadi pour freshwater into the lagoon only when torrential rain occurs, reaching concentrations of dissolved and particulate metals in water for a few hours before returning to baseline levels after 24–48 h (Marín-Guirao *et al*., 2007). At the same time, primary producers and biofilms accumulate high concentrations of metals (Marín-Guirao *et al*., 2005). The "reference site" was located to the east of the lagoon, at a distance of approximately 6 km from the contaminated site, where the influence of nutrients and metals is considered negligible (Marín-Guirao *et al*., 2005, 2008).

Experimental design and sample collection

The study was designed to mimic the repeated pulse exposure of nutrients and metals that the lagoon may receive during flash floods of the wadis in the study area. Biofilms were grown on glass slides (39.52 cm2) to reduce the heterogeneity of the natural substrates. In the two sampling sites, at least 30 glass slides were attached to slide holders (four per treatments) and anchored 30 cm below the sea surface to avoid the influence of sediment suspension. The experiment was performed in June 2008 and lasted 20 days to avoid growth of macroalgae or epibionts on biofilms. Biofilms were initially grown for 10 days at each sampling site, and the treatments were applied on days 10, 13, 16 and 19 by placing the slide holders on plastic trays that contained the selected treatment solutions. At each site, each treatment consisted of the in situ pulse exposures (1 h) of nutrients (N), metals (M), a combination of metals and nutrients (MN), and seawater from each site used as the control treatment (C). The selected metals were Zn and Pb because they were dominant in wadi drainage (Marín-Guirao *et al*., 2005). The nominal concentrations for the M treatments were 100 mg $Zn \cdot L^{-1}$ ($ZnSO_4 \cdot 7H_2O$, Panreac) plus 50 mg $Pb \cdot L^{-1}$ ($PbSO_4$, Panreac); for N treatments, 80 µmol $NO_3^- \cdot L^{-1}$ (KNO_3, Panreac) plus 5 µmol $PO_4^{3-} \cdot L^{-1}$ (KH_2PO_4, Panreac); for MN treatments, a mixture of metals and nutrients at the concentrations outlined above were added. Due to the short duration of the experimental pulse exposures and the high salt precipitation, the nominal concentrations of dissolved nutrients and metals are 4 to 10 times higher than those occasionally found in the vicinity of the "contaminated site" after of flash flood of the wadi (Lloret *et al*., 2005; Marín-Guirao *et al*., 2007).

Figure 1 Detailed images of sampling sites.

Colonised glass slides were removed at the end of the experiment (day 20) and were transported to the laboratory in a dark cool box. All the biofilm samples were kept frozen until analysed, except for those used in the diatom community analysis because they were fixed with a formaline solution (3%). Water samples were collected at each sampling site and in each treatment solution on days 1, 10, 13, 16, 19 and 20 to be transported to the laboratory in a dark cool box. All the samples were immediately filtered and kept frozen until analysis, and the samples for the metal analysis were acidified with 2% HNO3 (65% Suprapur®, Merck). On the same dates, water temperature, dissolved oxygen, pH and salinity were measured in situ with portable sensors (multiparametric recorder WTW, MultiLine P4).

Water quality at the sampling sites

Chloroplhyll *a* and suspended solids were analysed in filters (GF/F filters, Whatman) obtained after filtering seawater (1.5 L). For chlorophyll a extraction, 6 mL of acetone (90%) were added to the filters, and the concentration was spectrophotometrically assessed at 630, 647 and 664 nm following the method of Jeffrey and Humphrey (1975). The suspended solid content was calculated as the difference in the dry weight of filters before and after filtration. The nutrient content was quantified by ion chromatography (Metrohm), nitrate using a chromatography module with a UV detection system (844 UV/VIS Compact IC), and phosphate using a chromatography module with a CO_2 suppressor and a conductivity detection system. The dissolved Zn and Pb concentrations were measured polarographically by anodic stripping voltametry (VA 646 processor, Methrom) with a hanging mercury drop electrode following the methods described in Marín-Guirao *et al*. (2007).

Diatom communities

Four colonised slides per treatment (one per slide holder) were digested (70 °C, 2 h) with H2O2 (33%, Panreac) to detach biofilms from slides and to remove organic matter. Cleaned diatom frustules were filtered (0.2 µm GNWP nylon membrane filter, MILLIPORE), washed with distilled water, suspended in ethanol solution (70%) and mounted onto slides using Naphrax (R.I.1.69). At least 400 valves of diatom species were counted per replicate slide by light microscopy (Leica DMRB). The fine structure of diatoms was analysed under a scanning electron microscope (JEOL-6100). Taxa were identified at the species level, whenever possible, using taxonomic monographs from Hustedt (1959) and Witkowski *et al*. (2000). The diatom composition, the relative abundance of species (%), the Shannon–Wiener diversity index (natural log, H´), evenness (Pielou's J) and species richness (Margelef's d) were calculated for each sample and then summarized per treatment.

Definition of biological traits

The growth forms of species were analysed before biofilm detachment and were grouped according to the literature and personal observations. Preserved samples were also analysed by scanning electron microscopy. The different growth forms were distinguished according to whether a) diatoms were solitary cells, i.e., prostrate, unattached (mobile) and motile, or b) the cells were grouped into colonies; i.e. growing in an erect mucous tube, forming a rosette colony, zig-zag filaments, ribbons, chains or stalked colonies. Unattached (mobile) growth forms encompass all the solitary diatoms with a raphe structure, and the motile guild includes members of Navicula and Nitzschia sensu lato, which are generally selected as fast-moving mobile diatoms (Passy, 2007). Rosette shaped-colonies include pennate cells that produce a pad at one pole that sticks to a substrate; the cell divisions produce colonies that resemble rosettes (Rimet & Bouchez 2012).

Characterisation of biofilms

For each analysis, four replicates per treatments were run; each replicate corresponded to the biofilm detached from a colonised slide (one per slide holder). The Zn and Pb that accumulated in biofilms were determined as described in Marín-Guirao *et al*. (2007). Approximately 0.05 g of dried powdered sample was digested using 1 mL of a nitric, perchloric and sulphuric acid mixture (8:8:1, v:v:v) in two heat digestion cycles with step-wise increases in temperature (40–380 °C) until total evaporation. Diluted and acidified samples were polarographically analysed for Zn and Pb, as described above for seawater. For chlorophyll a extraction, 10 mL of acetone (90%) were added to each sample, and the concentration was determined by the methodology described above for water samples. Because EPS are composed mainly of polysaccharides, the content in each sample was spectrophotometrically measured by the modified phenol-sulphuric acid method (Pacepavicius *et al*., 1997). To determine the dry weight (DW), samples were dried at 60 °C until constant weight, and chlorophyll a and polysaccharides con-tents were normalised to gDW.

Data analysis

Prior to the statistical analyses, we removed the diatom taxa that contributed <2% of the total abundance of samples. The data of the relative abundance and the type of growth forms of species were square root transformed, and the analysis was performed using the various routines available in the PRIMER 6 & PERMANOVA + software package (Anderson *et al*., 2008). A ranked triangular similarity matrix was constructed using Bray–Curtis similarity. Next, a two-way PERMANOVA crossed design was performed (9999 permutations) to test the site-treatment interaction. Pair-wise tests were run to compare the C treatments between sites and with the three treatments (N, M, MN) at each site independently. Significant differences in the paired comparisons were checked using Monte Carlo p-values due to the restricted number of possible permutations ($p < 0.05$). PERMANOVA analysis is sensitive to differences in dispersion among groups, so PERMDISP (Distance-

based test for homogeneity of multivariate dispersions) analysis was implemented to verify if significant results of PERMANOVA are exclusively caused by the effects of the treatments.

Significant changes in species richness, evenness and the diversity index between the C treatments of both sites were analysed based on Kruskal Wallis, and differences with the three treatments (N, M, MN) at each site were analysed using one-way ANOVA and a post hoc Tukey test. To check significant changes in the biofilm parameters (Zn and Pb accumulated, chlorophyll a and polysaccharides content), two-way ANOVA was performed with site and treatment as the fixed factors. To compare C treatments between sites and with the three treatments (N, M, MN) at each site, a post hoc Tukey test was performed. The Zn and Pb data were square root and log transformed, respectively, because data normality was not met (Shapiro-Wilk normality test). If homocedasticity and normality of model residuals were not met, a more conservative approach was applied reducing the signification level ($p \leq 0.01$) and using post hoc analyses with Bonferroni correction (Underwood 1997; Rutherford 2001).

Table 6. Summary of the relative abundance (%) for each treatment (C: control, N: nutrients, M: metals, MN: metals + nutrients) at the two sampling sites and the growth form of diatom species. The dark shade indicates the percentage of relative abundance of each species.

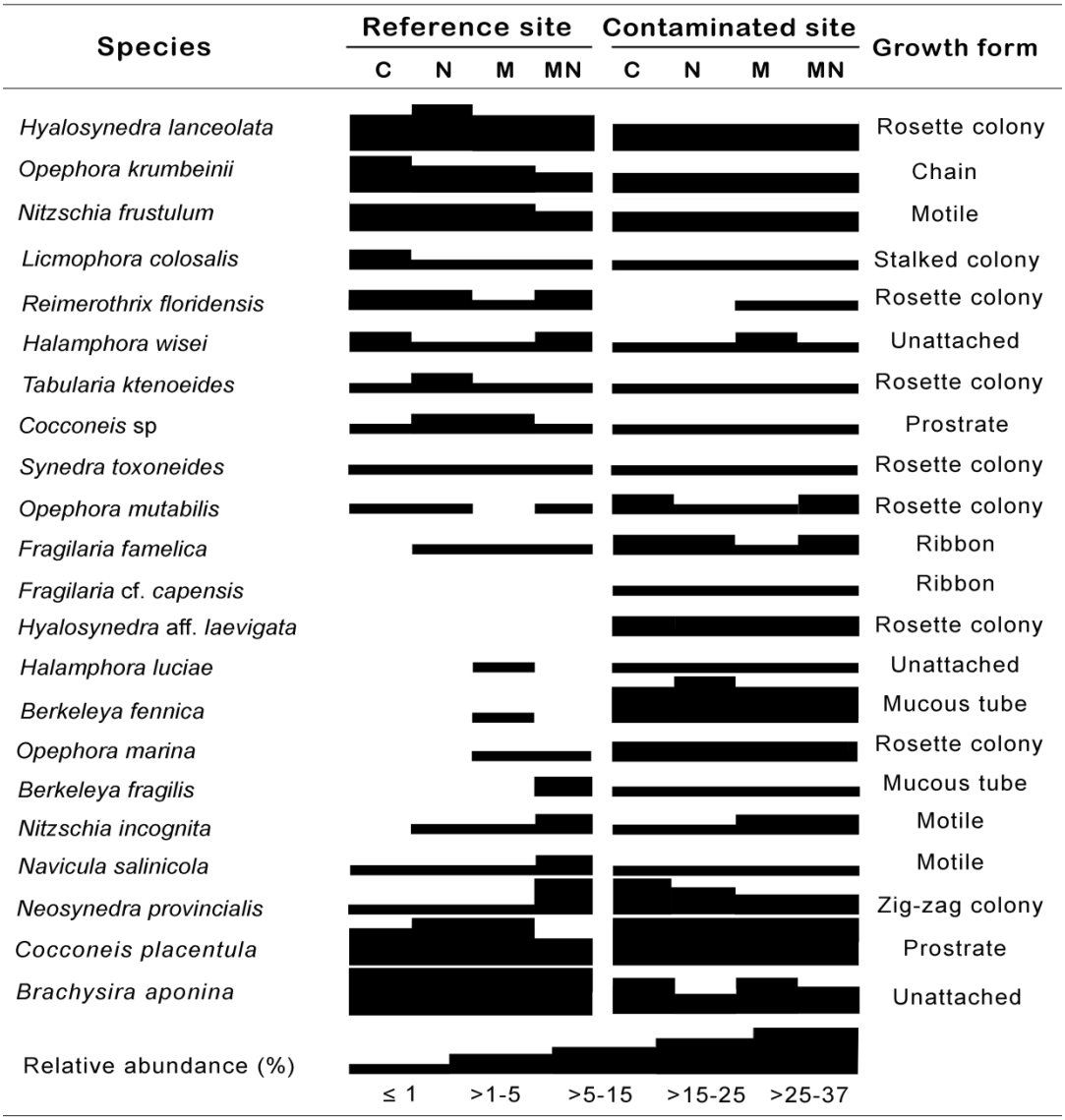

Table 7. Diatom community descriptive parameters (mean ± SD): species richness, evenness and diversity index values for each treated community at each site (n = 4). C: control, N: nutrients, M: metals, MN: metals + nutrients.

Parameter	Reference site			
	C	N	M	MN
Richness (Margalef d)	2.93 ± 0.08	2.84 ± 0.2	3.11 ± 0.23	3.32 ± 0.33
Evenness (Pielou J)	0.67 ± 0.04	0.65 ± 0.01	0.62 ± 0.04	0.72 ± 0.01
Diversity (Shannon–Wiener H´)	1.99 ± 0.13	1.89 ± 0.06	1.84 ± 0.13	2.2 ± 0.06
Parameter	**Contaminated site**			
	C	N	M	MN
Richness (Margalef d)	4.13 ± 0.91	4.09 ± 0.5	4.22 ± 0.28	4.39 ± 0.51
Evenness (Pielou J)	0.7 ± 0.04	0.63 ± 0.05	0.72 ± 0.04	0.72 ± 0.07
Diversity (Shannon–Wiener H´)	2.26 ± 0.25	2.06 ± 0.23	2.37 ± 0.16	2.39 ± 0.25

Generalized Linear Models (GzLM, two factors: site and treatment) were performed to analyse significant changes in the abundance of the different growth forms using a binomial distribution of errors because data were counts with an upper limit (Zuur *et al*., 2009). If the interaction was not significant, a Kruskal Wallis was used for comparison of the C treatments of both sites, and a one-way GzLM were performed to compare with the three treatments (N, M, MN) at each site. Significant changes in the abundance of the relevant taxa were similarly tested by one-way analysis. Model checking included a visual inspection of the variance-to-mean relationship and linearity of predictors. The ANOVAs and GzLMs were performed with the statistical software R (R Core Team, 2015).

Results

Characterisation of sites and treatments

The weather conditions during the experimental period were calm and sunny with no torrential rain, which would have washed metals into the lagoon, and no swells occurred that would have caused significant sediment suspension. Throughout the experimental period, dissolved metals (Zn and Pb), nitrates and suspended solids were slightly higher at the contaminated site than at the reference site, whereas other physico-chemical parameters of seawater (i.e., pH, salinity) were similar and remained constant at both sampling sites (Table Ap4 1). The dissolved metal and nutrient concentrations after 1 h of exposure time (+ 1 h) in the different treatments are summarized in Table Ap4 1. The concentrations did not vary significantly between sites and were lower than nominal levels due to absorption in biofilms and the low solubility of metals in the hypersaline water of the lagoon.

Changes in diatom community structure

The microalgae communities in the studied biofilms were dominated by diatoms, and 46 taxa were identified in the study area. The diatom assemblages from both sites were characterised by a few dominant diatom species and by many rare or less abundant taxa (Table 6). *Brachysira aponina* and *Cocconeis placentula* occurred abundantly (>15%) at both sites (Table 6), whereas *Opephora krumbeinii*, *Hyalosynedra lanceolata*, and *Nitzschia frustulum* were dominant (>11%) at the reference site and *Berkeleya fennica* and *Neosynedra*

provincialis at the contaminated site. The species richness (d) was significantly higher in C treatments from the contaminated site than at the reference ones (Table 7), and significant differences in the composition of taxa were also detected (PERMANOVA, Table 8). The evenness (J) and diversity index (H´) were not different between sites (Table 7, Table Ap 4 2). These changes were related with the fact that the dominant species in the reference biofilms *O. krumbeinii*, *H. lanceolata*, *N. frustulum* and *B. aponina* significantly decreased at the contaminated site, but without being eliminated. Therefore, all species found at the reference site, except *Opephora horstiana* and *Mastogloia* cf. *emarginata*, were also detected at the contaminated site. On the other hand, 12 species were exclusively found at the contaminated site e.g., *Hyalosynedra lanceolata*, *Opephora marina*, *Fragilaria* spp. and *B. fennica* (Table 6, Table Ap 4 3).

The selected community descriptive parameters (d, J, H') tended to decrease after N treatments and increased in M and MN treatments compared to controls at both sites, but not significantly (Table 7, Table S2). Two-way PERMANOVA results (Table 8) revealed that effects of the experimental treatments on diatom composition differed between sites. At the contaminated site, the relative abundance of *B. fennica* and *C. placentula* increased significantly after N treatments and Nitzschia incognita also responded positively to the M and MN treatments, but the community structure differed significantly to the C communities in any case (Table 8, Table Ap4 3). At the reference site, all the treatments (N, M and MN) promoted significant changes in the community structure compared to C treatments. The relative abundance of the dominant O. krumbeinii declined after all treatments (N, M and MN). In turn, the M treatment favoured the colonisation of the species characteristic at the contaminated site (e.g., *B. fennica*, *O. marina*, *Halamphora luciae*) and the increase of *B. aponina*. Nutrient inputs matched the occurrence of some species, e.g., *Fragilaria famelica*, *N. incognita*, and significantly increased the abundance of *Tabularia ktenoeides*, *H. lanceolata* and *C. placentula*. In the MN treatments, *O. krumbeinii*. *N. frustulum*, and *C. placentula* decreased significantly, and a subset of species proliferated significantly (*Berkeleya fragilis*, *N. incognita*, *Navicula salinicola*, *N. provincialis*), increasing their contribution to the total relative abundance from <2% to 27% (Table 6, Table Ap4 3). The MN treatments also favoured the appearance of some distinctive species from the contaminated site (e.g., *O. marina*, *F. famelica*). In the reference site, the Bray-Curtis dissimilarity values of each treatment compared to the C treatments were higher in the MN treatment (32.7) than for the N (18.3) and M (15.62) treatments. The PERMDIST analysis showed that dispersions remained constant for all the compared groups at each site ($p>0.05$), indicating that the significant results of PERMANOVA were exclusively due to effects of the treatments and not to the dispersion of the data.

Responses of biological traits

The two-way PERMANOVA results (Table 8) indicated that the global biofilm architecture changed significantly between sites (C treatments) (Figure 2.). The GzLM results showed that most growth form types differed significantly in abundance between the reference and contaminated sites (Table S4). Chains and rosette-shaped colonies, as well as the unattached (mobile) and motile cells, dominated in the reference biofilms (Figure 2.). In contrast, the abundance of the zig-zag colonies, mucous tubes, ribbons and prostrate cells was significantly higher at the contaminated site (Table Ap 4 4).

The global architecture of the reference biofilms was significantly modified after the N and MN treatments (PERMANOVA, Table 8). Both treatments promoted a significant decrease in chains. The MN treatment also reduced the abundance of prostrate cells whereas mucous tubes and zig-zag colonies significantly increased. Overall these shifts resulted in a higher complexity in the architecture of the reference biofilms that tended to be similar to those of the contaminated site (Figure 2.). At the contaminated site, mucous tubes significantly increased after N treatments, and unattached cells significantly decreased. After M treatments, motile species increased and zig-zag colonies decreased, but the global architecture was not significantly modified in any case (PERMANOVA, Table 8).

Table 8. Statistical two-way PERMANOVA results showing the interactive effects of sites and treatments on the diatom community structure and the abundance of the growth form. The results of the pair-wise tests indicate a) differences between sites when comparing C treatments (Ref.: reference site, Cont.: contaminated site) and b) significant differences among the treatments at each site (C: control, N: nutrients, M: metals, MN: metals + nutrients). Bold letters indicate significant differences

PERMANOVA	**Community structure**				**Biological traits**			
Main test	SS	MS	Pseudo-F	p	SS	MS	Pseudo-F	p
Site	9209	9209	71.83	**<0.001**	6888	6888	105.31	**<0.001**
Treatment	2027	675	5.27	**<0.001**	963	321	49.11	**<0.001**
Site x treatment	1550	516	4.03	**<0.001**	1259	419	64.17	**<0.001**
Pair-wise (a)	Between sites				Between sites			
C treatments	t	p (MC)			t	p (MC)		
	4.94	**<0.001**			5.19	**<0.001**		
Pair-wise (b)	Among treatments				Among treatments			
	Ref.		**Cont.**		**Ref.**		**Cont.**	
	t	p (MC)	t	p (MC)	t	p (MC)	t	p (MC)
C x N	2.03	**0.01**	1.58	0.07	18.36	**0.048**	17.26	0.06
C x M	1.86	**0.03**	1.66	0.05	15.95	0.10	14.67	0.12
C x MN	3.93	**<0.001**	1.48	0.11	45.42	**<0.001**	1.65	0.09
N x M	1.29	0.17	1.66	0.07	12.41	0.22	21.57	**0.02**
N x MN	3.92	**<0.001**	1.66	0.06	46.67	**0.001**	18.01	0.06
M x MN	3.96	**<0.001**	1.36	0.14	50.2	**<0.001**	13.69	0.16

Chemical characteristics of biofilms

The two-way ANOVA showed that the effects of the treatments significantly differed between the two sites for all the measured parameters (Table Ap 4 5). The biofilm Zn and Pb concentrations were significantly higher in the contaminated site than in the reference site, and the polysaccharide content was significantly lower in the contaminated site (Figure 3. , Table Ap 4 5). Metal exposure, either with or without nutrients, was generally reflected in an increased Zn and Pb content. The highest concentration of metal was measured in the MN treatments, being particularly high at the reference site. At this site, the chlorophyll a and polysaccharide contents increased significantly in the MN treatments (Figure 3.), whereas the polysaccharide content increased significantly after N and M enrichment at the contaminated site (Table Ap 4 5).

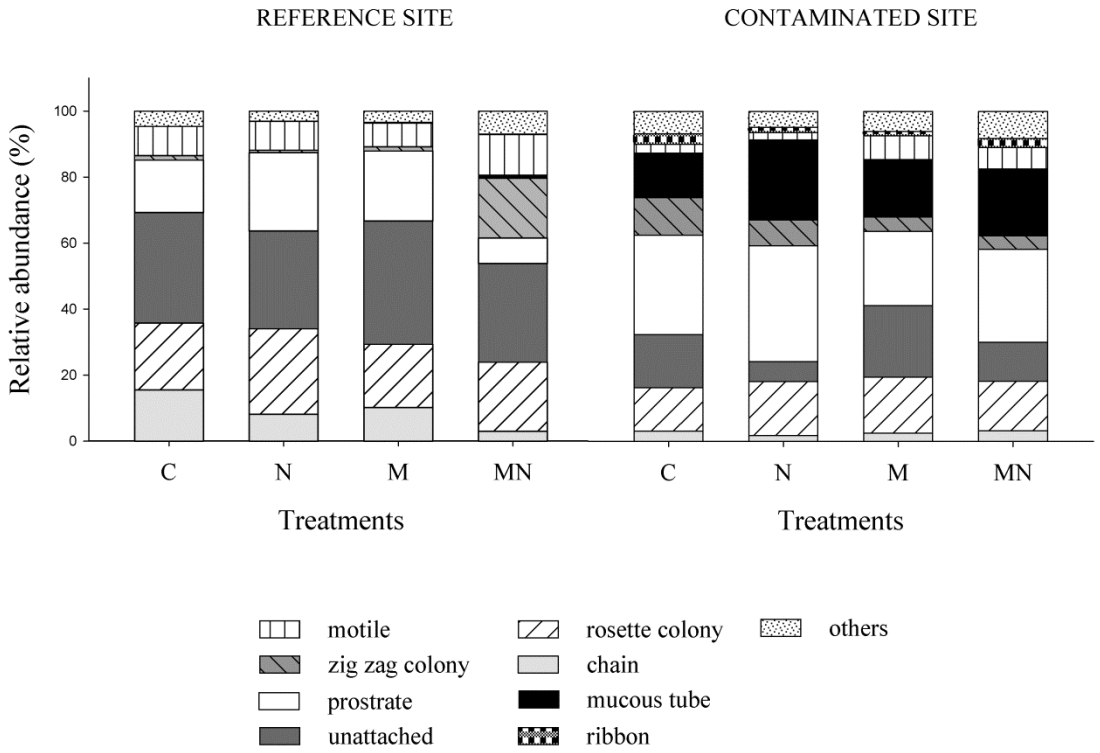

Figure 2. Percentage abundance of the different growth forms (biological traits) of diatom species after the experimental treatments (C: control, N: nutrients, M: metals, MN:metals + nutrients) at each site (Tukey test, n = 4)

Discussion

Our results show that pulse exposure of nutrient can amplify the metal effects on coastal biofilms communities with changes that vary with the diatom community composition and the growth form of species determined by the exposition history of the location (Figure 4.).

The structural differences between biofilms from the reference and contaminated sites, seemed to indicate that chronic discharge of metal and nutrients have reduced the success of *O. krumbeinii*, *N. frustulum* and *H. lanceolata*, than seem to be potential sensitive species, and favoured the colonisation (e.g., *H. lanceolata*, *H. luciae*, *O. marina* and *F. famelica*) and dominance (*Berkeleya* spp., *N. provincialis*) of some metal-tolerant species with high nutrient requirements. It has not been found information relative to metal tolerance of these species, but some of the taxa characteristic of this contaminated site have also been found under nutrient-enriched conditions in fresh and estuarine waters, such as *B. fennica* (Rinella and Bogan, 2004; Trobajo *et al*., 2004) and *F. famelica* (Rinella and Bogan, 2004; Ros *et al*., 2009). This replacement corresponds to the concept of toxicant-induced succession, TIS (Blanck, 2002), which was reflected in a more tolerant community to both metal and nutrients, in any case community structure was significantly altered, as expected for pre-exposed communities (Soldo and Behra, 2000). These structural changes were also reflected in a significant increase in species richness and a higher complexity of the architecture of biofilms at the contaminated site. This could be explained as an effect of the intermediate disturbance hypothesis (Townsend *et al*., 1997) because the intermittent frequency of the wadi discharges seemed to favour the occurrence of tolerant species with specific growth forms, such as mucous tubes and zig-zag colonies, which allow them to exploit vacant patches in these disturbed environments.

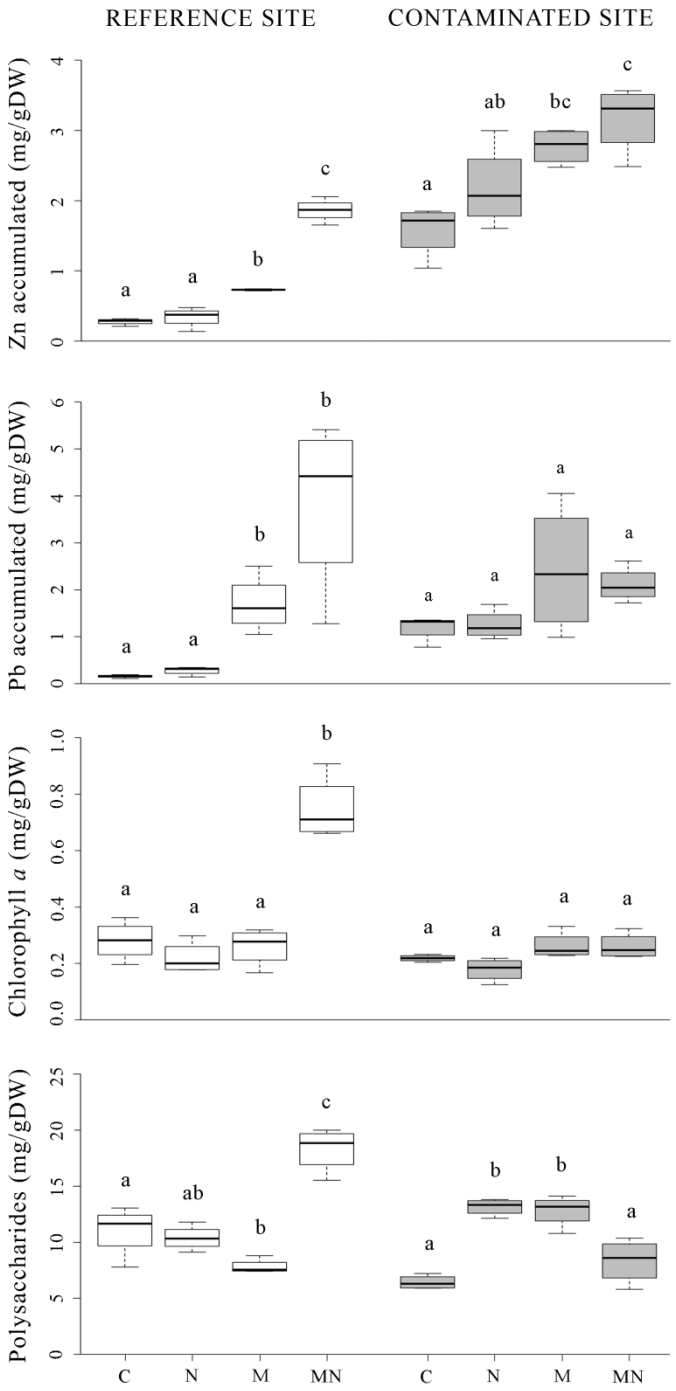

Figure 3. Chemical characterisation of the biofilms from both sites after each treatment. Different lower case letters above bars indicate significant differences between treatments (C: control, N: nutrients, M: metals, MN: metals + nutrients) at each site (Tukey test, n = 4).

Contrary to the weak responses of the biofilms from the contaminated site, the composition of reference biofilms was significantly modified by metal and nutrient exposures. The structural changes of the reference biofilms were reflected in a decrease in the species richness and diversity values after the nutrient and metal supply, while trend to increase after combined exposure, but not significantly. These findings are in agreement with the responses of microalgae communities within sediments from a shallow system (Larson *et al*., 2007) and seemed to be related to the fact that metals and nutrients triggered a reorganisation of diatom communities in different ways. Irrespective of the stressors and the scenarios, all reference communities displayed a decline in the abundance of the sensitive species *O. krumbeinii*. In turn, nutrient enrichment favoured the proliferation of rosette-colonies (*H. lanceolata* and *T. ktenoeides*) and the prostate *C. placentula*, which tended to dominate the biofilms. These responses agree with the high-nutrient tolerance of *C. placentula* (Wachnicka *et al*., 2011) and other *Tabularia* spp. (Hillebrand & Sommer 2000). Single metal inputs,

in contrast, favoured the colonisation of metal-tolerant species (e.g., *B. fennica* and *O. marina*) and promoted the transition towards biofilms from the contaminated site. Both stressors in combination drove more pronounced changes than when singly added, which matched with the amplification of accumulated metals and restructuration of diatom communities towards a composition and architecture similar to the ones found at the contaminated site. These findings suggested that nutrients seemed to hasten the succession of species towards tolerant-dominance communities. These effects included a prominent decline in the population of some dominant species, such as *O. krumbeinii* and *N. frustulum*, and even the opportunistic *C. placentula*. In turn, some taxa from the contaminated site such as *O. marina*; *N. provincialis*, which form zig-zag colonies; *B. fragilis*, which produce tubes; and even some other motile species (*Nitzschia* spp. and *Navicula* spp.) proliferated. Our findings are in agreement with data from shallow systems, where the biocide copper pyrithione produced stronger effects in nutrient-replete sediments (Larson *et al*., 2007; Sundbäck *et al*., 2007).

The transition of the more encrusting morphology in the reference biofilms (dominated by chains and rosette colonies) towards a dominance of long filaments (mucous tube and zig-zag colonies) after combined exposure was consists with the nature of biofilms from the contaminated site. Barranguet *et al*. (2002) indicated that Cu exposure caused the replacement of filamentous diatoms with a more encrusting growth form. Nutrient supply can increase the complexity of biofilms by increasing filamentous growth forms (Berthon *et al*., 2011; Passy, 2007). In our study, the proliferation of the long filamentous tubes of Berkeleya spp. and the zig-zag colonies of N. provincialis suggests that filamentous metal-tolerant species can dominate biofilms subjected to multiple stresses. The resistance to perturbations of species within mucous tubes, e.g., *Berkeleya* spp. and *Parlibellus* sp., could be related with the fact that tubes may represent a protective barrier against dissolved metals, as Rimet and Bouchez (2011) suggested for pesticides. These same species could also grow under enriched conditions due to the high demand of nutrients for tube production (Daniel *et al*., 1987; Hillebrand and Sommer, 2000). Among species forming zig-zag colonies, our results suggested N. provincialis as an interesting potential indicator of pollution. It has also been reported to be tolerant to the organic herbicide Irgarol 1501 (Dahl & Blanck 1996b; Eriksson *et al*., 2009). *Grammatophora* sp. also formed zig-zag colonies and was observed only at contaminated site, but its feasibility as an indicator should be further investigated. The response of motil taxa (e.g., *Nitzschia* and *Navicula*) to combined discharges in the reference site indicated a transition towards disturbed biofilms (Pass 2007) and may also agree with their classification as high competitors under nutrient-enriched conditions (Van der Grinten *et al*., 2004; Passy 2007; Ivorra *et al*., 2002; Delgado *et al*., 2012). However, the responses should be interpreted with caution because they can vary between species (*N. frustulum* was dominant at the reference site) and were clearer for short-term exposures than for chronic stresses.

Prostrate species (e.g., *C. placentula*) are considered pioneer colonisers of biofilms after metal pollution (Medley & Clements 1998; Corcoll *et al*., 2012). In our study, *C. placentula* was abundant at both sites, and could be considered as opportunistic because they grew well after nutrient exposure at both sites, consistent with the estuarine systems proposed by Trobajo *et al*. (2004). However, the decrease in prostate cells (*Cocconeis* spp.) seems to indicate that the increase in vertical complexity in biofilm architecture promotes a competitive exclusion of the organisms from deep biofilm layers, probably through limited resources (i.e., light, nutrients, surface). Finally *O. krumbeinii*, which forms chains and has the smallest sized cells (20 μm^3), showed more sensitive responses to both metal and nutrients in this hypersaline coastal system. Previous studies suggested that communities under chemical stress would tend to be dominated by small species in freshwater systems (Tlili *et al*., 2011; Ivorra *et al*., 1999). However, this was not observed in this study or in other marine shallow systems (Larson *et al*., 2007; Cunningham *et al*., 2003, 2005). Overall, our findings suggest that the growth form, the position and the size of cells can affect community responses to environmental metal and nutrients, similar to the findings of Ivorra *et al*. (2002) in a laboratory study, but the topic should be further investigated in marine coastal systems.

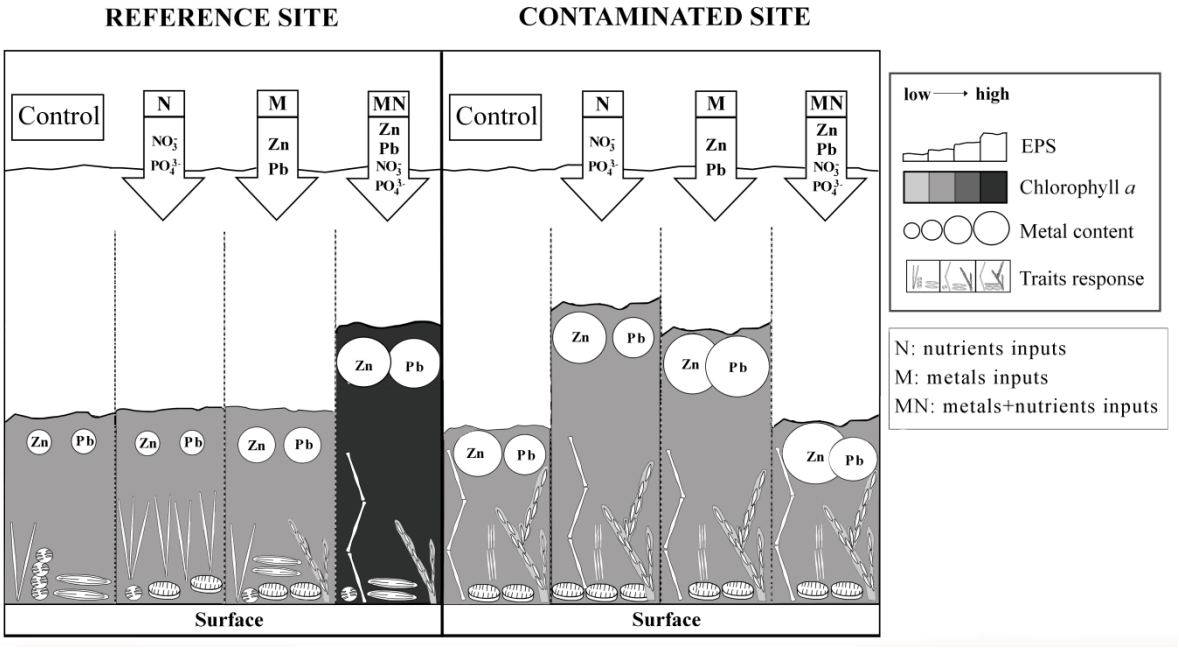

Figure 4. Conceptual diagram showing responses of coastal biofilms from reference and contaminated sites at the different levels analyzed: metal accumulation, EPS, chlorophyll a, and growth form.

Prostrate species (e.g., *C. placentula*) are considered pioneer colonisers of biofilms after metal pollution (Medley and Clements, 1998; Corcoll *et al*., 2012). In our study, *C. placentula* was abundant at both sites, and could be considered as opportunistic because they grew well after nutrient exposure at both sites, consistent with the estuarine systems proposed by Trobajo *et al*. (2004). However, the decrease in prostate cells (*Cocconeis* spp.) seems to indicate that the increase in vertical complexity in biofilm architecture promotes a competitive exclusion of the organisms from deep biofilm layers, probably through limited resources (i.e., light, nutrients, surface). Finally *O. krumbeinii*, which forms chains and has the smallest sized cells (20 μm^3), showed more sensitive responses to both metal and nutrients in this hypersaline coastal system. Previous studies suggested that communities under chemical stress would tend to be dominated by small species in freshwater systems (Tlili *et al*., 2011; Ivorra *et al*., 1999). However, this was not observed in this study or in other marine shallow systems (Larson *et al*., 2007; Cunningham *et al*., 2003, 2005). Overall, our findings suggest that the growth form, the position and the size of cells can affect community responses to environmental metal and nutrients, similar to the findings of Ivorra *et al*. (2002) in a laboratory study, but the topic should be further investigated in marine coastal systems.

The pronounced changes in the diatom composition within the reference biofilms after combined exposure coincided with a significant increase in chlorophyll a content compared to single metal inputs. This could indicate a higher biomass of autotrophic organisms in the presence of both stressors, which could be interpreted as an indirect top-down effect from the decrease in grazing by meiofauna (Larson *et al*., 2007). It could also indicate an increase in chlorophyll a synthesis to maintain effective conversion between light and chemical energy (Dahl, 1996; Dahl & Blanck 1996b), known as a protective mechanism against the toxicant "greening effect", but to understand if the increase of chlorophyll a is related to other effects at a functional level, the composition of pigments and the effects on photosynthesis efficiency in these communities should be addressed (Corcoll *et al*., 2012). An overproduction of polysaccharide was also observed after combined discharges in the reference site and as response to nutrients or metals in the contaminated site. We found no clear patterns of response to the different treatments at each site. In these multispecies biofilms, it could be related to variability in the species composition and the amount of extracellular polymeric substances produce each of the species (Tago & Aida 1977; Decho 1994). The presence of a raphe plays an important role in benthic

habitat colonisation by enabling diatoms to move and to secrete an exopolysaccharide matrix (Sims *et al*., 2006). In this study, some raphid species (*Nitzschia* spp., *Navicula* spp., *Berlekeya* spp., *C. placentula* spp) generally responded to short-term exposure, when EPS overproduction was also observed. Larras *et al*. (2014) suggested a phylogenetic relationship with resistance to various herbicides, and highlighted that araphid pennate diatoms were generally more sensitive than pennate raphid species. We found no clear patterns and a great variability between sites and species, suggesting that this hypothesis should be further investigated for metal pollution.

In conclusion, our findings indicate that the effects of metals combined with nutrients trigged more marked changes in the community composition and structure, in the chlorophyll a and EPS contents, promoting diatom communities dominated by tolerant species with specific growth forms. A biofilm dominated by filamentous mucous tubes, zig-zag colonies and prostrate cells seemed to indicate metal and nutrient environmental stress. We propose *Berkeleya* spp. and *N. provincialis* as tolerant species and *O. krumbe*inii as sensitive taxa to metal and nutrients contamination. We also suggest the incorporation of diatom growth forms into monitoring programmes as a potential easy and quick way to evaluate environmental pressures.

References

Anderson, M.J., Gorley, R.N., Clarke, K.R. 2008. Guide to software and statistical methods. *PERMANOVA+ for PRIMER*. University of Auckland and PRIMER-E, Plymouth.

Armitage, A.R., Frankovich, T.A., Fourqurean, J. W., 2006. Variable responses within epiphytic and benthic microalgal communities to nutrient enrichment. Hydrobiologia, 569 (1), 423-435.

Barranguet, C., Plans, M., van der Grinten, E., Sinke, J.J., Admiraal, W. 2002. Development of photosynthetic biofilms affected by dissolved and sorbed copper in a eutrophic river. Environmental Toxicology and Chemistry, 21: 1955-1965.

Berthon, V., Bouchez, A., Rimet, F. 2011. Using diatom life-forms and ecological guilds to assess organic pollution and trophic level in rivers: a case study of rivers in south-eastern France. Hydrobiologia, 673: 259-271.

Blanchard, G.F., Paterson, D.M., Stal, L.J., Richard, P., Galois, R., Huet, V., *et al*. 2000. The effect of geomorphological structures on potential biostabilisation by microphytobenthos on intertidal mudflats. Continental Shelf Research, 20: 1243-1256.

Blanck, H. 2002. A critical review of procedures and approaches used for assessing pollution-induced community tolerance (PICT) in biotic communities. Human and Ecological Risk Assessment 2002, 8: 1003–1034

Blanck, H., Eriksson, K.M., Grönvall, F., Dahl, B., Guijarro, KM., Birgersson, G., Kylin, H. 2009. A retrospective analysis of contamination and periphyton PICT patterns for the antifoulant irgarol 1051, around a small marina on the Swedish west coast. Marine Pollution Bulletin, 58(2): 230-7.

Breitburg, D.L., Sanders, J.G., Gilmour, C.C., Hatfield, C.A., Osman, R.W., Riedel, G.F., *et al*. 1999. Variability in responses to nutrients and trace elements, and transmission of stressor effects through an estuarine food web. Limnology and Oceanography 44: 837-863.

Cahoon, L.B. 2006. Upscaling primary production estimates: Regional and global scale estimates of microphytobenthos production In: Kromkamp J, de Brouwer JFC, Blanchard GF, Forster RM, Créach V, editors. *Functioning of microphytobenthos in estuaries*. Royal Netherlands Academy of Arts and Sciences pp. 99-106.

Corcoll, N., Bonet, B., Morin, S., Tlili, A., Leira, M., Guasch, H. 2012. The effect of metals on photosynthesis processes and diatom metrics of biofilm from a metal-contaminated river: a translocation experiment. Ecologial Indicators, 18, 620-631.

Cunningham, L., Stark, J.S., Snape, I., McMinn, A., Riddle, M.J. 2003. Effects of metal and petroleum hydrocarbon contamination on benthic diatom communities near Casey Station, Antarctica: An experimental approach. Journal of Phycology, 39: 490-503.

Cunningham, L., Raymond, B., Snape, I., Riddle, M.J. 2005. Benthic diatom communities as indicators of anthropogenic metal contamination at Casey Station, Antarctica Journal of Paleolimnology, 33: 499-513.

Dahl, B. 1996. On the ecotoxicology of antifouling agents. The use of marine microalgal communities in predictive and retrospective asessments. Ph. D. Thesis. University of Gothenburg, Sweden.

Dahl, B., Blanck, H. 1996a. Pollution-induced community tolerance (PICT) in periphyton communities established under tri-n-butyltin (TBT) stress in marine microcosms. Aquatic Toxicology, 34: 305-325.

Dahl, B., Blanck, H. 1996b. Toxic effects of the antifouling agent Irgarol 1051 on periphyton communities in coastal water microcosms. Marine Pollution Bulletin, 32: 342-350.

Daniel, G.F., Chamberlain, A.H.L., Jones, E.B.G. 1987. Cytochemical and electron microscopical observations on the adhesive materials of marine fouling diatoms. British Phycological Journal, 22: 101–118.

Decho, A.W. 1994. Molecular-scale events influencing the macroscale cohesiveness of exopolymers. In: Krumbein WE, Paterson D, Stal LJ, editors. Biostabilization of sediments. Verlag, Oldenburg, pp. 135-148.

Delgado, C., Pardo, I., Garcia, L. 2012. Diatom communities as indicators of ecological status in Mediterranean temporary streams (Balearic Islands, Spain). Ecological Indicators, 15: 131-139.

Desrosiers, C., Leflaive, J., Eulin, A., Ten-Hage, L. 2013. Bioindicators in marine waters: Benthic diatoms as a tool to assess water quality from eutrophic to oligotrophic coastal ecosystems. Ecological Indicators, 32: 25-34.

Dorigo, U., Berard, A., Rimet, F., Bouchez, A., Montuelle, B. 2010. In situ assessment of periphyton recovery in a river contaminated by pesticides. Aquatic Toxicology, 98: 396-406.

Eriksson, K.M., Clarke, A.K., Franzen, L.G., Kuylenstierna, M., Martinez, K., Blanck, H. 2009. Community-Level Analysis of psbA Gene Sequences and Irgarol Tolerance in Marine Periphyton. Applied and Environmental Microbiology, 75: 897-906.

Frankovich, T.A., Gaiser, E., Wachnicka, A., Zieman, J.C. 2006. Spatial and temporal distributions of epiphytic diatoms: relationships to salinity and nutrients in a subtropical ecosystem. Hydrobiologia 569, 259–271.

Guasch, H., Ivorra, N., Lehmann, V., Paulsson, M., Real, M., Sabater, S. 1998. Community composition and sensitivity of periphyton to atrazine in flowing waters: the role of environmental factors. Journal of Applied Phycology, 10: 203-213.

Guasch, H., Navarro, E., Serra, A., Sabater, S. 2004. Phosphate limitation influences the sensitivity to copper in periphytic algae. Freshwater Biology, 49: 463-473.

Hillebrand, H., Sommer, U. 2000. Effect of continuous nutrient enrichment on microalgae colonizing hard substrates. Hydrobiologia. 426: 185–192.

Hustedt, F. 1959. Die Kieselalgen Deutschlands, Österreichs und der Schweiz unter Berücksichtigung der ubrigen Länder Europas sowie der angrezenden Meeresgebiete. 2 Teil. In: Kryptogamen-Flora von Deutschland, Österreich und der Schweiz (Ed. By L. Rabenhorst). Akademische Verlagsgesellschaft, Leipzig, 845 pp.

Ivorra, N., Hettelaar, J., Tubbing, G.M.J., Kraak, M.H.S., Sabater, S., Admiraal,W. 1999. Translocation of microbenthic algal communities used for in situ analysis of metal pollution in rivers. Archives of Environmental Contamination and Toxicology, 37:19–28.

Ivorra, N., Hettelaar, J., Kraak, M.H.S., Sabater, S., Admiraal, W. 2002. Responses of biofilms to combined nutrient and metal exposure. Environmental Toxicology and Chemistry, 21: 626-632.

Jeffrey, S.W., Humphrey, G.F. 1975. New spectrophotometric equation for determining chlorophyll *a*, *b*, *c*1 and *c*2. Biochemie und Physiologie der Pflanzen, 167: 194-204.

Larras, F., Keck, F., Montuelle, B., Rimet, F., & Bouchez, A. 2014. Linking diatom sensitivity to herbicides to phylogeny: a step forward for biomonitoring?. Environmental Science & Technology, 48(3): 1921-1930.

Larson, F., Petersen, D.G., Dahllof, I., Sundback, K. 2007. Combined effects of an antifouling biocide and nutrient status on a shallow-water microbenthic community. Aquatic Microbial Ecology, 48: 277-294.

Lloret, J., Marín, A., Marín-Guirao, L., & Velasco, J. 2005. Changes in macrophytes distribution in a hypersaline coastal lagoon associated with the development of intensively irrigated agriculture. Ocean & Coastal Management, 48(9): 828-842.

Marín-Guirao, L., Atucha, A.M., Lloret, J., Lopez, E.M., Fernandez, A.J.G. 2005. Effects of mining wastes on a seagrass ecosystem: metal accumulation and bioavailability, seagrass dynamics and associated community structure. Marine Environmental Research, 60: 317-337.

Marín-Guirao, L., Lloret, J., Marín, A. 2008. Carbon and nitrogen stable isotopes and metal concentration in food webs from a mining-impacted coastal lagoon. Science of the Total Environment, 393: 118-130.

Marín-Guirao, L., Lloret, J., Marín, A., Garcia, G., Garcia-Fernández, A.J. 2007. Pulse-discharges of mining wastes into a coastal lagoon: Water chemistry and toxicity. Chemistry and Ecology, 23: 217-231.

Medley, C.N., Clements, W.H. 1998. Responses of diatom communities to heavy metals in streams: the influence of longitudinal variation. Ecological applications, 8, 631–644.

Morin, S., Duong, T.T., Boutry, S., Coste, M. 2008a. Mitigation of metal toxicity to freshwater biofilms development (Decazeville watershed, SW France). Cryptogamie Algologie, 29: 201-216.

Morin, S., Duong, T.T., Dabrin, A., Coynel, A., Herlory, O., Baudrimont, M., *et al*. 2008b. Long-term survey of heavy-metal pollution, biofilm contamination and diatom community structure in the Riou Mort watershed, South-West France. Environmental Pollution, 151: 532-542.

Navarro, E., Guasch, H., Sabater, S. 2002. Use of microbenthic algal communities in ecotoxicological tests for the assessment of water quality: the Ter river case study. Journal of Applied Phycology, 14: 41-48.

Ohlauson, C., Blanck, H. 2014. A comparison of toxicant-induced succession for five antifouling compounds on marine periphyton in SWIFT microcosms. Biofouling, 30: 41-50.

Pacepavicius, G., Lau, Y.L., Liu, D., Okamura, H., Aoyama, I. 1997. A rapid biochemical method for estimating biofilm mass. Environmental Toxicology, 12: 97-100.

Passy, S.I. 2007. Diatom ecological guilds display distinct and predictable behavior along nutrient and disturbance gradients in running waters. Aquatic Botany, 86: 171-178.

R Core Team, 2015. R: A language and environment for statistical computing.

Rimet, F., Bouchez, A. 2011. Use of diatom life-forms and ecological guilds to assess pesticide contamination in rivers: Lotic mesocosm approaches. Ecological Indicators, 11: 489-499.

Rimet, F., Bouchez, A. 2012. Life-forms, cell-sizes and ecological guilds of diatoms in European rivers. *Knowledge and management of Aquatic Ecosystems*, 406: 01, pp. 12.

Rinella, D.J., Bogan, D.L. 2004. Toward a Diatom Biological Monitoring Index for Cook Inlet Basin, Alaska, Streams. University of Alaska Anchorage, U.S. Environmental Protection Agency, Seattle.

Ros, M.D., Marin-Murcia, J.P., Aboal, M. 2009. Biodiversity of diatom assemblages in a Mediterranean semiarid stream: implications for conservation. Marine and Freshwater Research, 60: 14-24.

Rutherford, A. 2001. Introducing ANOVA and ANCOVA a GLM Approach. SAGE Publications, London, U.K.

Sabater, S., Guasch, H., Ricart, M., Romani, A., Vidal, G., Kluender, C., *et al*. 2007. Monitoring the effect of chemicals on biological communities. The biofilm as an interface. Analytical and bioanalytical chemistry, 387: 1425-1434.

Serra, A., Guasch, H., Admiraal, W., Van der Geest, HG, Van Beusekom SAM, 2010. Influence of phosphorus on copper sensitivity of fluvial periphyton: the role of chemical, physiological and community-related factors. Ecotoxicology. 19: 770-780.

Sims, P.A., Mann, D.G., Medlin, L.K. 2006. Evolution of the diatoms: Insights from fossil, biological and molecular data. Phycologia. 45, 361−402.

Soldo, D., Behra, R. 2000. Long-term effects of copper on the structure of freshwater periphyton communities and their tolerance to copper, zinc, nickel and silver. Aquatic Toxicology, 47: 181-189.

Sundbäck, K., Petersen, D.G., Dahllof, I., Larson, F. 2007. Combined nutrient-toxicant effects on a shallow-water marine sediment system: sensitivity and resilience of ecosystem functions. *Marine Ecology Progress Series*, 330: 13-30.

Tago, Y., Aida, K. 1977. Exocellular mucopolysaccharide closely related to bacterial floc formation. Applied and environmental microbiology, 34: 308-314.

Terrados, J., Ros, J. 1991. Production dynamics in a macrophyte dominates ecosystem: the Mar Menor coastal lagoon (SE Spain). Oecologia aquatica, 10: 255-270.

Tlili, A., Berard, A., Roulier, J-L, Volat, B., Montuelle, B. 2010. PO_4^{3-} dependence of the tolerance of autotrophic and heterotrophic biofilm communities to copper and diuron. Aquatic Toxicology, 98: 165-177.

Tlili, A., Corcoll, N., Bonet, B., Morin, S., Montuelle, B., Berard, A., *et al*. 2011. In situ spatio-temporal changes in pollution-induced community tolerance to zinc in autotrophic and heterotrophic biofilm communities. Ecotoxicology 20: 1823-1839.

Townsend, C.R., Scarsbrook, M.R., Dolédec, S. 1997. The intermediate disturbance hypothesis, refugia, and biodiversity in streams. Limnology and Oceanography, 42(5): 938-949.

Trobajo, R., Quintana, X.D., Sabater, S. 2004. Factors affecting the periphytic diatom community in Mediterranean coastal wetlands (Emporda wetlands, NE Spain). Archiv für Hydrobiologie, 160: 375-399.

Underwood, A.J. 1997. Experiments in Ecology: Their Logical Design and Interpretation Using Analysis of Variance. Cambridge University Press, Cambridge, U.K.

Van der Grinten, E., Janssen, M., Simis, S.G.H., Barranguet, C, Admiraal, W. 2004. Phosphate regime structures species composition in cultured phototrophic biofilms. Freshwater Biology, 49: 369-381.

Velasco, J., Lloret, J., Millan, A., Marín, A., Barahona, J., Abellan, P. *et al*. 2006. Nutrient and particulate inputs into the Mar Menor lagoon (Se Spain) from an intensive agricultural watershed. Water Air and Soil Pollution, 176: 37-56.

Wachnicka, A., Gaiser, E., Boyer, J. 2011. Ecology and distribution of diatoms in Biscayne Bay, Florida (USA): Implications for bioassessment and paleoenvironmental studies. Ecological Indicators, 11: 622-632.

Witkowski, A., Lange-Bertalot, H., Metzeltin, D. 2000. Diatom flora of marine coasts I. In: Lange-Bertalot H, editor. Iconographia Diatomologica. Annotated Diatom Micrographs. Diversity-Taxonomy-Identification. Ruggell: A.R.G. Gantner Verlag KG, Vol. 7. pp. 1-925.

Zuur, A.F., Ieno, E.N., Walker, N., Saveliev, A.A., Smith, G.M. 2009. Mixed Effects Models and Extensions in Ecology with R. Springer, New York.

General Discussion

General Discussion

Benthonic diatoms can act as biological indicators of anthropogenic impacts in the coastal Mar Menor lagoon, as the present data evidence. However, more taxonomic and floristic studies, and *in vitro* bioassays and experiments, are needed to suitably characterise the ecological ranges and the bioindicator potential of the different species of any environmental impact. Any work on bioindicators needs to be based on sound floristic knowledge, but such information is often lacking in a marine environments. This is the scenario of the present thesis because previously no information has been available about the composition of the benthonic diatom communities in the Mar Menor Lagoon area. The only work that could be used as a reference for taxonomical studies was the doctoral thesis by Tomás (1988) which provides information on the flora of two saltpans located near the lagoon, called El Cotorillo and Marchamalo. Thus the 47 species included in the works of the present thesis are considered new citations for this lagoon ecosystem, two of which *Licmophora colosalis* and *Hyalosynedra lanceolata,* have been recently described as new species for science. In the field material, the populations of both species presented wide morphological variability as far as size and shape of valves are concerned, which could lead to incorrect identifications if no in-depth molecular and morphological study is done. For example, different populations are found for *H. lanceolata* of cell lengths of some 20 µm, 60 µm, and some longer than 100 µm. For *L. colosalis*, variability is also observed for rimoportulae and number of stria, as Chapter 2 explains. Hence all our results reveal the importance of using cultures and molecular techniques to correctly identify such species in dynamic and complex environments like those found in coastal lagoon, which agrees with what has been suggested for such environmental estuary species. Despite many works that have focused on marine benthic species having increased in recent years (Car *et al*., 2012; Li *et al*., 2016; Lobban *et al*., 2015; Álvarez-Blanco and Blanco, 2014), many species lack a thorough morphological study conducted with SEM, and an original description does not allow to clearly distinguish them as some taxonomic aspects are not described. For instance, some species of the genus *Limophora*, like *L. tenuis*, for which Chapter 2 provides new information on some taxonomic aspects and SEM images, even large-sized species which would, initially, be easy to identify, have only a partial description, but no reference illustrations (e.g., *Licmophora gigantea*). All this makes the work of identifying and comparing them with other species very difficult. Some recent studies have described several gender and species from conducting taxonomic reviews with material from coastal areas (Li *et al*., 2016). The review of the genus *Hyalosynedra*, done in Chapter 1, has resulted in the description of a new species, and points out the uncertainty in the taxonomic position of *Synedra toxoneides* (recently proposed for the genus *Hyalosynedra* in Álvarez-Blanco & Blanco, (2014). What all this evidences is the need to do taxonomic reviews of diatoms in areas with such singular conditions like those in the hypersaline Mar Menor Lagoon because, surprisingly, some of the most abundant genera have been barely studied to date.

The coastal Mar Menor Lagoon is classified as natural coastal-type water, and according to Water Framework Directive (WFD) guidelines, some biological elements are indicated to assess their ecological status, including phytoplankton (measures of chlorophylls concentrations), macrophytes and macroinvertebrates, for which some quality indices are proposed. Benthic diatoms are not, however, proposed as a monitoring tool. This makes sense in open coastal water where these communities do not develop at any great depth, but develop well in shallow coastal systems like estuaries and coastal lagoons. Indeed we found high biomass values in the shallow areas we studied. In 2008, values reached 2.6 g AFDW /m^2 in June and 8.5 g AFDW /m^2 in July (taken in artificial substrate for 20 days under the conditions described in Chapter 5). The results of this thesis also show how benthic diatom communities are an ideal tool to monitor and detect the release of metal and nutrients relatively quickly. The microbial biofilm serves as a tool to detect sporadic metal discharges because the mere addition of four 1-hour pulses reflected an increased Zn concentration, which more than doubled in all the analysed biofilms. This behaviour also reflected the influence of waste from former mining activity because the Zn concentration in the biofilms in the contaminated area was 5.5-fold higher than in the reference area. No rainfall events took place during the experiment indicated in Chapter 5, thus the high content of metals in this compartment indicates the bioavailability of sediment metals in contaminated areas; e.g., in the surrounding area of Beal Wadi, which agrees with what Marín-Guirao *et al*. (2005) suggested.

The diatom assemblages from study sites were characterised by a few dominant diatom species and by many rare or less abundant taxa. Some species are proposed as potential bioindicators, but a characterisation of the bioassay-based tolerance profile is necessary, specifically in terms of toxins and nutrients. *Berkeleya fennica* and *Neosynedra provincialis* seem to well tolerate the presence of high concentrations of metals and nutrients. Despite very little bibliography existing that provides information about the environmental preferences of marine species, the results of some works support the proposal of these species being ideal bioindicators. For instance, some *Berkeleya* species have been proposed as spillage indicators of wastewater in Argentina (Becherucci *et al*., 2016). *B. fennica* has been specifically detected in waters with high productivity (Trobajo *et al*., 2004), *N. provincialis* has also been reported to be tolerant to the organic herbicide Irgarol 1501 (Dahl & Blanck, 1996; Eriksson *et al*., 2009). Moreover, *C. placentula* could be considered opportunistic, which agrees with that proposed by Trobajo *et al*. (2004), and with its high-nutrient tolerance (Wachnicka *et al*., 2011). Some other interesting species for future ecological studies would be: *N. frustulum*, which has been found to be dominant in communities on the Ciervo Isle (the "reference" area), but which has appeared with some abundance (5-15%) in the contaminated area (Beal Wadi). Some studies have cited it as a typical species in waters with a high nutrient content (Delgado *et al*., 2012; Tomás, 1988). *O. krumbeinii* has been cited as a potentially sensitive species to this environmental stress as it abundance diminished with any releases in the reference area, and is barely found in the areas surrounding the contaminated area. This is the smallest species of all those analysed (30 μm^3), and its response pattern does not coincide with what former studies have suggested because it has been generally indicated as a small cell-sized species that tends to dominate in areas contaminated by metals (Morin *et al*., 2008). Thus more detailed research is required. All these observations need to be investigated in more depth and by bioassays to obtain basic information about the tolerance limits of each highlighted species.

Regarding community changes, it is worth stressing the combined releases of metals and nutrients that may alter the structure of communities in areas that remain relatively unaltered after a few days (one 1-hour pulse for 4 days). The presence of both stress factors leads to much more marked alterations in benthic communities if these factors act separately, and can amplify accumulated metals and the restructuration of diatom communities towards a similar composition and architecture to those found at the historically contaminated site. These findings suggest that nutrients seem to hasten the succession of species towards tolerant-dominance communities. Although those communities that live at the historically contaminated site can better support such stress, in structural terms it has been observed that inputs of metals or nutrients can induce mucilage production that can negatively affect sediment communities or macrophytes.

Our results also show that using certain species biological traits, like growth form, can provide further information about species' ecology; e.g., on the one hand, the tube of the *Berkeleya* species could act as a physical barrier against toxic agents; on the other hand, the same species could also grow under enriched conditions due to the high demand of nutrients needed for tube production (Daniel *et al*., 1987; Hillebrand & Sommer, 2000). Biofilm's growth forms and 3-dimensional structure could affect the interaction among different community components, and thus the final response of the whole community. Although more studies are needed, the biofilm's 3-dimensional structure could act as a fast warning-system for certain contamination types as greater 3-dimensional complexity has been found in the contaminated areas than in the reference ones. Research based on such metrics requires previously studying fresh material. Conventionally however, taxonomic studies into diatoms have been done by analysing processed and clean material. So despite the valuable information that fresh material contributes, it is difficult to find information about growth forms, not even about the nature of chloroplasts, in the literature (Round *et al*., 1990).

Many freshwater studies have suggested the growth form of species as being valuable biological traits to detect environmental changes (e.g. Rimet and Bouchez, 2011; Rimet and Bouchez, 2012), but these research works based on such metrics are rare in the marine environment (Svensson *et al*., 2014) Ulanova and Snoeijs, 2006). Specifically, stalked diatoms have been indicated as a good candidate to discriminate different trophic statuses in freshwater ecosystems (Berthon *et al*., 2011; Passy, 2007). Some peduncle-forming marine species

can form huge mucilaginous masses, like those described in Chapter 4 for *Licmophora colosalis* and *L. flabellate* (Ravizza & Hallegraeff, 2015). In the Tyrrhenian and Adriatic Seas, massive mucilage proliferations have been observed in both pelagic and benthic environments, and a positive relation between these events and abnormal temperature episodes has been pointed out (Cerrano *et al*., 2006; De Philippis *et al*., 2005). As to how temperature affects microalgae communities, there is some controversy about the results; e.g., there is a general idea that increased temperature diminishes cell size. Many studies have suggested that this effect is due to fewer nutrients to a greater extent than directly to temperature. The results in Chapter 4 reveal a clear interaction between the stoichiometric N:P ratio of water and the effect of increased temperature and the stress that species like *L. colosalis,* which can normally live in environments with high temperatures in summer like the Mar Menor (31 °C in August), are very sensitive if future temperatures increase if climate change forecasts come true. Their thermal tolerance limit does not exceed 36 °C, a temperature that may be reached in a few years time at Mar Menor in shallow areas as the summer of 2017 has already detected temperatures of 33 °C in July. This may change the population dynamics of the species in particular, and in benthic communities in general, as previous studies have indicated (Svensson *et al*., 2014). It has also been found that *L. colosalis* could better withstand future increases in temperature if water presents a stoichiometric N:P ratio close to 16, otherwise most of the population would die, and would favour the production of huge mucilaginous benthic masses. This result suggests the urgent requirement to stop spillages of nutrients in the Mar Menor, where the main source of contamination by nutrients is nitrates from the intensive agricultural practices in the region. As previously described in taxonomy sections, *L. colosalis* forms large masses, which can be seen by the naked eye, composed mainly of mucilage peduncles. Significant peduncle production has been found to be related with lack of P in water (high N:P ratio values). These results agree with the massive production patterns of the river *Didymosphenia geminata* species e.g., Bothwell & Kilroy (2011). Although this needs to be empirically verified for *L. colosalis*, as checked in *Didymosphenia*, this response could be related with the organic phosphorus capturing capacity by peduncles, which allows species to develop when growth is limited by lack of P. What all this evidences is that this characteristic of *L. colosalis* could also initially serve as an indicator of the areas with spillages of nutrients in the coastal Mar Menor Lagoon. All these results may be very interesting in a wider area than the Mar Menor as *L. colosalis* has also been found in the Red Sea and Florida Bay. Some species of the genus *Licmophora* form part of these mucilaginous proliferations on coasts of the Adriatic Sea, and also in Australia, as biofouling formers on crop farms.

In global terms, this thesis shows the high potential of benthic diatoms as bioindicators of the environmental impact on the studied lagoon. All the provided data can act as a baseline to consider the design of environmental monitoring at the lagoon. However, it is first necessary to extend floristic knowledge in other study areas. These data could serve to compare the current state of benthic communities after the eutrophication process, which has threatened the lagoon since 2015, and for the rapid detection of contamination sources to act on the area, and to facilitate follow-ups of evolution if recovery measures of the lagoon ecosystem are contemplated.

References

Álvarez-Blanco, I., Blanco, S. 2014. Benthic diatoms from Mediterranean Coasts. Vol 60: Bibliotheca Diatomologica.

Becherucci, M. E., Santiago, L., Benavides, H. R., & Vallarino, E. A. 2016. Assessing sewage impact in a South-West Atlantic rocky shore intertidal algal community. Marine pollution bulletin, 106(1): 388-394.

Berthon, V., Bouchez, A., Rimet, F. 2011. Using diatom life-forms and ecological guilds to assess organic pollution and trophic level in rivers: a case study of rivers in south-eastern France. Hydrobiologia, 673: 259-271.

Bothwell, M. L., & Kilroy, C. 2011. Phosphorus limitation of the freshwater benthic diatom Didymosphenia geminata determined by the frequency of dividing cells. Freshwater Biology, 56 (3): 565-578.

Car, A., Witkowski, A., Dobosz, S., Burfeind, D.D., Meinesz, A., Jasprica, N., *et al*. 2012. Description of a new marine diatom, Cocconeis caulerpacola sp. nov. (Bacillariophyceae), epiphytic on invasive Caulerpa species. European Journal of Phycology , 47: 433-448.

Cerrano, C., Totti, C., Sponga, F., Bavestrello, G. 2006. Summer disease in *Parazoanthus axinellae* (Schmidt, 1862) (Cnidaria, Zoanthidea). Italian Journal of Zoology, 73:355–361

Dahl, B., Blanck, H. 1996. Toxic effects of the antifouling agent Irgarol 1051 on periphyton communities in coastal water microcosms. Marine Pollution Bulletin, 32: 342-350.

Daniel, G.F., Chamberlain, A.H.L., Jones, E.B.G. 1987. Cytochemical and electron microscopical observations on the adhesive materials of marine fouling diatoms. British phycological journal, 22(2): 101-118.

De Philippis, R., Faraloni, C., Sili, C., & Vincenzini, M. 2005. Populations of exopolysaccharide-producing cyanobacteria and diatoms in the mucilaginous benthic aggregates of the Tyrrhenian Sea (Tuscan Archipelago). Science of the total environment, 353(1): 360-368.

Delgado, C., Pardo, I., Garcia, L. 2012. Diatom communities as indicators of ecological status in Mediterranean temporary streams (Balearic Islands, Spain). Ecological Indicators, 15: 131-139.

Eriksson, K.M., Clarke, A.K., Franzen, L.G., Kuylenstierna, M., Martine, K., Blanck, H. 2009. Community-Level Analysis of psbA Gene Sequences and Irgarol Tolerance in Marine Periphyton. Applied and Environmental Microbiology, 75: 897-906.

Hillebrand, H., Sommer, U., 2000. Effect of continuous nutrient enrichment on microalgae colonizing hard substrates. Hydrobiologia, 426: 185–192.

Li, C.L., Ashworth, M.P., Witkowski, A., Lobban, C.S., Zglobicka, I., Kurzydlowski, K.J., *et al*. 2016. Ultrastructural and molecular characterization of diversity among small araphid diatoms all lacking rimoportulae. I. Five new genera, eight new species. Journal of Phycology, 52: 1018-1036.

Lobban, C.S., Ashworth, M.P., Car, A., Herwig, W., Ulanova, A. 2015. Licmosphenia revisited: transfer to Licmophora, redescription of L. clevei Mereschkowsky and descriptions of three new species. Diatom Research , 30: 227-236.

Marin-Guirao, L., Atucha, A.M., Lloret, J., Lopez, E.M., Fernandez, A.J.G. 2005. Effects of mining wastes on a seagrass ecosystem: metal accumulation and bioavailability, seagrass dynamics and associated community structure. Marine Environmental Research , 60: 317-337.

Morin, S., Duong, T.T., Dabrin, A., Coynel, A., Herlory, O., Baudrimont, M., *et al*. 2008. Long-term survey of heavy-metal pollution, biofilm contamination and diatom community structure in the Riou Mort watershed, South-West France. Environmental Pollution, 151: 532-542.

Passy, S.I. 2011. Diatom ecological guilds display distinct and predictable behavior along nutrient and disturbance gradients in running waters. Aquatic Botany, 86: 171-178.

Ravizza, M., Hallegraeff, G. 2015. Environmental conditions influencing growth rate and stalk formation in the estuarine diatom Licmophora flabellata (Carmichael ex Greville) C.Agardh. Diatom Research , 30: 197--208.

Rimet, F., Bouchez, A. 2011. Use of diatom life-forms and ecological guilds to assess pesticide contamination in rivers: Lotic mesocosm approaches. Ecological Indicators, 11: 489-499.

Rimet, F., Bouchez, A. 2012. Life-forms, cell-sizes and ecological guilds of diatoms in European rivers. Knowledge and Management of Aquatic Ecosystems , 12.

Round, F.E., Crawford, R.M., Mann, D.G. 1990. The Diatoms - Biology & Morphology of the genera: Cambridge University Press.

Svensson, F., Norberg, J., Snoeijs, P. 2014. Diatom Cell Size, Coloniality and Motility: Trade-Offs between Temperature, Salinity and Nutrient Supply with Climate Change. Plos One, 9.

Tomás, X. 1988. Diatomeas de las aguas epicontinentales saladas del litoral mediterráneo de la Penínnsula Ibérica. University of Barcelona, Spain.

Trobajo, R., Quintana, X.D., Sabater, S. 2004. Factors affecting the periphytic diatom community in Mediterranean coastal wetlands (Emporda wetlands, NE Spain). Archiv Fur Hydrobiologie, 160: 375-399.

Ulanova, A., Snoeijs, P. 2006. Gradient responses of epilithic diatom communities in the Baltic Sea proper. Estuarine Coastal and Shelf Science, 68: 661-674.

Wachnicka, A., Gaiser, E., Boyer, J. 2011. Ecology and distribution of diatoms in Biscayne Bay, Florida (USA): Implications for bioassessment and paleoenvironmental studies. Ecological Indicators, 11: 622-632.

General Conclusions

General Conclusions

1. The floristic knowledge provided by this thesis can serve as a baseline to develop strategies to monitor the lagoon, but it is necessary to extend knowledge in different areas and in seasonality terms. The 47 taxa dealt with in this thesis are new cites of benthic diatoms for the Mar Menor lagoon, and two new species are described for Science: *Hyalosynedra lanceolata* and *Licmophora colosalis*. New information is provided to clarify the phylogenetic relationship among closely related taxa, such as *Hyalosynedra* species and *S. toxoneides*.

2. *Licmophora* is very well represented at the Mar Menor lagoon. Six species are found only in summer months, and they all seem to be eurihaline. *L. colosalis* is the most abundant early in summer months, while *L. remulus* is more abundant in September. New information and illustrations of some morphological characters of *L. tenuis* are provided, and some nomenclatural changes are proposed for the closely related taxa with *L. colosalis.*

3. The presented data evidence the need to carry out taxonomic reviews of marine benthic diatom genera, including a phylogenetic point of view, and to acquire information about their ecological tolerances and their suitability as a biological indicator.

4. The global change effects on *L. colosalis* populations are driven more by the combined effects of temperature stress and the N:P stoichiometry of water than by the direct effects of temperature. *L. colosalis* seems to be adapted to coastal water with stoichiometric N:P ratio values that ranged between 16 and 21, and an optimal growth temperature close to 26 °C. However, the value of 36 °C, predicted in the Mar Menor lagoon, can be lethal.

5. *Licmophora colosalis* could overcome the increase of 5 °C, from 26 °C to 31 °C, by inhabiting environments with a balanced N:P stoichiometry. While this thermal stress can have deleterious effects on populations that inhabit places with an unbalanced N:P stoichiometry of water as it can reduce cell growth and promote high mortality rates. In turn, it was found that, as observed for other diatom species, strongly limited growth by an unbalanced N:P stoichiometry was reflected by high levels of accumulated carbohydrates.

6. Stalks overproduction by *L. colosalis* is specifically observed when growth lowers by P-limited conditions. Since stalks production patterns remain constant at both 26 °C and 31 °C, we suggest that this species could serve as a sentinel for nitrate pollution in the lagoon.

7. Benthic diatom communities may serve as biological indicators of anthropogenic impacts on the coastal Mar Menor lagoon. They are a suitable tool to detect sporadic exposures of metal and nutrients, and the chronic influence of wadis drainages from the areas surrounding the lagoon. The biofilms from the chronically contaminated site are dominated by tolerant species, and may better overcome future sporadic metal and nutrient loads than those from unaltered sites. In contrast, both single and combined short exposures of metal and nutrients may strongly alter the biofilm communities from unaltered sites.

8. Metals and nutrients triggered the reorganisation of diatom communities in different ways and, by acting in combination, metal seemed to favoured the colonisation of metal-tolerant species, and nutrients seemed to benefit the proliferation of some tolerant-metal species with a specific growth form; e.g., tube forming and zig-zag colonies. Therefore, both stressors in combination drove more pronounced changes than when singly added, which matched the amplification of accumulated metals and the restructuring of diatom communities towards a similar composition and architecture to those found at the contaminated site. These findings suggest that nutrients seemed to hasten the succession of species towards tolerant-dominance communities.

9. A biofilm dominated by mucous tubes, zig-zag colonies and prostrate cells seemed to indicate metal and nutrient environmental stress. A study approach based on the biological traits of species may reflect further information on species' ecology (interaction between species) and, therefore, a better understanding of all the

whole community's responses. We suggest, therefore, incorporating diatom growth forms into monitoring programmes as a potentially quick and easy way to evaluate environmental pressures.

10. The epilithic diatom assemblages from the Mar Menor are characterised by a few species dominating in early summer months. Based on the abundance patterns, three groups of species are distinguished: *Brachysira aponina* and *Cocconeis placentula* that occur abundantly (>15%) at both the study sites, and *Opephora krumbeinii*, *Hyalosynedra lanceolata* and *Nitzschia frustulum,* which are dominant at the reference site, while *Berkeleya fennica* and *Neosynedra provincialis* dominated at the contaminated ones (>11%). Based on the occurrence at each study site, and the responses to sporadic metal and nutrient impacts, we propose *O. krumbeinii* as a potential sensitive species that is dominant at the reference site, and is negatively affected by both metal and nutrient stress. Conversely, *Berkeleya spp* and *Neosynedra provincialis* drove assemblages from the chronically contaminated sites and tended to dominate impacted-reference biofilms, and could therefore be proposed as potential tolerant species to both metals and nutrients. *Cocconeis placentula* is recognised as an opportunistic species as it appears relatively abundantly at the two study sites and tends to be abundant after nutrient enrichment.

Supporting Information

Appendix 1. Supporting information of chapter 1.

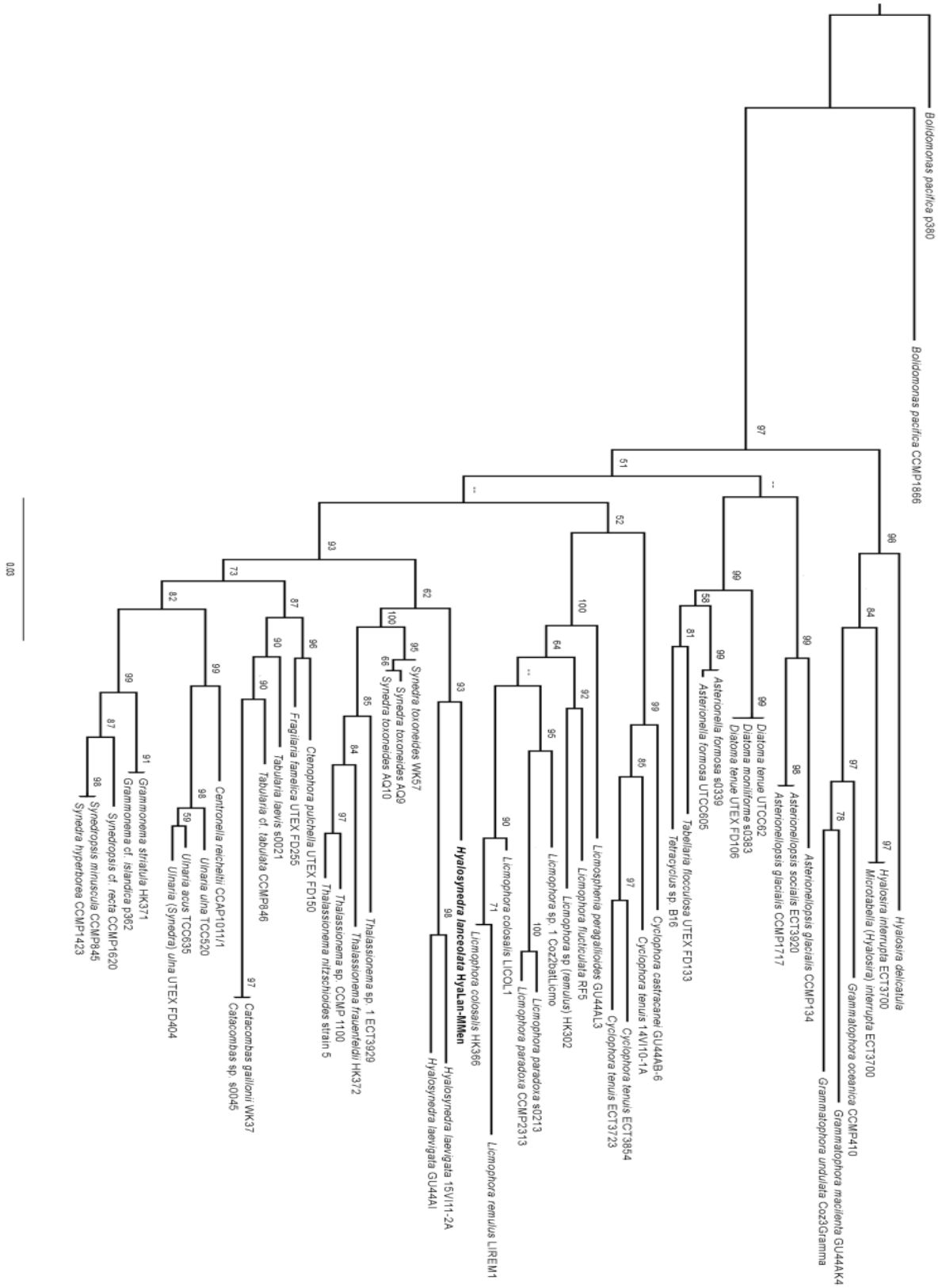

Figure Ap1 1. Maximum likelihood tree inferred from a concatenated alignment of SSU rRNA and *rbc*L markers of 56 araphid diatoms with constrained *S. toxoneides* and *Thalassionema* as the monophyletic clade. The numbers on the nodes are maximum likelihood bootstraps (MLb). The newly described species is shown in bold. Any support values lower than 50% were omitted.

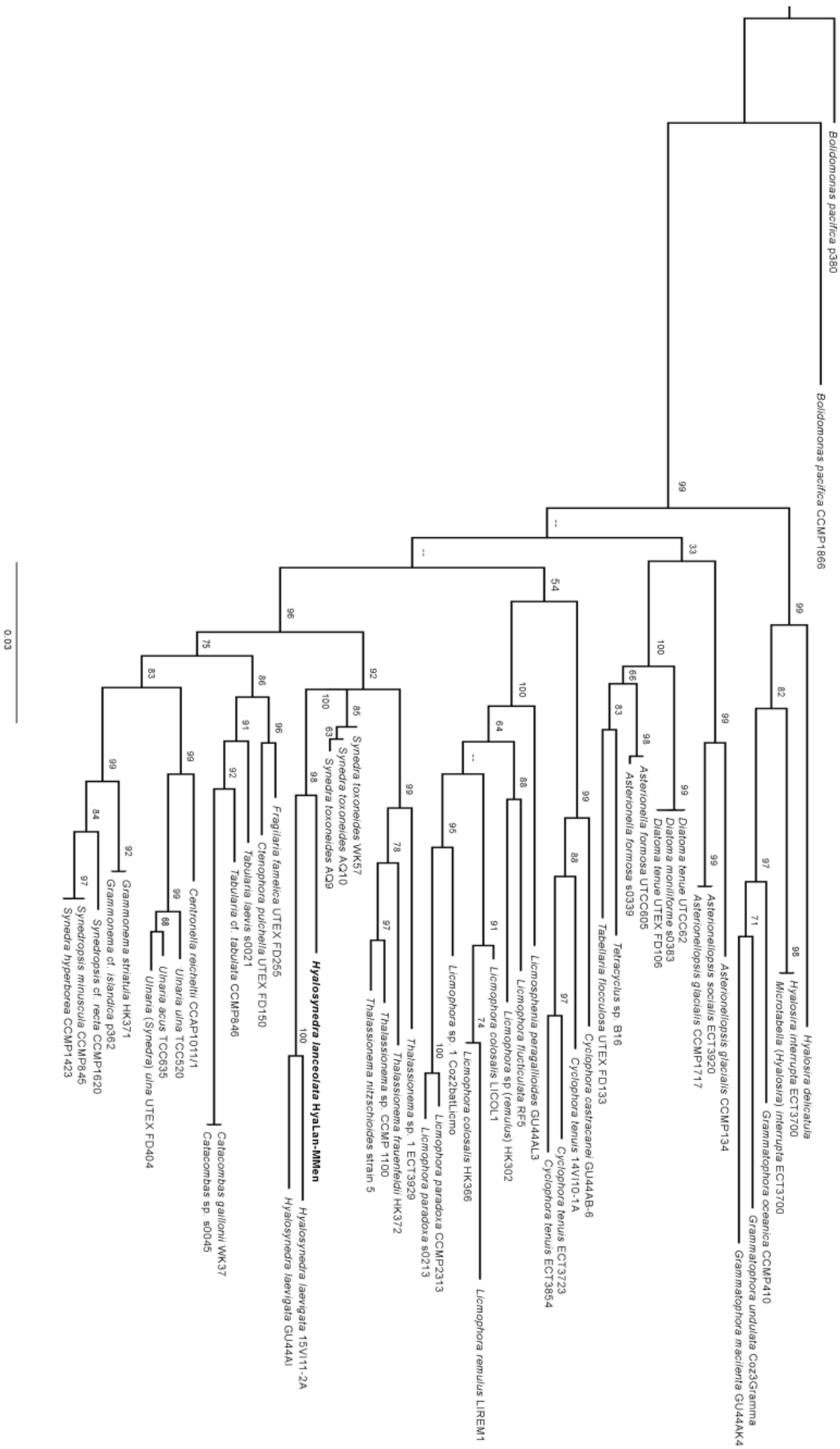

Figure Ap1 2. Maximum likelihood tree inferred from a concatenated alignment of SSU rRNA and *rbc*L markers of 56 araphid diatoms with constrained *S. toxoneides* and *Hyalosynedra* as the monophyletic clade. The numbers on the nodes are maximum likelihood bootstraps (MLb). The newly described species is shown in bold. Any support values lower than 50% were omitted.

Table Ap1 1. Maximum likelihood tree inferred from a concatenated alignment of SSU rRNA and *rbc*L markers of 56 araphid diatoms with constrained *S. toxoneides* and *Thalassionema* as the monophyletic clade. The numbers on the nodes are maximum likelihood bootstraps (MLb). The newly described species is shown in bold. Any support values lower than 50% were omitted.

Code	Taxon	Accesión number	
		SSU rDNA	rbcL
Afor	*Asterionella formosa UTCC605*	HQ912633	HQ912497
Afor1	*Asterionella formosa s0339*	AB430595	AB430671
Asoc	*Asterionellopsis socialis ECT3920*	JX413545	JX413562
Agla	*Asterionellopsis glacialis CCMP1717*	HQ912646	HQ912510
Agla1	*Asterionellopsis glacialis CCMP134*	HQ912613	HQ912477
Bpac	*Bolidomonas pacifica p380*	AB430618	AB430698
Bpac1	*Bolidomonas pacifica CCMP1866*	HQ912557	HQ912421
Cgai	*Catacombas gaillonii WK37*	EF423402	-
Csp	*Catacombas sp. s0045*	KR048195	KR048217
Crei	*Centronella reicheltii CCAP1011/1*	HQ912635	HQ912499
Cten	*Cyclophora tenuis ECT3723*	HQ912660	HQ912524
Cten1	*Cyclophora tenuis ECT3854*	JN975240	JN975254
Cten2	*Cyclophora tenuis 14VI10-1A*	JN975241	JN975255
Ccas	*Cyclophora castracanei GU44AB-6*	JN975242	JN975256
Cpul	*Ctenophora pulchella UTEX FD150*	HQ912611	HQ912475
Dten	*Diatoma tenue UTCC62*	HQ912622	HQ912486
Dten1	*Diatoma tenue UTEX FD106*	HQ912593	HQ912457
Dmon	*Diatoma moniliforme s0383*	AB430597	AB430674
Ffam	*Fragilaria famelica UTEX FD255*	HQ912588	HQ912452
Goce	*Grammatophora oceanica CCMP410*	HQ912634	HQ912498
Gmac	*Grammatophora macilenta GU44AK4*	JX401241	JX401259
Gund	*Grammatophora undulata Coz3Gramma*	JX401240	JX401258
Gstr	*Grammonema striatula HK371*	KF701591	KF701600
Gisl	*Grammonema cf. islandica p362*	AJ535190	-
Hlae	*Hyalosynedra laevigata 15VI11-2A*	JX401235	JX401253
Hlae1	*Hyalosynedra laevigata GU44AI**	JX401236	JX401254
Hlan	***Hyalosynedra lanceolata* HyaLan-MMen**	KY679465	KY679464
Hint	*Hyalosira interrupta ECT3700*	JN975247	JN975261
Hdel	*Hyalosira delicatula*	AF525654	AB430678
Lflu	*Licmophora flucticulata RF5*	HQ997923	JN975262
Lpar	*Licmophora paradoxa s0213*	AB430601	AB430679
Lpar1	*Licmophora paradoxa CCMP2313*	HQ912612	HQ912476
Lsp1	*Licmophora sp. 1 Coz2batLicmo*	JX401238	JX401256
Lsp	*Licmophora sp (remulus) HK302/GU52-O*	JN975248	JN975263
Lcol	*Licmophora colosalis HK366/ECT3907*	JX401239	JX401257
Lcol1	*Licmophora colosalis LICOL1*	KT321974	KT321972
Lrem	*Licmophora remulus LIREM1*	KT321975	KT321973
Lper	*Licmosphenia peragallioides GU44AL3*	JX401237	JX401255
Mint	*Microtabella (Hyalosira) interrupta ECT3700*	JN975247	JN975261
Stox1	*Synedra toxoneides AQ9**	KP981383	-
Stox2	*Synedra toxoneides AQ10**	KP981384	-
Stox3	*Synedra toxoneides WK57*	EF423421	-
Srec	*Synedropsis cf. recta CCMP1620*	HQ912616	HQ912480
Smin	*Synedropsis minuscula CCMP845*	EF423415	JN162825
Shyp	*Synedra hyperborea CCMP1423*	HQ912621	HQ912485
Ttab	*Tabularia cf. tabulata CCMP846*	AY485475	HQ912479
Tlae	*Tabularia laevis s0021*	AB430610	AB430690
Tflo	*Tabellaria flocculosa UTEX FD133*	HQ912584	HQ912448
Tesp	*Tetracyclus sp. B16*	KJ577873	KJ577910
Thsp	*Thalassionema sp. CCMP 1100*	EF192983	FJ002114
Thsp1	*Thalassionema sp. 1 ECT3929*	JX401234	JX401252
Thfr	*Thalassionema frauenfeldii HK372*	KF701592	KF701601
Thni	*Thalassionema nitzschioides strain 5*	KJ671712	KJ671820
Uacu	*Ulnaria acus TCC635*	KF959659	KF959645
Uuln1	*Ulnaria ulna TCC520*	KC736643	KC736614
Uuln2	*Ulnaria (Synedra) ulna UTEX FD404*	HQ912590	HQ912454

Table Ap1 2. Estimates of the evolutionary divergence between the SSU rDNA gene sequences. Values correspond to the p-distance between sequences, as a percentage.

	Stox2	Stox1	Hlae	Hlae1	Stox3	Hlan	Ffam	Srec	Uuln2	Gstr	Gisl	Crei	Cgai	Ttab	Tlae	Cpul	Goce	Gmac	Cten	Ccas	Cten1	Afor	Afor1	Tflo	Dten	Dten1	Dmon	Asoc	Agla	Agla1	Hint	Hdel	Gund	Mint	Cten2	Smin	Shyp	Uacu	Uuln1	Tesp	Thsp	Thfr	Thsp1	Lper	Lflu	Lpar	Lsp1	Lpar1	Lsp	Lcol	Lrem	Lcol1	Bpac	Bpac1	Csp
Stox1	0.10																																																							
Hlae	1.58	1.68																																																						
Hlae1	1.47	1.57	0.11																																																				
Stox3	0.00	0.10	1.58	1.47																																																			
Hlan	1.26	1.36	0.74	0.63	1.26																																																			
Ffam	0.84	0.94	1.79	1.78	0.84	1.36																																																		
Srec	1.26	1.15	2.10	1.99	1.26	1.57	0.84																																																	
Uuln2	2.09	2.20	2.84	2.72	2.09	2.30	2.09	2.20																																															
Gstr	1.47	1.36	2.31	2.20	1.47	1.78	1.05	0.42	2.20																																														
Gisl	1.47	1.36	2.31	2.20	1.47	1.78	1.05	0.42	2.20	0.00																																												
Crei	1.68	1.57	2.21	2.20	1.68	2.20	1.05	1.26	1.78	1.36	1.36																																											
Cgai	1.47	1.57	2.31	2.30	1.47	2.09	1.26	1.78	2.51	1.78	1.78	1.68																																										
Ttab	0.84	0.94	1.58	1.57	0.84	1.36	0.52	1.05	1.88	0.94	0.94	1.05	1.15																																										
Tlae	0.84	0.94	1.58	1.57	0.84	1.36	0.21	0.84	2.09	1.05	1.05	0.84	1.05	0.31																																									
Cpul	0.94	1.05	1.89	1.88	0.94	1.47	0.10	0.84	2.09	1.05	1.05	1.05	1.26	0.63	0.31																																									
Goce	3.14	3.25	3.36	3.25	3.14	3.14	2.83	3.25	3.98	3.25	3.25	3.66	3.66	3.14	2.83	2.93																																								
Gmac	2.94	3.05	3.47	3.36	2.94	3.05	2.73	3.15	3.68	3.15	3.15	3.57	3.47	3.05	2.73	2.84	0.74																																							
Cten	1.78	1.68	2.63	2.51	1.78	2.09	1.99	1.99	3.25	2.20	2.20	2.62	2.72	1.99	1.99	2.09	3.46	3.68																																							
Ccas	2.62	2.51	3.05	3.04	2.62	2.93	2.41	2.41	3.46	2.51	2.51	2.62	3.14	2.41	2.41	2.41	3.98	4.20	1.99																																						
Cten1	1.78	1.68	2.73	2.62	1.78	2.20	1.99	1.78	3.04	1.99	1.99	2.41	2.83	1.99	1.99	1.99	3.46	3.68	0.21	1.78																																						
Afor	1.88	1.99	2.52	2.51	1.88	2.20	1.68	1.88	2.83	1.99	1.99	2.30	2.51	1.68	1.68	1.68	3.46	3.47	2.20	2.09	1.99																																						
Afor1	1.88	1.99	2.52	2.51	1.88	2.20	1.68	1.88	2.83	1.99	1.99	2.30	2.51	1.68	1.68	1.68	3.46	3.47	2.20	2.09	1.99	0.00																																						
Tflo	1.88	1.99	2.52	2.51	1.88	2.20	1.68	1.88	2.83	1.99	1.99	2.30	2.51	1.68	1.68	1.68	3.46	3.47	2.20	2.09	1.99	0.21	0.21																																						
Dten	1.78	1.88	2.42	2.41	1.78	2.09	1.57	1.78	2.72	1.99	1.99	2.20	2.41	1.57	1.57	1.57	3.46	3.47	2.09	2.09	1.88	0.31	0.31	0.31																																						
Dten1	1.78	1.88	2.42	2.41	1.78	2.09	1.57	1.78	2.72	1.99	1.99	2.20	2.41	1.57	1.57	1.57	3.46	3.47	2.09	2.09	1.88	0.31	0.31	0.31	0.00																																						
Dmon	1.78	1.88	2.42	2.41	1.78	2.09	1.57	1.78	2.72	1.99	1.99	2.20	2.41	1.57	1.57	1.57	3.46	3.47	2.09	2.09	1.88	0.31	0.31	0.31	0.00	0.00																																						
Asoc	2.09	1.99	2.84	2.72	2.09	2.41	2.09	1.88	3.14	1.88	1.88	2.30	2.93	2.09	2.09	2.09	3.56	3.78	1.78	2.30	1.57	1.78	1.78	1.78	1.78	1.78	1.78																																						
Agla	2.09	1.99	2.84	2.72	2.09	2.41	2.09	1.88	3.14	1.88	1.88	2.30	2.93	2.09	2.09	2.09	3.56	3.78	1.78	2.30	1.57	1.78	1.78	1.78	1.78	1.78	1.78	0.00																																						
Agla1	1.99	1.88	2.73	2.62	1.99	2.30	1.99	1.78	3.04	1.78	1.78	2.20	2.62	1.99	1.99	1.99	3.46	3.68	1.68	2.20	1.47	1.68	1.68	1.68	1.68	1.68	1.68	0.31	0.31																																						
Hint	3.14	3.25	3.57	3.56	3.14	3.25	2.72	3.25	3.87	3.56	3.56	3.56	3.56	2.83	2.72	2.83	1.78	1.68	3.77	4.19	3.77	3.66	3.66	3.66	3.56	3.56	3.56	4.08	4.08	3.98																																						
Hdel	5.24	5.35	5.36	5.35	5.24	5.14	4.93	5.35	5.45	5.35	5.35	5.35	5.14	5.35	5.03	4.93	4.93	3.67	3.68	5.35	5.77	5.45	5.35	5.35	5.35	5.35	5.35	5.35	5.66	5.66	5.56	4.09																																						
Gund	3.25	3.35	3.36	3.25	3.25	3.14	2.83	3.25	4.08	3.25	3.25	3.66	3.56	3.14	2.83	2.93	0.31	0.84	3.35	3.87	3.35	3.35	3.35	3.35	3.35	3.35	3.35	3.35	3.46	3.46	3.35	1.88	3.56																																						
Mint	3.14	3.25	3.57	3.56	3.14	3.25	2.72	3.25	3.87	3.56	3.56	3.56	3.56	2.83	2.72	2.83	1.78	1.68	3.77	4.19	3.77	3.66	3.66	3.66	3.56	3.56	3.56	4.08	4.08	3.98	0.00	4.09	1.88																																						
Cten2	1.68	1.57	2.63	2.51	1.68	2.09	1.88	1.68	2.72	1.88	1.88	2.30	2.72	1.88	1.88	1.88	3.56	3.57	0.73	1.88	0.52	1.99	1.99	1.99	1.78	1.78	1.78	2.09	2.09	1.99	3.66	5.35	3.46	3.66																																						
Smin	1.26	1.15	2.10	1.99	1.26	1.57	1.05	0.21	2.09	0.21	0.21	1.36	1.78	0.84	1.05	1.05	3.46	3.36	1.99	2.41	1.78	1.88	1.88	1.88	1.78	1.78	1.78	1.88	1.88	1.78	3.46	5.45	3.46	3.46	1.68																																						
Shyp	1.26	1.15	2.10	1.99	1.26	1.57	1.05	0.21	2.09	0.21	0.21	1.36	1.78	0.84	1.05	1.05	3.46	3.36	1.99	2.41	1.78	1.88	1.88	1.88	1.78	1.78	1.78	1.88	1.88	1.78	3.46	5.45	3.46	3.46	1.68	0.00																																						
Uacu	2.20	2.30	2.94	2.83	2.20	2.41	2.09	2.20	0.21	2.20	2.20	2.20	1.78	2.62	1.88	2.09	2.09	3.98	3.89	3.25	3.46	3.04	2.83	2.83	2.83	2.72	2.72	2.72	3.14	3.14	3.04	3.87	5.35	4.08	3.87	2.72	2.09	2.09																																						
Uuln1	2.51	2.62	3.26	3.14	2.51	2.72	2.51	2.62	0.42	2.62	2.62	2.20	2.93	2.30	2.51	2.51	4.40	4.10	3.66	3.87	3.46	3.25	3.25	3.25	3.14	3.14	3.14	3.35	3.35	3.25	4.29	5.77	4.50	4.29	3.14	2.51	2.51	0.42																																						
Tesp	2.09	2.20	2.73	2.72	2.09	2.41	1.88	2.09	3.04	2.20	2.20	2.51	2.72	1.88	1.88	1.88	3.66	3.68	2.41	2.30	2.20	0.42	0.42	0.42	0.31	0.31	0.31	1.99	1.99	1.88	3.87	5.56	3.56	3.87	2.09	2.09	2.09	3.04	3.46																																						
Thsp	0.63	0.73	1.37	1.26	0.63	1.26	1.05	1.26	1.88	1.26	1.26	1.36	1.15	0.63	0.84	1.15	3.35	3.15	2.20	2.62	2.20	2.09	2.09	2.09	1.99	1.99	1.99	2.30	2.30	1.99	3.35	5.35	3.35	3.35	3.35	2.09	1.05	1.05	1.99	2.30	2.30																																						
Thfr	0.84	0.94	1.79	1.68	0.84	1.47	1.26	1.47	2.30	1.36	1.36	1.78	1.36	0.84	1.05	1.36	3.46	3.26	2.41	2.62	2.41	2.20	2.20	2.20	2.20	2.20	2.20	2.41	2.41	2.09	3.56	5.56	3.46	3.56	2.30	1.26	1.26	2.41	2.72	2.41	0.42																																						
Thsp1	0.73	0.84	1.68	1.57	0.73	1.36	1.15	1.36	2.20	1.36	1.36	1.68	1.26	0.73	0.94	1.26	3.04	3.05	2.30	2.93	2.30	2.20	2.20	2.20	2.09	2.09	2.09	2.41	2.41	2.09	3.25	5.35	3.25	3.25	2.20	1.15	1.15	2.30	2.62	2.41	0.31	0.52																																						
Lper	1.99	1.88	2.10	2.20	1.99	1.99	1.99	2.09	2.83	2.30	2.30	2.62	2.72	1.99	1.99	2.09	3.46	3.57	1.88	2.51	1.99	1.57	1.57	1.57	1.47	1.47	1.47	2.30	2.30	2.20	3.56	5.35	3.35	3.56	1.99	2.09	2.09	2.83	3.25	1.78	2.20	2.41	2.30																																						
Lflu	2.62	2.51	3.15	3.25	2.62	2.72	2.51	2.41	3.25	2.51	2.51	2.93	3.35	2.51	2.51	2.51	3.87	4.10	2.09	2.51	1.88	1.57	1.57	1.68	1.78	1.78	1.78	1.88	1.88	1.78	3.98	5.66	3.77	3.98	2.41	2.41	2.41	3.25	3.66	1.88	2.83	2.93	2.93	1.78																																						
Lpar	2.62	2.52	3.47	3.56	2.62	2.94	2.52	2.62	3.25	2.83	2.83	3.14	3.56	2.73	2.73	2.52	3.98	4.10	2.31	3.04	2.10	2.10	2.10	2.10	1.99	1.99	1.99	2.41	2.41	2.31	3.88	5.67	3.88	3.88	2.52	2.62	2.62	3.25	3.67	2.31	3.04	3.25	3.14	1.78	1.05																																						
Lsp1	2.20	2.09	2.84	2.93	2.20	2.51	1.88	1.78	3.04	2.20	2.20	2.20	2.72	2.09	1.88	1.88	3.77	3.68	1.88	2.41	1.68	1.78	1.78	1.78	1.68	1.68	1.68	1.88	1.88	1.78	3.46	5.35	3.66	3.46	1.88	1.99	1.99	3.04	3.46	1.99	2.41	2.62	2.51	1.68	1.26	1.36																																						
Lpar1	2.73	2.62	3.58	3.67	2.73	3.04	2.62	2.73	3.35	2.94	2.94	3.25	3.67	2.83	2.83	2.62	4.09	4.21	2.41	3.14	2.20	2.20	2.20	2.20	2.10	2.10	2.10	2.52	2.52	2.41	3.98	5.56	3.98	3.98	2.62	2.73	2.73	3.35	3.77	2.41	3.14	3.35	3.25	1.89	1.15	0.10	1.47																																						
Lsp	2.51	2.41	2.84	2.93	2.51	2.62	2.41	2.51	3.25	2.62	2.62	2.93	3.35	2.41	2.41	2.51	3.87	4.20	2.20	2.83	2.20	1.88	1.88	1.88	1.99	1.99	1.99	2.09	2.09	1.99	4.08	5.45	3.77	4.08	2.72	2.51	2.51	3.25	3.66	2.09	2.62	2.83	2.83	1.88	0.84	1.36	1.57	1.26																																						
Lcol	3.04	3.14	3.47	3.35	3.04	3.25	3.04	3.25	3.77	3.46	3.46	3.77	3.98	3.04	3.04	3.14	4.40	4.41	2.51	3.25	2.51	2.41	2.41	2.41	2.30	2.30	2.30	2.83	2.83	2.72	4.50	5.87	4.29	4.50	2.93	3.25	3.25	3.77	4.19	2.62	3.14	3.46	3.35	2.20	1.78	2.20	2.20	2.10	1.78																																						
Lrem	3.04	3.14	3.47	3.35	3.04	3.25	3.04	3.25	3.77	3.46	3.46	3.77	3.98	3.04	3.04	3.14	4.40	4.41	2.51	3.25	2.51	2.41	2.41	2.41	2.30	2.30	2.30	2.83	2.83	2.72	4.50	5.87	4.29	4.50	2.93	3.25	3.25	3.77	4.19	2.62	3.14	3.46	3.35	2.20	1.78	2.20	2.20	2.10	1.78	0.00																																						
Lcol1	2.41	2.30	2.63	2.72	2.41	2.72	2.30	2.20	2.93	2.41	2.41	2.51	3.14	2.30	2.30	2.30	3.77	4.10	1.88	2.30	1.68	1.57	1.57	1.57	1.26	1.26	1.26	1.88	1.88	1.78	3.87	5.56	3.66	3.87	1.99	2.20	2.20	2.93	3.35	1.57	2.41	2.83	2.72	1.36	0.94	1.05	0.94	1.15	1.05	1.68	1.68																																						
Bpac	4.08	3.98	4.94	4.82	4.08	4.29	4.08	3.98	4.71	3.87	3.87	4.40	4.61	3.98	4.08	4.08	5.55	5.57	3.87	4.71	3.77	4.40	4.40	4.40	4.40	4.40	4.40	4.40	4.40	3.77	3.77	3.87	5.86	7.55	5.55	5.86	3.98	3.87	3.87	4.71	5.13	4.50	3.98	4.08	4.08	4.50	4.50	4.72	4.50	4.82	4.50	5.34	5.34	4.50																																						
Bpac1	4.29	4.19	5.36	5.24	4.29	4.71	4.50	4.50	5.03	4.40	4.40	4.92	5.13	4.40	4.50	4.61	5.76	5.78	4.29	5.24	4.29	4.71	4.71	4.71	4.71	4.71	4.71	4.08	4.08	4.19	6.07	7.97	5.86	6.07	4.50	4.40	4.40	5.03	5.45	4.82	4.40	4.50	4.50	4.71	4.82	5.03	4.82	5.14	4.71	5.55	5.55	4.82	0.84																																						
Csp	0.63	0.84	1.89	1.88	0.63	1.46	0.63	1.05	2.09	1.05	1.05	0.84	0.00	0.42	0.42	0.63	4.18	4.00	1.67	2.51	1.67	0.84	0.84	0.84	0.84	0.84	0.84	1.67	1.67	1.46	4.18	6.50	4.18	4.18	1.67	1.05	1.05	2.30	2.93	1.05	0.63	0.63	0.63	1.46	2.30	2.94	2.09	3.14	2.72	2.72	2.72	2.30	2.93	3.56																																						
Thnl	0.42	0.64	1.50	1.27	0.42	1.27	0.85	0.85	1.49	0.85	0.85	0.64	0.64	0.64	0.64	0.85	4.03	3.85	1.49	2.34	1.49	1.06	1.06	1.06	1.06	1.06	1.06	1.49	1.49	1.27	4.46	6.60	4.03	4.46	1.49	0.85	0.85	1.70	2.34	1.27	0.00	0.42	0.42	1.49	2.34	2.98	2.12	3.19	2.55	2.34	2.34	1.91	2.76	3.40	0.64																																						

Appendix 2. Supporting information of chapter 3.

Table Ap2 1. List of taxa and Genbank accession numbers for SSU rDNA and *rbc*L sequences used in the phylogenetic analysis. Bold letters indicate sequences of this study. * Names proposed for change in Genbank, see text. The strain and location of taxon is indicated when provided by the database.

Taxon	Accession number		Location
	SSU rDNA	rbcL	
Hyalosira delicatula	AF525654	AB430678	
Grammatophora undulata	JX401240	JX401258	
Licmosphenia peragallioides GU44AL3	JX401237	JX401255	Guam (Pacific Ocean)
Licmophora normaniana	KJ577860	KJ577897	
Licmophora communis	AY633756	-	
Licmophora flabellata	AY633757	-	
Licmophora flabellata WK58	EF423410	-	
Licmophora flabellata WK47	EF423409	-	
Licmophora juergensii-1	AY633759	-	
Licmophora juergensii-2	AF525661	-	
Licmophora reichardtii WK63	EF423412	-	
Licmophora grandis WK62	EF423411	-	
Licmophora sp CSL-2013	JX401238	JX401256	Guam (Pacific Ocean)
Licmophora gracilis	AY633758	-	
Licmophora flucticulata RF5	HQ997923	JN975262	Guam (Pacific Ocean)
Licmophora paradoxa s0213	AB430601	AB430679	
Licmophora paradoxa CCMP2313	HQ912612	HQ912476	
*Licmophora sp HK302**	JN975248	JN975263	Guam (Pacific Ocean)
*Licmophora colosalis HK366/ECT3907**	JX401239	JX401257	Florida Bay (Atlantic Ocean)
Licmophora remulus LIREM1	KT321975	KT321973	Mar Menor (Mediterranean Sea)
Licmophora colosalis LICOL1	KT321974	KT321972	Mar Menor (Mediterranean Sea)

Appendix 3. Supporting information of chapter 4.

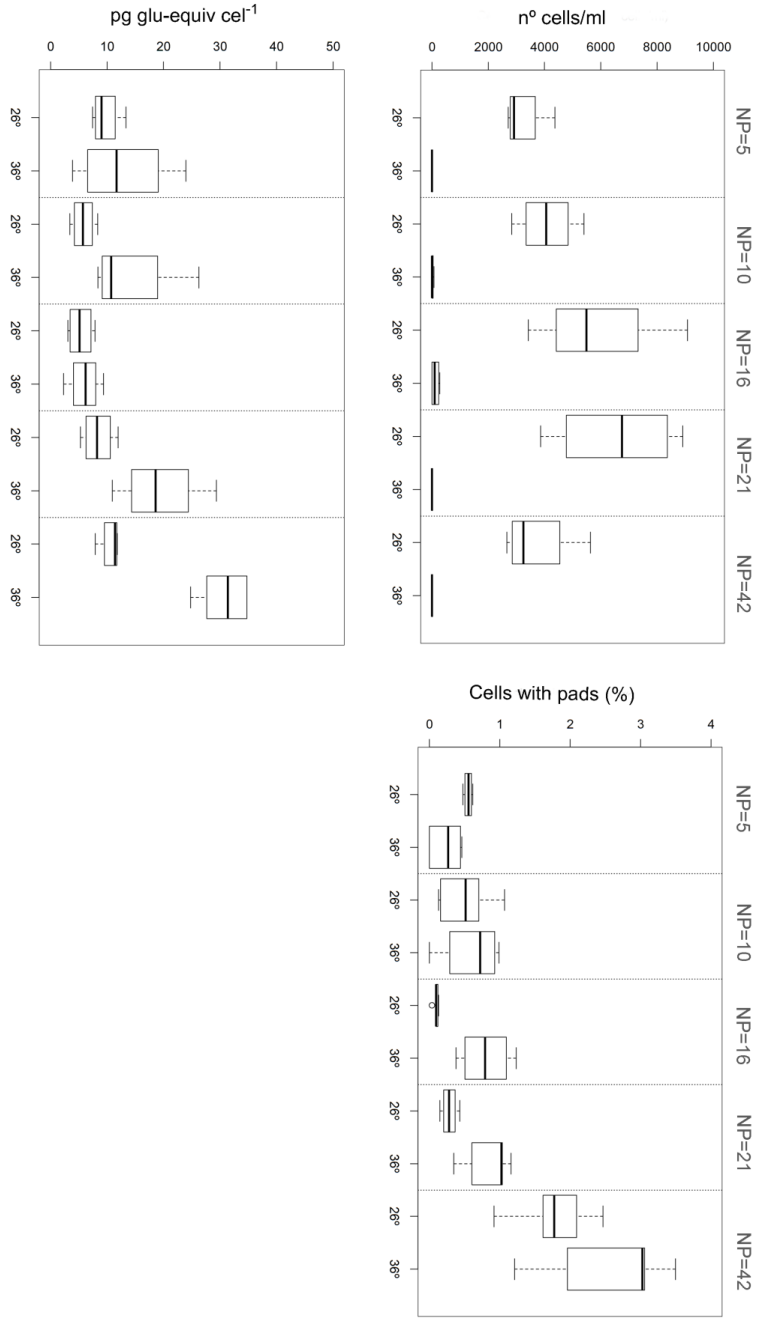

Figure Ap3 1. . Summary of responses to the gradient of N:P ratios at 26 and 36°C.

Appendix 4. Supporting information of chapter 5

Table Ap4 1. Summary of the physical and chemical parameters of the water column (mean±SD) analysed at the reference and contaminated sites during the field experiment, including control treatments (C). The nominal concentration of metals and nutrients in the different treatments (N: nutrients, M: metals, MN: metals+nutrients) and the concentrations found after 1 h (+1 h) of the treatment are indicated at the bottom.

Water parameter (C treatments)	**Reference site**	**Contaminated site**
Salinity	44.16±0.32	44.36±0.66
pH	8.11±0.24	8.10±0.17
Temperature (ºC)	26.80±2.06	27.6±2.25
Dissolved O2 (mg · L-1)	8.66±2.09	7.80±0.26
Chlorophyll a (mg · m-3)	1.07±0.33	0.85±0.19
Suspended solids (mg · L-1)	10.10±6.48	12.30±7.17
NO3- (µmol · L-1)	2.96±0.39	3.72±1.13
PO43 – (µmol · L-1)	<1.05	<1.05
Zn (µg · L-1)	<0.45	0.99±0.57
Pb (µg · L-1)	3.01±2.80	5.23±1.83

Treatments (N, M, MN)	**Nominal**	**Reference site (+1 h)** Min-Max (Mean)	**Contaminated site (+1 h)** Min-Max (Mean)
Nutrients (N)			
NO3- (µmol · L-1)	80	42.18-74.7 (58.44)	47.52-85.56 (66.5)
PO43 – (µmol · L-1)	5	<1.05-4.51 (2.80)	<1.05-3.05 (2.37)
Metals (M)			
Zn (mg · L-1)	100	24.9-47.7 (40.17)	34.9-55.7 (48.77)
Pb (mg · L-1)	50	2.7-8.6 (3.98)	3.2-8.08 (5.83)
Metals+Nutrients (MN)			
NO3- (µmol · L-1)	80	55.71-66.36 (61.03)	40.38-61.70 (51.04)
PO43 – (µmol · L-1)	5	<1.05-2.92 (2.17)	<1.05-2.92 (2.15)
Zn (mg · L-1)	100	61.1-74.6 (67.53)	33.12-65.38 (49.76)
Pb (mg · L-1)	50	5.19-11.9 (5.83)	4.1-16.4 (11.06)

Table Ap4 2. Results of the one-way statistical analyses applied to the selected diatom community descriptive parameters, namely the Kruskal Walis test to compare the control communities (C) between sites and a post-hoc Tukey test to compare C with the other three treatments (N: nutrients, M: metals, MN: metals+nutrients) at each site. Bold letters indicate significant differences.

Kruskal Walis	**Between sites**	
	χ^2	p
Richness (Margalef d)	5.33	0.02
Evenness (Pielou J)	1.35	0.25
Diversity (Shannon–Wiener H´)	3.00	0.08

Tukey test	**Reference site**		**Contaminated site**	
Richness (Margalef d)	t	p	t	p
CxN	-0.5	0.95	-1.2	0.58
CxM	1.12	0.68	0.67	0.91
CxMN	2.3	0.13	0.79	0.85
Evenness (Pielou J)	t	p	t	p
CxN	-0.9	0.75	-1.77	0.32
CxM	-1.8	0.21	0.73	0.87
CxMN	2.46	0.054	0.69	0.89
Diversity (Shannon–Wiener H´)	t	p	t	p
CxN	-1.4	0.45	0.67	0.91
CxM	-2.15	0.19	-1.29	0.58
CxMN	2.8	0.06	0.79	0.85

Table Ap4 3. List of all the taxa found in this study. Significant differences in the abundance of relevant species between the control treatments of both sites (Ref: reference site, Cont: contaminated site) and among treatments at each site are indicated (p-value). If there is no significant response, "x" indicates presence in the control communities from each site.

Amphora pseudohyalina Simonsen			x
Ardissonea fulgens (Greville) Grunow		x	
Berkeleya fragilis Greville		C<MN (z=6.13, p=0.01)	x
Berkeleya fennica Juhlin-Dannfelt	Ref<Cont (χ^2=6.03, p=0.01)		C<N (z=7.85, p<0.001) C<M (z=3.7, p<0.001) C<MN (z=6.02, p<0.001)
Brachysira sp		x	x
Brachysira aponina Kützing	Ref>Cont (χ^2=5.46, p=0.01)	C<M (z=3.34, p<0.01)	C>N (z=-9.05, p<0.001) C>MN (z=-3.7, p<0.001)
Caloneis liber (W.Smith) Cleve			x
Chamaepinnularia sp			x
**Cocconeis placentula* var. *euglypta* (Ehrenberg) Grunow var. *lineata* (Ehrenberg) Van Heurck	Ref=Cont (χ^2=3.00, p=0.08)	C<N (z=7.06, p<0.001) C<M (z=4.91, p<0.001) C>MN (z=-5.24, p<0.001)	C<N (z=3.5, p<0.01) C>M (z=-4.6, p<0.001)
Cocconeis scutellum Ehrenberg		C>MN (z=-2.5, p=0.04)	x
Cocconeis sp		x	x
Cyclotella striata (Kützing) Grunow		x	x
Diploneis sp		x	x
Entomoneis sp		x	x
Fragilaria cf *capensis* Grunow			x
Fragilaria famelica (Kützing) Lange-Bertalot			x
Grammatophora marina (Lyngbye) Kützing			x
Halamphora luciae (Cholnoky) Levkov			x
Halamphora sp		x	x

Halamphora wisei (M.M.Salah) I.Álvarez-Blanco & S.Blanco		x	x
Hyalosynedra aff *laevigata* (Grunow) D.M.Williams & Round			x
Hyalosynedra aff *sublaevigata* Álvarez-Blanco & S.Blanco	Ref>Cont (χ^2=5.39, p=0.02)	C<N (z=3.29, p<0.01)	x
Licmophora colosalis Belando, Aboal & Jiménez		x	x
Licmophora debilis (Kützing) Grunow ex Van Heurck		x	x
Licmophora flabellata (Greville) C.Agardh		x	x
Licmophora proboscidea Mereschkowsky		x	x
Licmophora tenuis (Kützing) Grunow		x	x
Mastogloia cf *emarginata* Hustedt		x	
Navicula salinicola Hustedt		C<MN (z=6.58, p<0.001)	x
Neosynedra provincialis (Grunow) D.M.Williams & Round	Ref<Cont (χ^2=5.6, p=0.02)	C<MN (z=13.01, p<0.001)	C>M (z=-7.24, p<0.001) C>MN (z=-7.45, p<0.001)
Nitzschia aff *closterium* (Ehrenberg) W.Smith		x	x
Nitzschia frustulum (Kützing) Grunow	Ref>Cont (χ^2=5.6, p=0.017)	C>MN (z=-4.04, p<0.001)	x
Nitzschia incognita Legler & Krasske		C<MN (z=6.14, p=0.01)	C<M (z=3.62, p<0.01) C<MN (z=3.99, p<0.001)
Opephora horstiana Witkowski		x	
Opephora krumbeinii A.Witkowski, Witak & K.Stachura	Ref>Cont (χ^2=5.33, p=0.02)	C>N (z=-7.22, p<0.01) C>M (z=-5.56, p<0.01) C>MN (z=-1139, p<0.001)	x
Opephora marina (W.Gregory) Petit			x
Opephora mutabilis (Grunow) Sabbe & Wyverman		x	x
Parlibellus sp			x
Pleurosigma sp			x
Proshkinia sp		x	x

Reimerothrix floridensis A.K.S.K.Prasad	x	x
Seminavis cf *insignis* Álvarez-Blanco & S.Blanco	x	x
Synedra toxoneides Castracane	x	x
Tabularia ktenoeides M.Kuylenstierna	C<N (z=4.45, p<0.001)	x
Toxarium undulatum J.W.Bailey	x	x

*Two varieties of *Cocconeis placentula* have been jointly analyzed because they responded similarly

Table Ap4 4. Results of the GzLM analysis (two factors) applied to the relative abundances of the type of growth form of diatom species. Significant changes in abundance between sites (control treatments) and among treatments at each site (C: control, N: nutrients, M: metals, MN: metals+nutrients) are indicated in bold. S: Site (df=1), T: treatment (df=3), SxT: Site x Treatment (df=3). *Main test not significant.

	Main test		Between sites	Pair-wise among treatments	
				Reference site	Contaminated site
		χ^2 / p-value	χ^2 / p-value	(χ^2 or z/ p-value)	(χ^2 / p-value)
Chain	S T SxT	61.94/**<0.001** 31.95/**<0.001** 12.57/**<0.01**	28.67/**<0.001**	C>N (10.87/**0.01**) C=M (5.45/0.23) C>MN (29.89/**<0.001**) MN<M (14.56/**<0.01**) MN<N (9.06/**0.03**)	C=N (1.88/1.00) C=M (0.39/1.00) C=MN (0.01/1.00)
Zig-zag colony	S T SxT	4.83/**0.02** 55.81/**<0.001** 121.40/**<0.001**	23.79/**<0.001**	C=N (1.23/1.00 C=M (0.11/1.00) C<MN (38.40/**<0.001**) MN>M (36.40/**<0.001**) MN>N (28.37/**<0.001**)	C=N (2.64/0.51) C>M (11.75/**<0.01**) C>MN (13.03/**<0.01**) MN<N (9.63/**<0.05**)
Motile	S T SxT	26.64/**<0.001** 13.86/**<0.01** 15.9/**<0.01**	13.34/**<0.001**	C=N (0.02/1.00) C=M (1.10/1.00) C=MN (2.78/0.57)	C=N (0.25/1.00) C<M (8.96/**<0.05**) C=MN (7.38/0.06)
Unattached	S T SxT	157.43/**<0.001** 35.47/**<0.001** 17.73/**<0.001**	30.59/**<0.001**	C=N (1.55/0.85) C=M (1.19/0.85) C=MN (0.63/0.85)	C>N (19.72/**<0.001**) C=M (4.06/0.30) C=MN (2.48/0.57) M>N (37.21/**<0.001**) M>MN (12.37/**<0.01**)
Prostrate	S T SxT	69.91/**<0.001** 25.25/**<0.001** 31.67/**<0.001**	24.57/**<0.001**	C=N (6.70/0.07**)** C=M (3.57/0.29) C>MN (11.34/**<0.01**) MN<M (25.40/**<0.001**) MN<N (31.78/**<0.001**)	C=N (1.47/0.67) C=M (6.54/0.07) C=MN (0.19/0.95) N>M (14.10/**<0.01**)
Mucous tube	S T SxT	421.03/**<0.001** 22.20/**<0.001** 5.85/0.12	6.05/**0.01**	6.75/0.08*	C<N (4.15/**<0.001**) C=M (1.99/0.18) C<MN (3.56/**<0.01**)
Ribbon	S T SxT	40.35/**<0.001** 4.15/0.25 3.68/0.29	6.40/**0.01**	-	-
Rosette colony	S T SxT	19.05/**<0.001** 4.73/0.19 3.46/0.32	4.80/<**0.05**	-	-
Stalked colony	S T SxT	0.02/0.88 1.16/0.76 2.52/0.47	-	-	-

Table Ap4 5. Two-way ANOVA results (two factors) showing the interactive effect of the site and treatment on the biofilm parameters. Significant differences between the control biofilms of both sites and the treatment at each site (C: control, N: nutrients, M: metals, MN: metals+nutrients) are indicated in bold. Ref.: reference site, Cont.:

	Zn		Pb		Chlorophyll *a*		Polysaccharides	
Two-way ANOVA	F	*p*	F	*p*	F	*p*	F	*p*
Site /df=1	293.48	**<0.001**	33.06	**<0.001**	43.78	**<0.001**	10.61	0.003
Treatment /df=3	50.33	**<0.001**	37.64	**<0.001**	37.81	**<0.001**	14.04	**<0.001**
Site x Treatment /df=3	6.24	<**0.01**	15.69	**<0.001**	26.38	**<0.001**	42.81	**<0.001**
Tukey test	F	*p*	F	*p*	F	*p*	F	*p*
Between sites /df=1 (C treatment)	73.59	**<0.001**	48.45	**<0.001**	1.99	0.47	19.35	**<0.001**
Among treatments /df=1 (F/*p*-value)	**Ref.**	**Cont.**	**Ref.**	**Cont.**	**Ref.**	**Cont.**	**Ref.**	**Cont.**
C x N	0.2/ 1.00	6.7/ 0.11	3.4/ 0.31	0.03/ 1.00	1.9/ 1.00	0.8/ 1.00	0.3/ 1.00	41.1/ **<0.001**
C x M	15.1/ **0.001**	24.0/ **<0.001**	65.3/ **<0.001**	4.2/ 0.28	0.2/ 1.00	0.9/ 1.00	9.4/ **0.01**	37.1/ **<0.001**
C x MN	98.5/ **<0.001**	38.8/ **<0.001**	113.3/ **<0.001**	4.0/ 0.28	110.3/ **<0.001**	0.9/ 1.00	47.9/ **<0.001**	3.3/ 0.20
N x M	11.2/<**0.01**	5.3/ 0.25	38.8/ **<0.001**	3.4/ 0.31	0.8/ 1.00	3.5/ 0.52	6.01/ 0.057	0.1/ 1.00
N x MN	87.9/ **<0.001**	13.2/ <**0.01**	77.4/ **<0.001**	3.3/ 0.31	141.6/ **<0.001**	3.4/ 0.52	56.81/ **<0.001**	21.0/ **<0.001**
M x MN	36.4/ **<0.001**	1.7/ 1.00	6.5/ 0.083	0.002/ 1.00	120.4/ **<0.001**	0.001/ 1.00	99.8/ **<0.001**	17.1/ **<0.001**